09,2023
Volume 1 Issue 2

Agricultural & Rural Studies

ISSN 2959-9784
02 >
9 772959 978235

SCC PRESS

https://sccpress.com/ars

OPEN ACCESS

ISSN 2959-9784

Cover Story

Siniscola, situated on Sardinia's northeastern coastline, Italy, (39 m above sea level) encapsulates a mosaic of historical, cultural, and developmental dynamics. Tracing its origins to the Nuragic civilization, the village's evolution has been imprinted by successive influences including Phoenician, Carthaginian, and Roman epochs, contributing to its multifaceted identity. With a population of approximately 11,000 inhabitants, Siniscola is anchored by its agrarian heritage. The landscape is adorned with cereal fields, vineyards, and olive groves, representing its agricultural heritage and intertwining with the island's broader agricultural context. Distinctive to Siniscola is the "pompia," a citrus fruit renowned for its rough, thick, and irregular skin, used to create the eponymous sweet delicacy. "Sa pompia" has been cultivated in this region since antiquity. Representing traditional Siniscola cuisine is the iconic dish "sa suppa Thiniscolesa," a culinary delight.

Siniscola's development is reflected in its infrastructure evolution. From its fortified origins, the village has transitioned into a bridge between tradition and modernity. The historical significance of both the tourism and agriculture industries mirrors the economic fluctuations that have shaped Sardinia's trajectory. The contemporary rise in tourism, allured by pristine beaches, marks the most recent phase of transformation. Essentially, Siniscola captures Sardinia's essence—a harmony of past and present. The coexistence of age-old traditions and modern progress reflects the island's resilience. In this coastal enclave, Sardinia's story resonates—a testament to its journey guided by echoes of the past, embracing the timeless sea rhythms and the beauty of its unspoiled beaches.

(Giuseppe Pulighe, Researcher at CREA - Research Centre for Agricultural Policies and Bioeconomy, via Po 14, 00198 Rome, Italy.)

Agricultural & Rural Studies

Vol. 1, No. 2 September, 2023

Contents

0007 Trapped in the Past: The Decline of Italian Olive Groves in the Face of Traditional Visions and Policies, Emerging Challenges and Innovation
Giuseppe Pulighe

0008 Research on Progress of Forest Fire Monitoring With Satellite Remote Sensing
Ying Zheng, Gui Zhang, Sanqing Tan and Lanbo Feng

0009 The Relationship between Agri-Food Production and Macro-Economic Dynamics: A Study on Soybeans in Brazilian South and Chinese Mainland
Ângelo Belletti and Sérgio Schneider

0010 Analysis of Spatial Unbalance and Convergence of Agri- cultural Total Factor Productivity Growth in China—Based on Provincial Spatial Panel Data From 1978 to 2020
Chaozhu Li and Xiaoliang Li

0011 Evaluation of the Streamflow Response to Agricultural Land Expansion in the Thiba River Watershed in Kenya
Brian Omondi Oduor, Benedict Mutua, John Ng'ang'a Gathagu and Raphael Wambua

0012 An Atlas of Desertification for Spain
Jaime Martínez-Valderrama

About the Journal

Agricultural & Rural Studies (**A&R**, **ISSN 2959-9784**) is a quarterly journal to be an international, multi-/inter-disciplinary platform for communicating advances in fundamental and applied studies on contemporary agricultural, rural and farmers' issues and policies, as broadly defined by the disciplines of economics, sociology, human geography and cognate subjects.

A&R is a digital-only, double-blind peer-reviewed, open-access (OA) journal. Article Publishing Charges (APC) are waived in the first four years. The journal publishes various materials – perspective, review, original research, and commentary articles – and it is dedicated to serving as an efficient, professional, and innovative platform for scholars in the field of agricultural and rural studies.

In a nutshell, the A&R Journal:

(1) covers multidisciplinary and interdisciplinary subjects such as economics, sociology, human geography and cognate subjects that are relevant to contemporary agricultural, rural and farmers' issues and policies.

(2) Is served by a renowned, dedicated, and international editorial board.

(3) Is a fully independent Open Access (OA) platform: http://sccpress.com/ars, which promotes your article worldwide.

(4) Offers supportive, efficient, and professional publication services. We understand that authors are unique, and each paper is different. That is why our full-time professional editors are ready to help authors with structure matters and support them with reference management to simplify their research life.

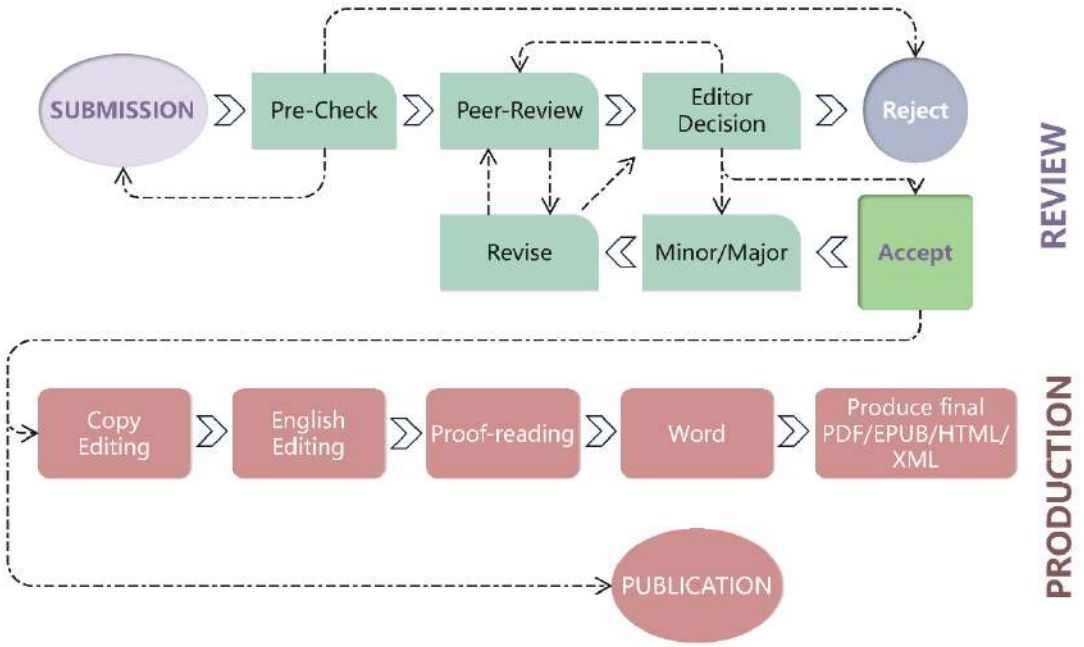

Agricultural & Rural Studies

Perspective

Trapped in the Past: The Decline of Italian Olive Groves in the Face of Traditional Visions and Policies, Emerging Challenges and Innovation

Giuseppe Pulighe

Research Centre for Agricultural Policies and Bioeconomy, 00184 Rome, Italy; giuseppe.pulighe@crea.gov.it

Abstract: Italy has long been a key player in olive crop production, but the sector is currently facing an unprecedented crisis. This is evident by shrinking cultivated areas, farms, production levels, and investments. Multiple factors contributed to this decline, including traditional cultivation practices, limited innovation and competitiveness, siloed-oriented policies, landscape protection measures, and unsustainable agricultural systems. Phytosanitary issues, such as the spread of *Xylella fastidiosa* and the effects of climate change and drought, further compounded these challenges. Over the last decade, the sector has undergone preservation efforts focused on the perpetuation of traditional narratives and implementing policies to protect smallholder farmers, old cultivars, and safeguard traditional agri-food products. However, these approaches hinder the sector's ability to adapt and compete in the market, perpetuating stagnation rather than driving the necessary changes. To reverse this decline, the olive sector must undergo necessary evolution, as seen in other sectors, such as viticulture and tree crops. This entails embracing a comprehensive strategy encompassing research and development, infrastructure investment, the promotion of modern cultivation techniques, and policies that support the sector's evolution. Without such measures, the future of Italy's olive industry remains uncertain, with significant implications for its cultural heritage and economy. Italy must recognize the economic and cultural consequences of continued decline and take immediate action for long-term viability.

Keywords: olive crop decline; siloed-oriented policies; CAP; competitiveness; sustainability

Citation: Pulighe, G. Trapped in the Past: The Decline of Italian Olive Groves in the Face of Traditional Visions and Policies, Emerging Challenges and Innovation. *Agricultural & Rural Studies*, 2023, *1*, 0007. *https://doi.org/10.59978/ar01020007*

Received: 31 July 2023
Revised: 9 August 2023
Accepted: 23 August 2023
Published: 1 September 2023

Publisher's Note: SCC Press stays neutral with regard to jurisdictional claims in published maps and institutional affiliations.

1. Introduction

Italy's olive groves (*Olea europaea* L.) and olive oil industry have been an essential part of the country's cultural and economic heritage for centuries (Bartolini & Petruccelli, 2002). Italy is one of the world's leading countries in olive crop production and land use of olive groves, accounting for approximately 11% of the world's cultivated area (Torrecillas & Martínez, 2022). However, over the past few decades, the olive sector is facing a crisis of unprecedented proportions, with a decline well represented by numbers (Cola & Sarnari, 2020). The downturn of the olive sector is reflected in several statistical indicators, such as cultivated areas, olive farms, production, oil mills, trade balance, and investments. The total olive-growing area in Italy is approximately 1,129 million hectares in 2021, equal to 8% of the utilized agricultural area (Council for Agricultural Research and Economics, 2022). Although cultivated areas have been quite stable over the past decade, 'Italy's olive orchard' is characterized by the massive presence of ancient olive trees (only 3% of the olive trees are less than 11 years old) and relatively low tree density per hectare (Figure 1). The most recent data indicate a contraction with a loss of about 17,000 hectares almost entirely confined to the Apulia (the most important region for olive production in Italy) due to the effects of infection of *Xylella fastidiosa* first appeared in 2013 (Schneider et al., 2020).

Figure 1. Traditional olive grove in Italy with wide planting spacing. Credit: Achim Ruhnau, Unsplash.

The general agricultural census data of the year 2020 indicate that the olive sector includes 619,378 farms, with a decrease of about one-third from the 2010 census. For production, the data indicate a trend decline beyond the traditional olive tree alternate bearing, which furthermore is more pronounced in ancient productive trees. Over the past decade, the production of olive oil in Italy has experienced a significant decline, dropping from more than 500,000 tons in 2010 to approximately 235,000 tons in 2022 (Cola & Sarnari, 2020; International Olive Council, 2023).

The fragmentation of the production structure is also evident from the high number of active mills, amounting to 4,448 (CREA, 2022), in comparison with Spain where there are less than 1,700 (Cola & Sarnari, 2020). Although the widespread presence of mills can ensure rapid olive processing and thus the hygienic-nutritional quality of the oil, as well as an added value in terms of tourism (Lombardo et al., 2022), it also results in a low average production per olive mill of only 74 tons in 2021.

Regarding trade balance, Italy is positioned as a net importer of olive oil, with a deficit amounting to 263,000 tons and 62 million euros in 2019, continuing the reduction observed in the past three years (Cola & Sarnari, 2020). Spain is the main supplier, accounting for more than 60 percent of imported olive oil, mainly extra-virgin olive oils (EVOO). In the context of worldwide olive oil production, an annual average of 3 million tons of olive oil is harvested, with the European Union (EU) being a prominent contributor for approximately 2 million tons of this annual yield. Among the key Member States, Spain leads with 66% of EU production, trailed by Italy at 15%, Greece at 13%, and Portugal at 5%. The EU constitutes the largest consumer of olive oil, with an approximate annual consumption of 1.5 million tons, and holds the position of the foremost exporter of olive oil, with an annual export volume of approximately 570,000 tonnes (IOC, 2023). Overall, the causes of this decline are multifaceted and weave together traditional views of cultivation, scarce innovation and competitiveness, lack of cooperation, siloed-oriented policies, landscape protection and unsustainable agricultural systems. In addition, in recent years the exacerbation of phytosanitary problems such as *Xylella fastidiosa* and the accentuation of climate change and drought have exacerbated the conditions of many operators in the olive supply chain. It has been estimated that if the expansion of the infected area is not stopped, the economic impact on Italy could grow to 5.2 billion euros (Schneider et al., 2020).

The convergence of these challenges has hindered the progress of the olive sector, resulting in its apparent stagnation in terms of farm structure and the agri-food system. As a result, the sector has been unable to attain the transition necessary for achieving market competitiveness.

In this essay, we claim that the olive sector stagnation is strongly influenced by the peasantry and utopian envision and narratives (self-supported by the agricultural policies and subsidies) that would like to safeguard smallholder farmers and their income, old cultivars, agrarian landscape and traditional agrifood products, which instead just perpetuates the status quo.

We argue that a necessary evolution is required in the olive sector, similar to advancements observed in other agricultural sectors such as viticulture and fruit growth. It is crucial to strike a

balance between preserving cultural heritage and embracing necessary changes to modernize the industry, promote sustainability, and ensure its long-term viability. By challenging traditional visions and narratives, fostering disruptive innovations, enhancing cooperation, and implementing supportive policies, the olive sector can overcome its current challenges and regain its position as a dynamic and competitive industry. Taking proactive measures to address the multifaceted causes of decline will not only safeguard Italy's cultural heritage but also contribute to economic growth and sustainability in the agricultural sector. In the following, we will critically discuss these multifaceted challenges and explore the role of innovation in revitalizing the sector.

2. Characteristics of the Value Chain

The value chain for the olive sector in Italy encompasses a comprehensive set of characteristics that span the pillars of agricultural production, industrial processing, and commercialization phases. Notably, a significant proportion of agricultural farms in this sector exhibit an average size of less than two hectares, highlighting the predominance of small-scale cultivation practices (Cola & Sarnari, 2020).

The modest size of these farms is linked to high production costs and reduced inclination for innovation and market orientation, as evidenced by the higher average age of the farmers involved. Additionally, the presence of an aging workforce is more pronounced in the olive industry compared to other agricultural sectors. On the other hand, the production stage of the olive value chain in Italy benefits from a wealth of regional cultivars, encompassing a remarkable diversity of more than 500 distinct landraces (Pannelli & Perri, 2012).

However, this abundance of regional cultivars can pose challenges if their features and potential are not adequately evaluated and valorized. Indeed, despite the high number of oils with Protected Designation of Origin (PDO) or Protected Geographical Indication (PGI) (Lombardo et al., 2021), these landraces have a minimal impact on the overall production volumes and, furthermore, are often poorly recognized or unknown to consumers (Cola & Sarnari, 2020). It seems intuitive how it is impossible to individually enhance all these cultivars in the market when instead a strategy would be needed to synthesize this botanical richness into new pathways.

As previously mentioned, the industrial phase of the value chain is characterized by a significant concentration of small olive oil mills, predominantly located in southern Italy. In addition to small mills, the olive sector in Italy also comprises large companies that purchase olive oil and engage in bottling operations. However, the presence of a large number of mills can result in diminished economic efficiency, elevated production costs, and a postponed implementation of technological advancements. These factors, in turn, have the potential to impede the achievement and maintenance of high-quality standards in olive oil production.

Despite being a major producer, Italy holds the distinction of being the world's foremost importer of olive oil, as well as the second largest exporter. As indicated above, large bottling companies import the product to enhance its value through export. Italy's trade deficit in olive oil accounts for 28% of the total volume but represents just 2% of the corresponding value in commercial exchanges (Cola & Sarnari, 2020). The olive sector's significant export orientation underscores a key advantage that should be further fostered and expanded.

3. Traditional Visions

The olive groves hold a significant place as an iconic and symbolic representation of the Mediterranean regions, reflecting their extensive agricultural heritage and playing a crucial role in shaping the landscape. Beyond their cultural and historical significance, the olive groves have substantial economic, cultural, and ecological importance, along with viticulture and cereal cultivation (Giourga & Loumou, 2002). The olive tree, along with the vine and wheat, also holds a significant and sacred role within the symbolism of Christianity, representing consecrated alimentary products such as oil, wine, and bread. Its presence shapes the visual aesthetics of the Mediterranean landscape, reflecting a long-standing agricultural tradition deeply intertwined with the cultural identity of the local communities. Culturally, olives trees, local landraces and olive oil have deep-rooted traditions and are integral to Mediterranean cuisine. They are essential components of local dishes, representing a shared culinary heritage. Furthermore, olives and olive branches have symbolic meanings, representing peace, prosperity, and unity, and are often associated with the cultural identity of the Mediterranean regions. From an ecological perspective, olive groves contribute to the preservation of biodiversity and the conservation of natural resources. These groves create unique habitats for various plant and animal species, promoting ecological diversity (Fekete et al., 2023). Traditional and labor-intensive cultivation practices, including terracing, in the past have bolstered soil conservation and fostered sustainable land resource utilization in olive-growing regions (Giourga & Loumou, 2002). Nevertheless, as suggested by Duarte et al. (2008) traditional olive orchards have limited economic sustainability. Their viability depends on accepting reduced

opportunity costs for family labor and engaging in part-time olive growing, which ultimately results in an economically marginal status.

The culmination of these intertwined elements, perpetuated for centuries, remains evident in contemporary times, where Italian olive cultivation epitomizes a narrative deeply ingrained in peasant traditions. This narrative would guarantee the preservation of the timeless landscape, local olive landraces, and a production system rooted in traditional peasant practices. However, these visions, while preserving the cultural heritage, have contributed to the decline of the industry by failing to address the evolving needs of olive farming in the face of mounting challenges.

4. The Role of the Policies

The EU has historically placed significant attention on the olive oil sector, offering subsidies to support farmers engaged in olive oil production through the Common Agricultural Policy (CAP) (de Graaff & Eppink, 1999). Support for the olive sector has taken various forms, with consumption aid playing a significant role as a primary form until 1994. Between 1994 and 1999, consumption subsidies were significantly reduced and eventually abolished in 1998. They were gradually replaced by subsidies aimed at olive oil production. Between 2000 and 2005, there were relatively few changes in the support measures for the olive sector, while the 2004 reform incorporated support for olive oil production into the single payment scheme (Agrosynergie, 2009). Decoupling has been permitted in order to prevent the abandonment of olive groves in marginal areas, accompanied by the introduction of cross compliance for Good Agricultural and Environmental Conditions (GAEC) (Duarte et al., 2008). The CAP for the period 2023–2027 in Italy introduces targeted sectoral support for the production of olive oil and table olives. This support is implemented through co-financing programs that focus on the operational programs of producer organizations and their associations. The allocation of funds is closely tied to the actual production levels delivered to the market. Moreover, the CAP 2023–2027 also introduces eco-schemes which should encourage farmers to adopt environmentally friendly practices, by obtaining up to € 586 hectare (AgroNotizie, 2023). Substantially, the focus of the interventions is still on maintaining the status quo and tend to discourage innovation or does not encourage investment capacity and strategic orientation.

One of the main problems of the sector policies is that have demonstrated limited effectiveness as they have primarily prioritized problem mitigation rather than addressing the underlying causes. The logic of policy intervention has consistently treated the sector as static, primarily because olive growing is a long-term endeavor, leading to inertia and slower emergence of changes compared to annual production. Indeed, the various reforms of the CAP have consistently overlooked the central role of olive growers in terms of supporting their competitiveness and entrepreneurial capabilities. Instead, the focus of these reforms has primarily been on the widespread allocation of aid to small-scale producers following price-production dynamics, rather than tailoring interventions to address the specific requirements and challenges associated with various forms of olive cultivation and land management, or new consumption habits.

For instance, one aspect that has been insufficiently addressed in the reforms is the issue of fragmented land structures, which impose limitations on the competitiveness and investment capacity within the olive sector. It is worth noting that the average farm size in Apulia, for instance, is reported to be approximately 1.7 hectares, significantly smaller compared to the average farm size of 8 hectares observed in Andalusia in Spain.

As stated by Duarte et al. (2008) the main causes of abandonment are closely related to farm profitability, the main issue being the low yields of traditional olive groves. This low profitability is further exacerbated by the size of the farms, which hampers the implementation of innovative strategies. This interconnected relationship forms a self-reinforcing cycle wherein limited profitability due to low yields contributes to farm abandonment, and the inability to invest in productivity-enhancing measures further perpetuates the cycle of low profitability.

Evidence that policies intervention in the sector has not promoted an increase in high quality and competitive products in the market is indicated by consumer behaviors. Although Italy has the highest number of certified EVOO recognized as PDO or PGI (Lombardo et al., 2021), recent findings suggest that only 36% of consumers broadly understood health claims on EVOO (Lombardi et al., 2021). Despite various studies indicated an increasing willingness to pay for premium products (Di Vita et al., 2021), Lombardi et al. (2021) argued that low perceived health claims on EVOO hinders the ability of producers to take advantage derived from higher prices of the perceived high quality of these products.

5. The Innovation Imperative

The gradual decline of the olive sector in Italy highlights the urgent need for innovation. This calls for a combination of policy reforms and significant cultural shifts to support the necessary changes. To tackle the aforementioned challenges, the olive sector needs to initiate innovation in its growing practices. This involves adopting a new approach that moves away from traditional

orchards and towards a model that emphasizes farm-centered strategies and farmer-led with robust professional skills. An entrepreneurial mindset should guide this transformation, with a strong focus on incorporating innovation and leveraging new technologies at its core, as in the case of grape growing and fruit cultivation.

A viable innovation path is the shift toward intensification adopting high density or super high density planting system which allow for huge increases in production efficiency with a reduction of production costs (Lo Bianco et al., 2021) (Figure 2).

Previous research has established that these system plantings based on integral mechanization can be both economic and environmentally sustainable (Camposeo et al., 2022), able to improve soil carbon sequestration (Mairech et al., 2020). As suggested by Camposeo et al. (2021) super high density planting systems are able to produce nutraceutical EVOOs rich in polyphenols compounds, as demonstrated with "Lecciana" that is the first olive cultivar of Italian descent suitable for super high-density orchards.

Figure 2. Mechanized harvesting in a super high density olive orchard in Italy.

A recent study by Flamminii et al. (2023) conducted in the Abruzzo region examined allochthonous cultivars suitability for super high density systems and concluded that it is possible to obtain nutraceutical EVOOs comparable to traditional ones.

In such a framework, innovation's contribution to revitalizing Italian olive farming should include:

- New planting systems. Should ensure tree canopies suitable for mechanical operations and precision management.
- New suitable cultivars. The adoption of new olive cultivars, adapted to the changing climate, suitable for new planting systems, resistant to pests and diseases, low vigor, with better yields and oil quality. In the future, new plantations will be benefiting from new cultivars obtained with conventional and new breeding techniques.
- Mechanization. The adoption of integrated mechanization in olive farming for all cultivation stages can help reduce labor costs and improve efficiency. Mechanization facilitates the swift processing of olives at the mills within a few hours of harvest.
- Precision agriculture. The use of disruptive agriculture techniques, such as sensors, drones, and data analytics, to optimize irrigation and water management, fertilization, and pest management. Precision agriculture can help reduce the use of resources, increase yields, and improve oil quality.
- Climate-Smart Certification and Labeling: Implementing a climate-smart certification and labeling system for olive products can help consumers identify products that are produced using sustainable and climate-friendly practices. This can create incentives for farmers to adopt environmentally friendly approaches and differentiate their products in the market.
- Investment in education and training. Providing continuous education and training programs to olive farmers can ensure that they are up-to-date with the latest innovations, best practices, and market trends. Well-informed farmers are better equipped to make informed decisions and adapt to changing circumstances effectively.

To foster the growth of the olive oil sector in Italy, the government should adopt a comprehensive set of development policies that encompass various dimensions. Firstly, investing in new olive trees plantings to increase and rationalize production oriented only towards producing nutraceutical EVOOs products. Secondly, prioritizing research and development efforts to enhance mechanization practices becomes crucial. Considering the impending labor shortage in this sector, its significant impact on costs and final income is evident. Thirdly, it becomes imperative to implement targeted measures for the modernization of olive mills and their strategic placement within the territory. These innovative solutions require research, investment, and collaboration between farmers, researchers, policymakers, and other stakeholders. The adoption of these solutions can help ensure the long-term sustainability of Italian olive farming and contribute to the development of a more resilient and vibrant rural economy. It is only through innovation that the Italian olive farming industry can overcome the challenges it faces and ensure a sustainable future.

6. Summary

The paper provides insights into the current state of Italian olive groves, discussing their strengths and weaknesses. It highlights the factors contributing to their decline, while also acknowledging the potential of Italian olive oil sector and its ability to increase production, although it currently falls short of fulfilling domestic needs. To address these challenges, adopting new sustainable practices is crucial. One such measure involves increasing planting densities to improve productivity. However, it's essential to balance this approach with meeting minimum sustainability goals, including considerations for yield, labor, costs, as well as proper irrigation and fertilization practices. The perception of olive trees as low-maintenance crops has hindered advancements in care and management techniques. Nevertheless, there are opportunities to enhance the productivity of traditional olive groves through improved pruning, biostimulant-based fertilization, and incorporating modern machinery. Moreover, integrated mechanization could help counterbalance the potential scarcity of labor in the olive sector in the future.

Embracing innovation and sustainable practices is vital for the long-term success of the olive industry. A forward-looking approach should consider promoting the coexistence of multiple olive cultivation systems, such as terraced olive agro-ecosystems, catering to diverse needs and consumers. By diversifying and meeting varying market demands, the Italian olive industry can enhance its resilience and competitiveness. In conclusion, the revitalization of Italian olive groves necessitates the adoption of innovative and sustainable practices, alongside a willingness to challenge traditional perspectives. By taking these steps, the olive sector can unlock its full quality potential, fulfill domestic demands, and ensure a prosperous future for both olive growers and consumers.

CRediT Author Statement: This is a single author paper and the author was solely responsible for the content, including the concept, design, analysis, writing, and revision of the manuscript.

Data Availability Statement: Not applicable.

Funding: This research received no external funding.

Conflicts of Interest: The author declares no conflict of interest.

Acknowledgments: Not applicable.

References

AgroNotizie. (2023, March 8). *Olivo, con la nuova Pac 586 euro in più ad ettaro*. https://agronotizie.imagelinenetwork.com/agricoltura-economia-politica/2023/03/08/olivo-con-la-nuova-pac-586-euro-in-piu-ad-ettaro/78185

Agrosynergie. (2009). *Evaluation des mesures appliquées au secteur oléicole dans le cadre de la politique agricole commune. Rapport final*. https://rica.crea.gov.it/download.php?id=784

Bartolini, G., & Petruccelli, R. (2002). *Classification, origin, diffusion and history of the olive*. Food & Agriculture Organization.

Camposeo, S., Vivaldi, G. A., Montemurro, C., Fanelli, V., & Cunill Canal, M. (2021). Lecciana, a new low-vigour olive cultivar suitable for super high density orchards and for nutraceutical evoo production. *Agronomy*, *11*(11), 2154. https://doi.org/10.3390/agronomy11112154

Camposeo, S., Vivaldi, G. A., Russo, G., & Melucci, F. M. (2022). Intensification in olive growing reduces global warming potential under both integrated and organic farming. *Sustainability*, *14*(11), 6389. https://doi.org/10.3390/su14116389

Cola, M., & Sarnari, T. (2020). *La competitività della filiera olivicola analisi della redditività e fattori determinanti (in italian)*. https://www.reterurale.it/flex/cm/pages/ServeBLOB.php/L/IT/IDPagina/22376

Council for Agricultural Research and Economics. (2022). *Annuario dell'agricoltura italiana 2021 (in italian)*. https://www.crea.gov.it/documents/68457/0/Annuario_CREA_2021_Volume_LXXV.pdf/49fc57e1-a325-50f4-22bb-d044d0f24dbe?t=1671527592245

CREA. (2022). ANNUARIO DELL'AGRICOLTURA ITALIANA 2021 (in italian). CREA.

de Graaff, J., & Eppink, L. A. A. J. (1999). Olive oil production and soil conservation in southern Spain, in relation to EU subsidy policies. *Land Use Policy*, *16*(4), 259–267. https://doi.org/10.1016/S0264-8377(99)00022-8

Di Vita, G., Zanchini, R., Falcone, G., D'Amico, M., Brun, F., & Gulisano, G. (2021). Local, organic or protected? Detecting the role of different quality signals among Italian olive oil consumers through a hierarchical cluster analysis. *Journal of Cleaner Production*, *290*,

125795. https://doi.org/10.1016/j.jclepro.2021.125795
Duarte, F., Jones, N., & Fleskens, L. (2008). Traditional olive orchards on sloping land: Sustainability or abandonment? *Journal of Environmental Management*, *89*(2), 86–98. https://doi.org/10.1016/j.jenvman.2007.05.024
Fekete, R., Vincze, O., Süveges, K., Bak, H., Malkócs, T., Löki, V., Urgyán, R., & Molnár V., A. (2023). The role of olive groves in the conservation of Mediterranean orchids. *Global Ecology and Conservation*, *44*, e02490. https://doi.org/10.1016/j.gecco.2023.e02490
Flamminii, F., Gaggiotti, S., Chiaudani, A., Compagnone, D., & Cichelli, A. (2023). The introduction of allochthonous olive variety and super high-density system in the abruzzo region: A study on olive oil quality. *Foods*, *12*(6), 1292. https://doi.org/10.3390/foods12061292
Giourga, C., & Loumou, A. (2002). Olive groves: "The life and identity of the Mediterranean". *Agriculture and Human Values*, *20*(1), 87–95.
International Olive Council. (2023). *Production of olive oil 2022–2023.*
Lo Bianco, R., Proietti, P., Regni, L., & Caruso, T. (2021). Planting systems for modern olive growing: strengths and weaknesses. *Agriculture*, *11*(6), 494. https://doi.org/10.3390/agriculture11060494
Lombardi, A., Carlucci, D., Cavallo, C., De Gennaro, B., Del Giudice, T., Giannoccaro, G., Paparella, A., Roselli, L., Vecchio, R., & Cicia, G. (2021). Do consumers understand health claims on extra-virgin olive oil? *Food Research International*, *143*, 110267. https://doi.org/10.1016/j.foodres.2021.110267
Lombardo, L., Farolfi, C., & Capri, E. (2021). Sustainability certification, a new path of value creation in the olive oil sector: The Italian case study. *Foods*, *10*(3), 501. https://doi.org/10.3390/foods10030501
Lombardo, L., Farolfi, C., Tombesi, S., Novelli, E., & Capri, E. (2022). Development of a sustainability technical guide for the Italian olive oil supply chain. In *Science of The Total Environment*, 820, 15332. https://doi.org/10.1016/j.scitotenv.2022.153332
Mairech, H., López-Bernal, Á., Moriondo, M., Dibari, C., Regni, L., Proietti, P., Villalobos, F. J., & Testi, L. (2020). Is new olive farming sustainable? A spatial comparison of productive and environmental performances between traditional and new olive orchards with the model OliveCan. *Agricultural Systems*, *181*, 102816. https://doi.org/10.1016/j.agsy.2020.102816
Pannelli, G., & Perri, E. (2012). *Scelte varietali in olivicoltura. Accademia Nazionale dell'Olivo e dell'Olio*.
Schneider, K., van der Werf, W., Cendoya, M., Mourits, M., Navas-Cortés, J. A., Vicent, A., & Oude Lansink, A. (2020). Impact of Xylella fastidiosa subspecies pauca in European olives. *Proceedings of the National Academy of Sciences*, *117*(17), 9250–9259. https://doi.org/10.1073/pnas.1912206117
Torrecillas, C., & Martínez, C. (2022). Patterns of specialisation by country and sector in olive applications. *Technology in Society*, *70*, 102003. https://doi.org/10.1016/j.techsoc.2022.102003

Agricultural & Rural Studies

Review

Research on Progress of Forest Fire Monitoring with Satellite Remote Sensing

Ying Zheng, Gui Zhang *, Sanqing Tan and Lanbo Feng

College of Forestry, Central South University of Forestry and Technology, Changsha 410000, China;
zoeysjz@163.com (Y.Z.); t19920990@csuft.edu.cn (S.T.); cahrmisty@163.com (L.F.)
* Correspondence: csfu3s@163.com

Abstract: With satellite remote sensing technology blooming, satellite remote sensing has become a common tool to detect forest fires, and played an important role in forest fire monitoring. This paper sort the research status and progress on satellite remote sensing monitoring for forest fires to provide directions and insights for subsequent research and applications. Through reviewing the literature on satellite remote sensing monitoring for forest fires, we present satellites and sensors for forest fire monitoring, describe forest fire monitoring methods through brightness temperature detection and smoke detection, and summarize current problems of satellite remote sensing monitoring of forest fires. Despite forest fire satellite remote sensing monitoring algorithms are becoming increasingly mature, it is not without problems such as slow migration of cloud detection algorithms, difficulties in unifying spatial and temporal characteristics, and difficulties in detecting small fires and low-temperature fires. Finally, in response to the problems identified, we list some recommendations with a view to providing useful references for future research on forest fire monitoring with satellite remote sensing.

Keywords: satellite remote sensing; sensors; forest fire monitoring; forest fire brightness temperature; forest fire smoke

Citation: Zheng, Y.; Zhang, G.; Tan, S.; Feng, L. Research on Progress of Forest Fire Monitoring with Satellite Remote Sensing. *Agricultural & Rural Studies*, 2023, *1*, 0008. *https://doi.org/10.59978/ar01020008*

Received: 27 July 2023
Revised: 7 August 2023
Accepted: 25 August 2023
Published: 5 September 2023

1. Introduction

The introduction should briefly place the study in a broad context and highlight why it is important. It should define the purpose of the work and its significance. The current state of the research field should be carefully reviewed and key publications cited. Please highlight controversial and diverging hypotheses when necessary. Finally, briefly mention the main aim of the work and highlight the principal conclusions. As far as possible, please keep the introduction comprehensible to scientists outside your particular field of research. Forest fire is a worldwide natural disaster. As it can destroy forest resources and cause global environmental pollution, governments are paying more attention to it. Forest fires occur randomly and unexpectedly, therefore timely monitoring of forest fires helps to reduce the loss caused by them.

With the vigorous development of satellite remote sensing technology, satellite remote sensing has become a frequently used tool for forest fire monitoring. When monitoring forest fires, relying on "low and medium altitude" tools is not only high-cost and technically difficult, but leaves blind spots for forest fire monitoring (Shu et al., 2005). However, satellite sensors can provide information with different spatial resolutions and different spectra on a global scale (Chuvieco et al., 2020), with the advantages of large monitoring range, short response time and strong anti-interference ability. They can effectively make up for the shortcomings, regarding the small monitoring range, poor stability and high cost, of "low altitude" cameras in forest areas (Barmpoutis et al., 2020; Wu et al., 2020), and solve problems of being subject to air control, weather conditions and short range of "mid-altitude" Unmanned Aerial Vehicles (UAVs) (Howard et al., 2018). Thus, satellite sensors meet the need for timely monitoring of forest fires in large areas (Qin et al., 2015). There are currently two main ways of using remote sensing technology for forest fire monitoring. One is to obtain the brightness temperature information through the infrared band of satellite remote sensing. The flames produced by forest fires have distinctive radiative characteristics, contrasting markedly with the background radiation of surrounding areas (Sun et al., 2020). The other is to detect forest fire smoke produced during forest fires. which can detect forest fires earlier than brightness temperature detection. In the early stages of forest fires, the incomplete combustion of

combustible materials can produce large amounts of smoke (Zheng et al., 2023), which can help to detect forest fires earlier than monitoring through brightness temperature detection.

This paper reviews the progress of research on satellite remote sensing for forest fire monitoring. We begin with an overview of the development and properties comparison of meteorological satellites and sensors commonly used for forest fire monitoring (Section 2). We then compared and analyzed methods of monitoring forest fires using brightness temperature detection and smoke detection (Section 3). Finally, we discuss the existing problems and future directions of satellite remote sensing monitoring for forest fires (Section 4). The above studies can provide useful references for the selection of satellites for forest fire monitoring, the adoption of monitoring methods, and the improvement of forest fire monitoring accuracy to point the way to further research.

2. Overview and Application of Meteorological Satellites and Sensors for Forest Fire Monitoring

2.1. Overview of Meteorological Satellites and Sensors for Forest Fire Monitoring

In recent years, with the advancement of remote sensing technology, the launch of a large number of remote sensing satellites and the low cost of usage, scholars worldwide have studied satellite remote sensing monitoring for forest fires.

At present, domestic and foreign mainly use meteorological satellites to monitor forest fires. According to their orbits, meteorological satellites are divided into two main categories: Polar Orbit Meteorological Satellite and Geostationary Meteorological Satellite. The capabilities' comparison of the two satellites is shown in Table 1. The Geostationary Meteorological Satellite, also known as Geosynchronous Satellite, usually orbits at an altitude of around 36,000 km, matching the speed of the Earth's rotation. The Geostationary Meteorological Satellites currently in orbit include China's Fengyun-2 (FY-2) and Fengyun-4 (FY-4), the US GEOS series, Japan's Himawari-9, Korea's GEO-KOMPSAT-2A(GK2A), etc. The Polar Orbit Meteorological Satellite, also known as Sun-synchronous Orbit Satellite, usually orbits at an altitude of around 500 to 800 km, travelling along a near-polar orbit between the North Pole and the South Pole. Due to the large inclination angle of the orbit of such satellite, it can only make earth observations during each fly-by. The Polar Orbit Meteorological Satellites presently in orbit include China's Fengyun-3 (FY-3), the US NOAA and the European Metop series, etc.

Table 1. The capability comparison between Polar Orbit Meteorological Satellite and Geostationary Meteorological Satellite.

Capability	Geostationary Meteorological Satellite	Polar Orbit Meteorological Satellite
Providing Continuous Observation Data	√	×
Temporal Resolution	High	Low
Spatial Resolution	Low	High
Enabling Continuous Monitoring of the Same Area over a Long Period	√	×
Orbital Position	Settled	Unsettled
Orbital Period	Long	Short

Satellite systems are based on sensors (Rafik et al., 2020). acquire images at multiple spatial and temporal resolutions by carrying different sensors. Satellites acquire images with multiple spatial and temporal resolutions by carrying different sensors. Sensors on board Geostationary Meteorological Satellites that are commonly used for forest fire monitoring include Advanced Himawari Imager (AHI), Advanced Baseline Imager (ABI), Advanced Geostationary Radiation Imager (AGRI), etc. Sensors on board Polar Orbit Meteorological Satellite include Advanced Along-track Scanning Radiometer (ATSR), Advanced Very High Resolution Radiometer (AVHRR), Moderate-resolution Imaging Spectroradiometer (MODIS), Visible Infrared Imaging Radiometer (VIIRS), etc.

The world's first meteorological satellite is the US TIROS-1, which was launched in 1960 and transmitted back the first satellite cloud images (Lv et al., 2003). From 1975-2010, the US launched four generations of the GOES series geostationary satellites. The temporal resolution, number of channels and imaging speed of the satellites have been gradually increased, and monitoring capabilities have been enhanced (Fang, 2014). Meanwhile, the third generation US Polar Orbit Meteorological Satellite, NOAA, went into operation in 1978, equipped with the AVHRR (Lu & Gu, 2016). In 2011, the SNPP satellite was successfully launched, primarily carrying the VIIRS with operational microlight detection capability.

The development of meteorological satellites in Europe began with the first Geostationary Meteorological Satellite Meteosat-1, launched in 1997. Europe's first Polar Orbit Meteorological

Satellite, Metop-A, was launched in 2006. Despite its late start, the satellite had a high technological starting point, with rapid advances in its imaging quality and the Infrared Atmospheric Sounding Interferometer (IASI) on board (Lu & Gu, 2016).

With the improvement of satellite remote sensing technology, Japan launched the Geostationary Meteorological Satellite Himawari-8 in 2014, equipped with the AHI, which is mainly used for the monitoring of natural disasters (He et al., 2020). And then the Himawari-9 was launched in 2016 and was to be in service in 2022.

China is one of the few countries in the world with both Geostationary Meteorological Satellites and Polar Orbit Meteorological Satellites (Tang et al., 2016). China has launched eight Polar Orbit Meteorological Satellites and nine Geostationary Meteorological Satellites, completing the transformation of meteorological satellites from experimental applications to operational services (Sun et al., 2020). In addition, China's High-resolution Earth Observation System was started at 2010. And GF-4 is China's first relatively high-resolution remote sensing satellite (Sun et al., 2020).

2.2. Applications of Meteorological Satellites and Sensors for Forest Fire Monitoring

As early as the 1980s, techies began being abuzz about research on forest fire monitoring using remote sensing technologies. With the advantages of the vast synchronous observation area, broad detection band and rapid sampling time, the AVHRR sensor equipped on NOAA satellite (NOAA/AVHRR), since its successful launch in 1978, has become the main data source for domestic and international scholars using satellites to monitor forest fires. Flannigan and Haar attempted to use NOAA/AVHRR to monitor the forest fire in north-central Alberta in June 1982. However, experiment results indicated that the satellite's visual field is susceptible to clouds and smoke, making it difficult to monitor forest fires (Flannigan & Haar, 1986). In 1996, Yi et al. conducted a simulation experiment based on NOAA/AVHRR data for the southwest forest of China, where forest fires occurred frequently and were difficult to monitor, and their results were basically at a practical level (Yi et al., 1996). In 1997, Pozo et al. compared forest fire information in southeastern Spain obtained by AVHRR Band 3 and 4, with real information of forest fires provided by the Andalusian Regional Government Environmental Directorate (Pozo et al., 1997). They verified the advantages of using remote sensing techniques for forest fire monitoring in forests containing complex features that are difficult to monitor fires by other tools. In 2012, to eliminate fire signal noise due to solar reflections, He et al. introduced a new test to filter forest fire detection results based on the 2004 mid-infrared band data of NOAA/AVHRR, reducing the number of false fire detections by 27.1% (He & Li, 2012). During this period, the accuracy of forest fire monitoring using remote sensing still needed to be improved, but the greater value of forest fire monitoring using remote sensing technology was initially confirmed.

At the beginning of the 21st century, the MODIS sensor began collecting remote sensing information as part of NASA's Earth Observing System (EOS) in 1999 on board the Terra satellite and in 2002 on board the Aqua satellite. MODIS sensor has specific bands and fire products for fire monitoring and has therefore become a research hotspot in the field of remote sensing monitoring for forest fires during this period. In 2002, Justice, a professor of the University of Maryland, and Kufuman, a staff of Goddard Space Flight Center, led a research team to conduct a simulation experiment on forest fire monitoring in African forests using MODIS data, and validated the results of the simulation experiment using the Advanced Spaceborne Thermal Emission and Reflection Radiometer (ASTER) data (Justice et al., 2002). In 2003, Giglio et al., members of the above research team, tested the effectiveness of MODIS data for forest fire detection and found that MODIS data were subject to interference from water et al. resulting in high false alarm rates for forest fire monitoring and difficulties in detecting small or low-temperature forest fires (Giglio et al., 2003). In 2007, they used MODIS data to compensate for the limitations of the Visible and Infrared Scanners in detecting forest fires in tropical and subtropical regions due to differences between day and night (Giglio, 2007). In 2016, Giglio et al. studied the 6th Version of MODIS data (collection 6) compiled by NASA, which improved the forest fire detection performance of MODIS by reducing false alarms caused by small bare land and missed alarms caused by thick smoke cover occurred in Version 5 data (Giglio et al., 2016). In 2004, Qin et al. detected forest fires in China, with an accuracy of 80%, based on band characteristics of MODIS (Qin & Yi, 2004). Furthermore, scholars collected information from higher spatial resolution sensors to validate the performance of MODIS for forest fire monitoring. In 2008, Schroeder et al. analyzed the MODIS fire detection product MOD14 using remote sensing imagery collected from the ASTER sensor and ETM+ sensor with the spatial resolution of 30m and showed that MODIS has difficulty detecting fires under the tree canopies (Schroeder et al., 2008). During this period, the complex environmental background of forests had a greater impact on forest fire monitoring using MODIS and required reliability verification through extensive experiments. But the feasibility and prospect of MODIS for forest fire monitoring was confirmed. Until 2019, MODIS was still used as an important tool for forest fire

monitoring, for example, Ba et al. used MODIS images for scene classification to detect early forest fires (Ba et al., 2019).

With the launch of more remote sensing satellites and sensors, satellites and sensors for monitoring forest fires tend to be diversified. In 2008, Giglio et al. used data from the ASTER sensor, carried on the Terra satellite, to detect the forest fire radiative power (FRP) to measure the forest fire intensity (Giglio et al., 2008). In 2011, He et al. combined data from the same temporal phase of ASTER and MODIS for forest fire detection to eliminate the effects of solar contamination and thermal-path-radiance, improving the accuracy of forest fire detection, but with a higher rate of detecting errors in deforested areas (He & Li, 2011). European ATSR sensor, onboard ERS satellites, provides multi-angle, near real-time thermal infrared measurement information for forest fire monitoring (Arino et al., 2012). In 2012, Arino et al. analyzed the time series of night fires provided by ATSR and verified that the ATSR data correlated well with MODIS data (Arino et al., 2012). As the Sea and Land Surface Temperature Instrument (SLSTR) sensor on the Sentinel-3 has similar characteristics to the ATSR and has a wider scanning area, Arino et al. proposed the use of the SLSTR as the supplement to the night fire information collected from ATSR and MODIS to address information saturation during the day (Arino et al., 2012). In 2012, Wooster et al. developed and tested a theoretical forest fire detection algorithm for SLSTR using MODIS and ASTER data and confirmed its high detection accuracy for small or low-temperature forest fires (Wooster et al., 2012). However, this experiment lacked validation using real SLSTR images. With the launch of the Sentinel-3 satellite with the SLSTR sensor in 2014, Xu et al. collected real images from SLSTR in 2020 to complement and update previous forest fire monitoring data and compared them with fire products from MODIS and VIIRS (Xu et al., 2020). Furthermore, in 2021, they confirmed that the F1 Band of SLSTR is of great application for forest fire detection (Xu et al., 2021). And they predicted that data from Sentinel-3/SLSTR could become the main source for midday and night forest fire detection in the future.

In 2011, the first VIIRS sensor was successfully launched on board the SNPP satellite, carrying two sets of independent multispectral Bands and providing images of global coverage. In 2014, Schroeder et al. developed a fire detection algorithm using VIIRS, which has superior mapping capabilities to MODIS (Schroeder et al., 2014). In 2017, Zhang et al. jointly used I-band at a spatial resolution of 375 m and M-band of 750 m from VIIRS to detect fire and its radiated power (FRP) for the first time, and were able to effectively detect small fires (Zhang et al., 2017). The Chinese GF-4 satellite has high temporal resolution and moderate spatial resolution, making it suitable for high-frequency forest fire monitoring. In 2021, Zhou et al. discovered that the Infrared Spectrum (IRS) sensor carried by the GF-4 has a band that is sensitive to forest fires. And they used this band for spatial alignment with MODIS and carried out forest fire monitoring experiments at Qinghai Lake and Siling Lake, obtaining a high degree of radiometric calibration agreement (Zhou et al., 2021). In 2022, Zhang et al. used data from the Panchromatic and Multispectral (PMS) sensor and IRS sensor carried by GF-4 to eliminate high-temperature anomalies when forest fires were not occurring, and used MODIS data to verify feasibility (Zhang et al., 2022). During this period, greater progress was made in forest fire monitoring using new satellites and sensors.

To achieve real-time monitoring of forest fires and improve the accuracy, scholars at home and abroad have devoted to research on multi-source satellite remote sensing monitoring for forest fires. In 2022, Tian et al. considered that remote sensing data from a single source could not meet the needs of forest fire monitoring, thus they combined Planet, Sentinel-2, MODIS, GF-1, GF-4 and Landsat-8 satellites to validate forest fires that occurred in March 2020 in Liangshan Yi Autonomous Prefecture, Sichuan Province, and the monitoring efficiency was significantly improved (Tian et al., 2022). In 2023, Yin et al. used GF-6 Wide Field of View (WFV) data and FY-3D Medium-Resolution Spectral Imager (MERSI) data to effectively identify forest fires in Anning, Yunnan Province, on 9 May 2020 (Yin et al., 2023).

3. Forest Fire Monitoring Methods with Satellite Remote Sensing

Nowadays, many countries have established satellite remote sensing systems for forest fire monitoring (He et al., 2022), and scholars have developed and improved a variety of forest fire monitoring algorithms for different remote sensing satellites. Forest fire monitoring algorithms can be mainly classified into Brightness Temperature detection-based forest fire monitoring methods and forest fire smoke detection-based forest fire monitoring methods.

3.1. Forest Fire Monitoring Methods Based on Brightness Temperature

The most common and basic method used in research on forest fire monitoring with satellite remote sensing technology is Brightness Temperature (BT) detection method. This method uses BT differences between forest fires and other categories of land cover in the Middle Infrared (MIR) and Thermal Infrared (TIR) channels of remote sensing imagery to construct forest fire detection

algorithms, and then combines the reflective properties of the visible or Near-infrared (NIR) channels to exclude spurious detections of forest fires.

3.1.1. Brightness Temperature Detection Based on Bi-spectral Method

Remote sensing infrared is highly sensitive to thermal radiation (Li & Jia, 2018). Forest fires occur at high temperatures, therefore the use of remote sensing infrared to discriminate the BT anomaly of land covers can be effective in detecting forest fires.

In 1981, Dozier (1981) proposed the bi-spectral detection method to calculate the temperature and area of sub-pixel fire points using MIR and TIR data from AVHRR, paying the way for forest fire monitoring using remote sensing infrared data. However, this method is premised on the assumption that there are only two temperature fields, the flame and the background, and both temperature fields have the same temperature (Dozier, 1981). This assumption is usually unrealistic and limits the applicability of the method. On this basis, scholars have made further improvements to the bi-spectral detection method. In 1990, Kaufman et al. (1990) improved the bi-spectral method by using AVHRR data to deal with the problem of high environmental impact during forest fire detection in the daytime. In 2006, Zhukov et al. (2006) used Dozier's bi-spectral method to summarize and analyze the mission experience of the bi-spectral infrared detection (BIRD) experimental small satellite and confirmed that it is more reasonable to quantitatively evaluate forest fires in terms of FRP than the effective fire temperature or the effective fire area. In 2008, Eckmann et al. (2008) proposed the multiple endmember spectral mixture analysis (MESMA) based on the bi-spectral method to address the uncertainties in the detection of fire size and temperature using MODIS et al. They estimated the size and temperature of each fire sub-pixel by pre-generating a library of fire end-members and background end-members at different temperatures to decompose the fire pixels (Eckmann et al., 2008). In 2013, Peterson et al. (2013) used MIR and TIR data from MODIS to develop a sub-pixel-based FRP algorithm, which incorporated a radiative transfer model to eliminate solar effects and was applied to monitoring large forest fires in California, bridging the gap of earlier studies (Dozier, 1981) where the algorithm effect could not be verified due to the lack of real data. Given the rapid replacement of satellites and sensors, this algorithm was designed to be suitable for other sensors with similar spectral properties (Peterson et al., 2013). In 2014, Giglio and Schroeder (2014) proposed a rejection test before using the bi-spectral method. They filtered detection errors caused by background interference on the basis of prior knowledge and performed a feasibility assessment using MODIS data over 10 years (Giglio & Schroeder, 2014) to further improve the application of the bi-spectral method in forest fire detection.

3.1.2. Brightness Temperature Detection Based on Threshold Method

The threshold method is based on the analysis and study of prior knowledge of an area or season to select the threshold for fire point identification. When the BT of one or more spectral channels exceeds the pre-selected threshold, it is considered to be the fire point pixel. The threshold methods used for forest fire monitoring can be divided into single-channel threshold (SCT) method and multi-channel threshold (MCT) method.

The SCT method relies only on the BT value T_4 in the MIR channel. If the BT value T_4 of a pixel is greater than the pre-selected threshold, this pixel is defined as having the fire point. In 1991, Setzer and Pereira (1991) carried out a study of forest fire detection in tropical forests, using a digital non-supervised clustering algorithm to set pixels in Band 3 of AVHRR with the radiometric temperature above 460°C as fire points. As AVHRR lacks a dedicated channel designed for fire detection, scholars attempted to migrate SCT to other sensors and demonstrated its feasibility, for example, Arino and Rosaz (Arino et al., 1999) applied SCT to ATSR for forest fire detection. SCT is better suited to areas with low temperatures or low solar reflection (Hua & Shao, 2017). And it is more effective in detecting forest fires at night, but during the day there are more detection errors due to the influence of solar reflection caused by surface bright objects.

To solve the problems of SCT, MCT is pre-processed by eliminating clouds, compensating for solar radiation generated by ground reflections et al. to improve the effectiveness of MIR and then rules out spurious forest fires by comparing the BT difference in channels between MIR and TIR (Li et al., 2001). In 1990, Kaufman et al. (1990) demonstrated that if in a pixel, the channel 3 (MIR) temperature T_3 and the channel 4 (TIR) temperature T_4 acquired from AVHRR simultaneously satisfy the following criteria, fires are defined in this pixel.

$$T_3 \geq 316K,\ T_3 \geq T_4 + 10K,\ T_4 > 250K \quad (1)$$

In Equations (1), T_3 represents the MIR temperature value, T_4 represents the TIR temperature value, and K represents the unit of temperature.

In 1994, Kennedy et al. (1994) upgraded the forest fire monitoring system in West Africa, based on Kaufman's study (Kaufman et al., 1990), by optimizing the threshold value for channels 3 and 4 and increasing the difference between T_3 and T_4 to further eliminate spurious forest fires. In 2004, Pu et al. (2004) used a series of threshold tests to eliminate spurious fire alarms caused by warm backgrounds (e.g. bare ground), highly reflective clouds, and surface bright objects.

The threshold method is highly territorial and is only applicable to local areas, which is difficult to cope with forest fire monitoring in different geographical areas or different seasons. Therefore, scholars need to select appropriate thresholds according to characteristics of different areas. For example, in 2004, Li et al. (2000) developed a forest fire monitoring threshold method for the unique environment of northern Canada, which discriminated all potential forest fire pixels while removing spurious forest fire pixels. This algorithm can detect most real forest fires without thick cloud interference, laying the foundation for local forest fire satellite monitoring systems. In response to the problem of poor adaptability of fixed-threshold methods, scholars have investigated forest fire monitoring algorithms with adaptive thresholds (He & Liu, 2008; Liu et al., 2020). However, the missed detection rate of forest fires was high.

3.1.3. Brightness Temperature Detection Based on Contextual Method

The threshold method uses multi-spectral information to detect forest fires step by step for individual pixels without taking into account the effect of surrounding pixels, i.e. the environmental background changes, on forest fire detection.

To solve this problem, in 1990, Lee and Tag (1990) proposed a contextual method, based on MCT, extending to spatial information. They set up a 3x3 pixel matrix centered on the target pixel, calculated the background temperature according to surrounding pixels, and compare it with the mean BT value within the matrix to discriminate the presence of fires in the target pixel (Lee & Tag, 1990). This method can be flexibly and effectively applied to scenes where the surface temperature varies considerably. In 1996, Flasse and Ceccato (1996) proposed a fire detection contextual algorithm. They used the threshold method to detect potential fires using AVHRR data, analyzed the neighboring pixel background, and then compared the potential fires and their backgrounds by the BT properties of background pixels to confirm the real fires (Flasse & Ceccato, 1996). This method was tested in tropical rainforests and proved to be suitable for detecting forest fires in different areas at different times. However, a limitation revealed by this study is that in 1999, Nakayama et al. (1999) found that when this method was applied to large burning areas of fire, the central point was wrongly detected as a non-fire point. In 2007, Li et al. (2007) proposed an enhanced contextual algorithm for detection of forest fire (ECFDA), which improved the neighboring pixels confirmation algorithm of potential fires by optimizing the size of the background matrix, and improved the criteria selection algorithm for real fires by introducing the concept of BT gradient. The ECFDA is sensitive to the detection of small-scale fires, but cannot be applied to large-scale forest fires.

MODIS has dedicated fire detection channels and is used more often in forest fire monitoring studies. In 2003, Giglio et al. (2003) proposed an improved contextual fire detection algorithm for MODIS, known as version 4, which provides considerable improvement over previous versions. The version 4, improving the detecting sensitivity to small fires and cold fires, classified pixels examined by MODIS as one of the following classes: missing data, cloud, water, non-fire, fire, or unknown (Giglio et al., 2003). In 2008, Schroeder et al. (2008) tested the performance of the MODIS fire product using ASTER and ETM+ images in Brazilian Amazonia by quantifying commission and omission error and improved contextual detection algorithms using BT profiles to reduce the commission error rate in tropical forests. To exclude the detection errors caused by small forest bare areas, smoke obscuration, etc. and to reduce the commission error rate of fire detection (Wang et al., 2009; Wang et al., 2007), in 2016, Giglio et al. (2016) improved the detecting algorithm using collection 6 MODIS data by introducing the forest clearing rejection test.

However, in 2006, Zhou and Wang (Zhou & Wang, 2006) demonstrated that the theoretical algorithm for forest fire detection using MODIS data, when applied to Chinese forests, misidentified non-forest fire areas with image noise interference as forest fires. Therefore, they used the contextual method to analyze fire points and their neighboring pixels of nine forest fire events in China, and improved the noise point filtering criteria to effectively eliminate the noise interference points (Zhou & Wang, 2006).

As the performance of satellites and sensors continues to improve, scholars have attempted to address problems of MODIS in forest fire detection using newer satellites and sensors. In 2014, Schroeder et al. (2014) proposed an improved contextual method based on VIIRS to eliminate spurious fire identification caused by daytime water bodies, sun glints, bright objects, etc. In 2017, Lin et al. (2017) proposed the use of infrared channel slope to analyze the difference between TIR and MIR information collected from FY-3/VIRR and combined the contextual fire detection method and dynamic threshold fire detection method for selecting fire pixels. This method could better suit

the global environment for fire detection. In 2020, Yin et al. (2020), based on the FY-3/MERSI data, improved the dynamic threshold method and the contextual method for forest fire detection, by setting the threshold criteria for the BT value in the MIR, which achieved the fast and effective detection of both large and small-scale fires. The contextual method detects forest fires based on the difference between the target and the background within the adaptive window. It expands the application range of algorithms and improves the accuracy of forest fire detection, but the application flexibility is limited by regional differences in monitoring.

3.1.4. Brightness Temperature Detection Based on Deep Learning Method

In recent years, scholars have paid increasing attention to the application of Deep Learning methods in various fields, including the field of forest fire monitoring, and have made great progress. The more commonly employed methods include Neural Networks (NN), Decision Tree and its ensemble learning algorithms, and Support Vector Machine (SVM), etc. In 2000, Arrue et al. (2000) constructed the "False Alarm Reduction System" for forest fire monitoring using Back Propagation (BP) NN, Radial Basis Function Network, and Dynamic Learning Vector Quantizer to calculate the probability values of forest fires using satellite infrared images. In 2009, Maeda et al. (2009) used the BP algorithm to train artificial neural networks (ANN) of different structures to detect forest fires in high-danger areas of the Brazilian Amazon using MODIS imagery, achieving 90% accuracy. This algorithm allowed for fast training of samples while maintaining detection accuracy for forest fires (Abid, 2021).

The BT detection method for forest fires is mainly implemented by satellites and sensors with TIR channels, such as MODIS, AVHRR, FY series, etc., but it is not suitable for satellites and sensors with only a single MIR channel for forest fire detection.

3.2. Forest Fire Monitoring Methods Based on Forest Smoke Detection

In the early stage of forest fires, the low temperatures from combustion make it difficult for satellites to receive sufficient infrared radiation for imaging. However, insufficient burning of combustible materials produces large amounts of smoke, and detection of forest fire smoke by satellite can lead to earlier detection of forest fires. Currently, there are fewer domestic and international studies on smoke detection using satellites to detect forest fires.

3.2.1. Forest Smoke Detection Based on Visual Identification Method

The visual identification method is the early forest fire smoke detection method. It uses computers to generate true-color or false-color images of forest fire smoke to visualize the shape and scale of forest fire smoke (Chung & Le, 1984; Ferrare et al., 1990), and then manually interprets the area and diffusion direction of the forest fire smoke. The visual identification method is intuitive and convenient, but it relies on artificial operation, which is not conducive to the automatic processing of forest fire smoke information, and the accuracy of smoke identification is low. To improve the accuracy of smoke detection and reduce the subjective dependence of the visual identification method, scholars have used infrared information in combination with the threshold method for forest fire smoke detection.

3.2.2. Forest Smoke Detection Based on MCT Method

MCT detects smoke pixels by utilizing the rich land cover information in remote sensing images, setting criteria based on characteristics of land covers such as clouds, water bodies, vegetation, etc., combining the spectral features of multiple infrared channels (Xie et al., 2007), and excluding non-smoke pixels by different thresholds.

In 2007, Chrysoulakis et al. (2007) identified the center of forest fire smoke, based on multi-temporal and multi-spectral features of remote sensing imagery, by comparing the anomalous pixels in the NIR channel and combining them with the Normalized Difference Vegetation Index (NDVI) index, and then used spectral and spatial filters to spatially extend the center to the entire area covered by the forest fire smoke plume. The proposed algorithm provided accurate estimates of the spatial characteristics of the forest fire smoke plume (Chrysoulakis et al., 2007). To improve the sensitivity of detecting small fires and low-temperature fires, in 2007, Wang et al. (2007) identified smoke pixels using the smoke mask technique based on information from the TIR channel and solar reflectance channel, and used the contextual method to detect missed forest fire events accompanied by significant smoke plumes. In addition, in 2008, Peng et al. (2008) set a forest fire smoke discrimination threshold based on the characteristics of tropical rainforests, and improved forest fire monitoring algorithm based on version 4 MODIS data by using the adaptive window adjustment technique of the smoke plume mask. This algorithm improved sensitivity to detection of small forest fires at low-temperature forest fires, especially fires with large scan angles (Peng et al., 2008).

However, smoke has no fixed spectral characteristics and shows similar features to clouds, dust and haze on the satellite spectral bands, thus making it difficult to distinguish them, resulting

in the MCT method not being able to effectively employ smoke detection for early warning of forest fires.

3.2.3. Forest Smoke Detection Based on Deep Learning

With the continuous launch of satellites, real-time access to remote sensing data has become a reality, and there is an urgent need to develop more effective and intelligent algorithms for the automated detection of forest fire smoke based on massive remote sensing data. In 2014, Li et al. (2014) separated smoke from other land cover types in satellite imagery and developed a smoke identification algorithm combining Fisher linear Discrimination and K-means clustering, which was validated using forest fire events in Greater Khingan Mountains (China), Amur Region (Russia), Australia and Canada, confirming that the algorithm could capture both heavy and dispersed forest fire smoke. In 2015, Li et al. (2015) trained and debugged the BPNN with samples acquired from MODIS data of three forest fire events occurring in China, Northeast Asia, and Russia, and verified that the algorithm was effective in capturing thick and thin smoke over land. In 2020, Qin et al. (2020) constructed a Decision Tree Identification model for forest fire smoke based on the reflectance of forest fire smoke in the visible and NIR channels of GF-1 and GF-2 satellite imagery. In 2023, Li et al. (2023) improved the subpixel mapping method based on the Random Forest model for identifying and locating forest fire smoke.

Scholars have further improved deep learning algorithms to address problems that have arisen in forest fire smoke detection research. The uneven spatial distribution of smoke and the complexity of its background result in smoke being difficult to detect due to its inconspicuous features in satellite imagery. To distinguish forest fire smoke from the background scene, in 2019, Ba et al. (2019) optimized the CNN, which improved the recognition accuracy of CNN for forest fire smoke based on remote sensing imagery, by introducing spatial and channel-wise attention mechanisms, and sorting out the spatial characteristic information of remote sensing images collected from medium- and high-resolution satellites. The acquisition of remote sensing image data containing forest fire smoke is limited by the constraints of satellite lifetime in orbit, geographical coverage, etc., which makes it difficult to collect a sufficiently large-scale dataset of forest fire smoke (Zheng et al., 2023). In 2018, ZHANG et al. (2018) performed forest fire smoke detection experiments based on the Faster R-CNN model, inserting real and simulated smoke into forest images to generate synthetic forest fire smoke samples. The results demonstrated that the method solves the problem of insufficient data while eliminating the need for sample labeling. In 2023, Sathishkumar et al. (2023) selected the Xception model as the optimal model, and fine-tuned it using the Learning Without Forgetting (LwF) algorithm to suit the new task. As a result, they investigated Transfer Learning of pre-trained models for forest fire smoke monitoring, which increased the data amount and decreased the long training time (Sathishkumar et al., 2023). In 2023, Zheng et al. (2023) used Himawari-8 satellite remote sensing images to construct a small-scale dataset and proposed a forest fire smoke detection model (SR-Net) combining CNN and Lightweight Vision Transformer (Lightweight ViT). The model employed CNN for inductive bias and the Global Attention Mechanism of Lightweight ViT to generate a lightweight forest fire smoke detection model with higher accuracy while consuming fewer training resources (Zheng et al., 2023).

4. Discussion and Conclusion

This study statistics and analyses research on satellite remote sensing for forest fire monitoring in recent decades based on bibliometric analysis, using the co-occurrence frequency of textual data located in titles, abstracts and keywords. We extracted data from the Web of Science search tool which contains a full range of papers. The input qualifiers were “remote sensing” and “forest fire monitoring”, and a total of 999 papers were retrieved (the data obtained up to 20 July 2023). We then used VOSviewer software to visually represent extracted data from 999 papers (Figure 1).

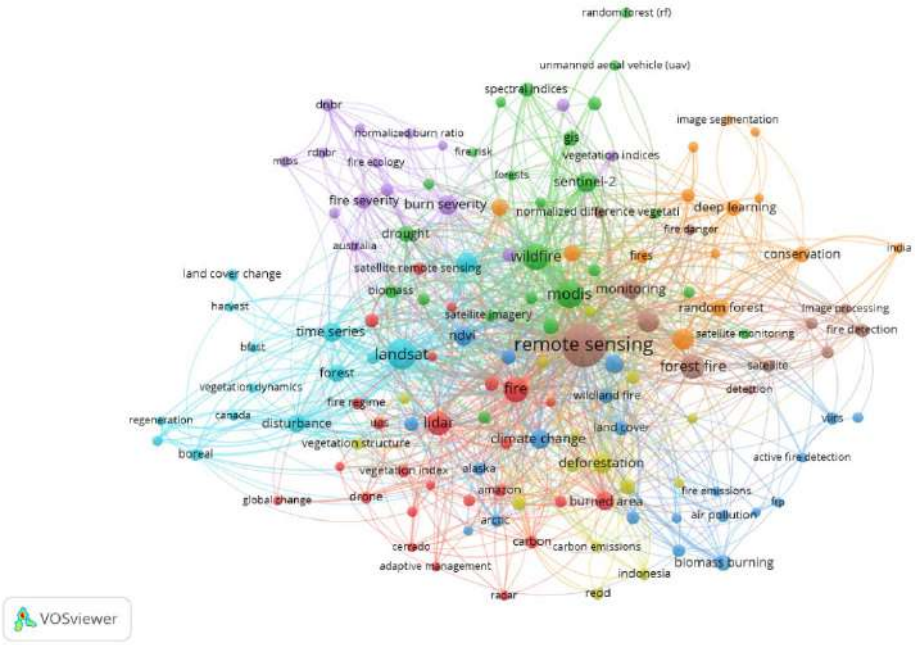

Figure 1. Data visualization based on keywords collected from Web of Science.

The results of the data network visualization show that satellites used more in forest fire satellite monitoring studies are Landsat, MODIS, Sentinel, etc., which all have obvious advantages and limitations in forest fire detection. Landsat provides detailed information on the spatial distribution of fires, but has a long revisit period (every 16 days) and a small geographical coverage area. MODIS has channels and products specifically designed for fires, with a resolution of the highest 250m and high detection accuracy, but the temporal resolution is not high enough to detect fires in time and then alarm it. Moreover, the methodology for satellite monitoring of forest fires shown in Figure 2 involves more terms such as “machine learning”, “time series” and “spectral indices”. It indicates that the research hotspots in forest fire monitoring focus on the introduction and development of Deep Learning in forest fire monitoring (machine learning), the improvement of the temporal efficiency of medium- and high-spatial-resolution satellites and sensors (time series), the improvement of monitoring algorithms for forest fires using the information of infrared channels (spectral indexes), and so on.

Figure 2. Publication numbers of research on satellite monitoring for forest fires in the Web of Science Core Collection database from 2009 to 2023. (The data obtained up to 20 July 2023.)

As the systems of satellites, sensors and forest fire monitoring technology, such as time series techniques to process data, deep learning methods, etc. (Santos et al., 2021), advance by leaps and

bounds, and the free remote sensing imagery springing up, the attention to satellite remote sensing monitoring of forest fires has gained a strong momentum. From the data provided by Web of Science, it can be seen that 2018 to 2023 (the data obtained up to 20 July 2023) are the most representative five years for domestic and international research on forest fire satellite remote sensing monitoring. Over these five years, satellite remote sensing monitoring algorithms for forest fires have become increasingly mature, but the current algorithms still have their own advantages and disadvantages, as shown in Table 2.

Table 2. Advantages and disadvantages of satellite remote sensing monitoring algorithms for forest fires.

Algorithms	Advantages	Disadvantages
Bi-spectral Method	Laying the theoretical foundations.	Based on unrealistic assumptions and lack of validation by actual data.
SCT Method	Simple technology.	Large daytime error.
MCT Method	High stability.	Not adapted to diverse environmental backgrounds.
Contextual Method	Highly adaptable to the environment.	High rate of missed and wrong judgements for small fires and low-temperature fires.
Deep Learning Method	Highly automated.	Relatively complex methods and techniques.

The review of literature revealed the following characteristics of satellite remote sensing monitoring of forest fires:

(1) Satellite remote sensing monitoring of forest fires is strongly influenced by the temporal and spatial resolution of satellites and sensors. It is difficult for current satellites and sensors to simultaneously fulfill the requirements of high temporal resolution and high spatial resolution for forest fire monitoring. Geostationary Meteorological Satellites have high temporal resolution but low spatial resolution, while Polar Orbit Meteorological Satellites have low temporal resolution but higher spatial resolution. Therefore, scholars at home and abroad have improved various algorithms for satellite remote sensing monitoring for forest fires, and are dedicated to making up for shortcomings of forest fire monitoring in time and space. For example, Himawari-8 can acquire surface information every 10 minutes, which is suitable for real-time monitoring of forest fires (Zhang et al., 2023), but suffers from the problem of low spatial resolution of pixels and large differences in the information contained in pixels. Therefore, Himawari-8 is more suitable to use deep learning algorithms for forest fire monitoring (Kang et al., 2022). On the contrary, MODIS has low temporal resolution and cannot rapidly detect forest fires, but it has high spatial resolution and can more accurately detect forest fires (Feng & Zhou, 2023).

Cloud masking impacts the effectiveness of forest fire monitoring. Current cloud identification algorithms have evolved to automatically and intelligently identify clouds using machine learning algorithms (Bing et al., 2023), but there are fewer studies applying them to data preprocessing for forest fire monitoring. Cloud masking can increase the satellite's reflectance in the visible band and decrease the BT value in the infrared band (Xie et al., 2018). Current cloud identification algorithms in forest fire monitoring mainly use the threshold method (Xu & Zhong, 2017), but the method is greatly affected by different time points and environments. Cloud identification using machine learning algorithms is more flexible than the threshold method, which has a simpler structure and higher accuracy, however, it requires manual extraction of training samples from different scenes (Tsagkatakis et al., 2019), and it is difficult for a single satellite or sensor to meet the number requirement of training samples.

Satellite monitoring algorithms for forest fire work to improve the sensitivity of monitoring small fires and fires with low bright temperatures. Due to the small burning area, insufficient combustion, low flame temperature and other features at the early stage of forest fires, and canopy shading, it leads to missed judgment and false judgment when using satellites and sensors to detect small fires or low-temperature fires.

Given the above characteristics, the future development trends of satellite remote sensing monitoring for forest fires are as follows:

(1) Using multi-source satellites and sensors to improve the spatial and temporal efficiency of forest fire monitoring. For instance, the combination of GF-6 WFV and FY-3 MERSI enables multi-aspect capture of forest fire information (Yin et al., 2023). The spatial resolution of GF-6 WFV data is 16m, the radiometric resolution is 12bit, its coverage is wide, and its imaging quality is high. FY-3 MERSI's monitoring scope is broad, observation frequency is dense, and it is sensitive to high-temperature heat reservoirs on the ground (Zheng et al., 2013). In addition, recent years have witnessed a spurt of progress in satellites and sensors. Research could incorporate an increasing number of advanced satellites for forest fire monitoring, such as China's HJ-1A and 1B satellites which can provide data up to 30m resolution (Sun et al., 2010), and South Korea's GK2A

satellite carrying an AMI sensor, which can provide a spatial resolution of up to 500m in the visible band, has a comparatively higher radiometric and spectral resolution, and has improved imaging time up to 10 minutes (Chen et al., 2022).

(2) Migrating and improving deep learning-based cloud detection algorithms to make them suitable for data preprocessing of forest fire monitoring. Deep learning captures more comprehensive and deeper features of cloud on remote sensing imagery, which can also be improved to be trained with small sample datasets (Zheng et al., 2023). Among the deep learning algorithms, CNN can classify and detect clouds with high accuracy (Segal-Rozenhaimer et al., 2020; Yu et al., 2020). U-Net can identify thin clouds, broken pieces of clouds (Segal-Rozenhaimer et al., 2020; Yu et al., 2020) and clouds in snow and ice regions (Jeppesen et al., 2019), distinguish between clouds and their shadows, and capture cloud boundaries (Bing et al., 2023). And BP NN are suitable for remote sensing imagery data containing complex underlying surfaces (Gao et al., 2018). However, the training time for cloud recognition using deep learning models is long and the model structure is complex, so they need to be migrated and improved to increase the computational efficiency when they are applied to forest fire monitoring.

(3) Increasing the accuracy of spatial positioning for satellite remote sensing monitoring of forest fires. Remote sensing imagery contains abundant feature types, but the spatial resolution of the highly temporal satellite data used in forest fire monitoring is low. The use of hybrid pixel decomposition combined with sub-pixel localization methods can effectively improve the spatial positioning accuracy during forest fire monitoring (Xu et al., 2022). There have been studies applying sub-pixel localization methods to other areas (Ling et al., 2010), but fewer use it in satellite remote sensing monitoring of forest fires.

CRediT Author Statement: Ying Zheng: Data curation, Writing-original draft and Writing – review & editing; **Gui Zhang:** Conceptualization, Methodology and Writing – review & editing; **Sanqing Tan:** Visualization, Supervision and Project administration; **Lanbo Feng:** Data curation and Validation.

Data Availability Statement: Not applicable.

Funding: This work was funded by the National Natural Science Foundation Project of China (32271879) and the Science and Technology Innovation Platform and Talent Plan Project of Hunan Province (2017TP1022).

Conflicts of Interest: The authors declare no conflict of interest.

Acknowledgments: Many thanks to people who took part in this paper.

References

Abid, F. (2021). A survey of machine learning algorithms based forest fires prediction and detection systems. *Fire Technology*, *57*(2), 559–590. https://doi.org/10.1007/s10694-020-01056-z

Arino, O., Casadio, S., & Serpe, D. (2012). Global night-time fire season timing and fire count trends using the ATSR instrument series. *Remote Sensing of Environment*, *116*, 226–238. https://doi.org/10.1016/j.rse.2011.05.025

Arino, O., Rosaz, J., & Atlas, F. (1999). 1997 and 1998 world atsr fire atlas using ers-2 atsr-2 data. *Proceedings of the joint fire science conference*.

Arrue, B. C., Ollero, A., & Dios, J. R. M. d. (2000). An intelligent system for false alarm reduction in infrared forest-fire detection. *IEEE Intelligent Systems and their Applications*, *15*(3), 64–73. https://doi.org/10.1109/5254.846287

Ba, R., Chen, C., Yuan, J., Song, W., & Lo, S. (2019). SmokeNet: Satellite smoke scene detection using convolutional neural network with spatial and channel-wise attention. *Remote Sensing*, *11*(14), 1702. https://doi.org/10.3390/rs11141702

Barmpoutis, P., Stathaki, T., Dimitropoulos, K., & Grammalidis, N. (2020). Early fire detection based on aerial 360-degree sensors, deep convolution neural networks and exploitation of fire dynamic textures. *Remote Sensing*, *12*(19), 3177. https://doi.org/10.3390/rs12193177

Bing, F., Jin, Y., Zhang, W., Xu, N., Yu, T., Zhang, L., & Pei, Y. (2023). Research progress of remote sensing image cloud detection based on machine learning. *Remote sensing technology and application*, *38*(1), 129–142. https://doi.org/10.11873/j.issn.1004-0323.2023.1.0129

Chen, J., Zheng, W., Wu, S., Liu, C., & Yan, H. (2022). Fire monitoring algorithm and its application on the GEO-KOMPSAT-2A geostationary meteorological satellite. *Remote Sensing*, *14*(11), 2655. https://doi.org/10.3390/rs14112655

Chrysoulakis, N., Herlin, I., Prastacos, P., Yahia, H., Grazzini, J., & Cartalis, C. (2007). An improved algorithm for the detection of plumes caused by natural or technological hazards using AVHRR imagery. *Remote Sensing of Environment*, *108*(4), 393–406. https://doi.org/10.1016/j.rse.2006.11.024

Chung, Y. S., & Le, H. V. (1984). Detection of forest-fire smoke plumes by satellite imagery. *Atmospheric Environment*, *18*(10), 2143–2151. https://doi.org/10.1016/0004-6981(84)90201-4

Chuvieco, E., Aguado, I., Salas, J., García, M., Yebra, M., & Oliva, P. (2020). Satellite remote sensing contributions to wildland fire science and management. *Current Forestry Reports*, *6*(2), 81–96. https://doi.org/10.1007/s40725-020-00116-5

Dozier, J. (1981). A method for satellite identification of surface temperature fields of subpixel resolution. *Remote Sensing of Environment*, *11*, 221–229. https://doi.org/10.1016/0034-4257(81)90021-3

Eckmann, T. C., Roberts, D. A., & Still, C. J. (2008). Using multiple endmember spectral mixture analysis to retrieve subpixel fire properties from MODIS. *Remote Sensing of Environment*, *112*(10), 3773–3783. https://doi.org/10.1016/j.rse.2008.05.008

Fang, Z. (2014). The evolution of meteorological satellites and the insight from it. *Advances in Meteorological Science and Technology*, *4*(6), 27–34. https://doi.org/10.3969/j.issn.2095-1973.2014.06.003

Feng, L., & Zhou, W. (2023). The forest fire dynamic change influencing factors and the impacts on gross primary productivity in China. *Remote*

Sensing, *15*(5), 1364. https://doi.org/10.3390/rs15051364
Ferrare, R. A., Fraser, R. S., & Kaufman, Y. J. (1990). Satellite measurements of large-scale air pollution: Measurements of forest fire smoke. *Journal of Geophysical Research: Atmospheres*, *95*(D7), 9911–9925. https://doi.org/10.1029/JD095iD07p09911
Flannigan, M. D., & Haar, T. H. V. (1986). Forest fire monitoring using NOAA satellite AVHRR. Canadian Journal of Forest Research, *16*, 975–982. https://doi.org/10.1139/x86-171
Flasse, S. P., & Ceccato, P. (1996). A contextual algorithm for AVHRR fire detection. *International Journal of Remote Sensing*, *17*(2), 419–424. https://doi.org/10.1080/01431169608949018
Gao, J., Wang, K., Tian, X., & Chen, J. (2018). A BP-NN based cloud detection method for FY-4 remote sensing images. *Journal of Infrared and Millimeter Waves*, *37*(4), 477–485. https://doi.org/10.11972/j.issn.1001-9014.2018.04.016
Giglio, L. (2007). Characterization of the tropical diurnal fire cycle using VIRS and MODIS observations. *Remote Sensing of Environment*, *108*(4), 407–421. https://doi.org/10.1016/j.rse.2006.11.018
Giglio, L., Csiszar, I., Restás, Á., Morisette, J. T., Schroeder, W., Morton, D., & Justice, C. O. (2008). Active fire detection and characterization with the advanced spaceborne thermal emission and reflection radiometer (ASTER). *Remote Sensing of Environment*, *112*(6), 3055–3063. https://doi.org/10.1016/j.rse.2008.03.003
Giglio, L., Descloitres, J., Justice, C. O., & Kaufman, Y. J. (2003). An enhanced contextual fire detection algorithm for MODIS. *Remote Sensing of Environment*, *87*(2), 273–282. https://doi.org/10.1016/S0034-4257(03)00184-6
Giglio, L., & Schroeder, W. (2014). A global feasibility assessment of the bi-spectral fire temperature and area retrieval using MODIS data. *Remote Sensing of Environment*, *152*, 166–173. https://doi.org/10.1016/j.rse.2014.06.010
Giglio, L., Schroeder, W., & Justice, C. O. (2016). The collection 6 MODIS active fire detection algorithm and fire products. *Remote Sensing of Environment*, *178*, 31–41. https://doi.org/10.1016/j.rse.2016.02.054
He, L., & Li, Z. (2011). Enhancement of a fire-detection algorithm by eliminating solar contamination effects and atmospheric path radiance: Application to MODIS data. *International Journal of Remote Sensing*, *32*(21), 6273–6293. https://doi.org/10.1080/01431161.2010.508057
He, L., & Li, Z. (2012). Enhancement of a fire detection algorithm by eliminating solar reflection in the mid-IR band: Application to AVHRR data. *International Journal of Remote Sensing*, *33*(22), 7047–7059. https://doi.org/10.1080/2150704X.2012.699202
He, Q., & Liu, C. (2008). Improved algorithm of self-adaptive five detection for MODIS data. *Journal of Remote Sensing*, (3), 448–453. https://doi.org/10.11834/jrs.20080361
He, R., Zhao, F., Zeng, Y., Zhou, R., Shu, L., & Ye, J. (2022). Application of multisource remote sensing imagery to forest fire monitoring. *World Forestry Research*, *35*(2), 59–63. https://doi.org/10.13348/j.cnki.sjlyyj.2021.0097.y
He, X., Feng, X., Han, Q., Kang, N., Guo, Q., & Peng, Y. (2020). Advances of the geostationary meteorological satellite in the world: A review. *Advances in Meteorological Science and Technology*, *10*(1), 22–29+41. https://doi.org/10.3969/j.issn.2095-1973.2020.01.005
Howard, J., Murashov, V., & Branche, C. M. (2018). Unmanned aerial vehicles in construction and worker safety. *American Journal of Industrial Medicine*, *61*(1), 3–10. https://doi.org/10.1002/ajim.22782
Hua, L., & Shao, G. (2017). The progress of operational forest fire monitoring with infrared remote sensing. *Journal of Forestry Research*, *28*(2), 215–229. https://doi.org/10.1007/s11676-016-0361-8
Jeppesen, J. H., Jacobsen, R. H., Inceoglu, F., & Toftegaard, T. S. (2019). A cloud detection algorithm for satellite imagery based on deep learning. *Remote Sensing of Environment*, *229*, 247–259. https://doi.org/10.1016/j.rse.2019.03.039
Justice, C. O., Giglio, L., Korontzi, S., Owens, J., Morisette, J. T., Roy, D. P., Descloitres, J., Alleaume, S., Petitcolin, F., & Kaufman, Y. J. (2002). The MODIS fire products. *Remote Sensing of Environment*, *83*(1), 244–262. https://doi.org/10.1016/S0034-4257(02)00076-7
Kang, Y., Jang, E., Im, J., & Kwon, C. (2022). A deep learning model using geostationary satellite data for forest fire detection with reduced detection latency. *GIScience & Remote Sensing*, *59*(1), 2019–2035. https://doi.org/10.1080/15481603.2022.2143872
Kaufman, Y. J., Tucker, C. J., & Fung, I. (1990). Remote sensing of biomass burning in the tropics. *Journal of Geophysical Research: Atmospheres*, *95*(D7), 9927–9939. https://doi.org/10.1029/JD095iD07p09927
Kennedy, P. J., Belward, A. S., & Gregoire, J. M. (1994). An improved approach to fire monitoring in West Africa using AVHRR data. *International Journal of Remote Sensing*, *15*(11), 2235–2255. https://doi.org/10.1080/01431169408954240
Lee, T. F., & Tag, P. M. (1990). Improved detection of hotspots using the AVHRR 3.7-um channel. *Bulletin of the American Meteorological Society*, *71*(12), 1722–1730. https://doi.org/10.1175/1520-0477(1990)071<1722:IDOHUT>2.0.CO;2
Li, X., & Jia, J. (2018). How the smallest clairvoyance in meteorological satellite was tempered?—The preparation of the infrared-detector chips of FY-4A multiple channel scanning radiation imager. *Chinese Journal of Nature*, *40*(2), 90–101. https://doi.org/10.3969/j.issn.0253-9608.2018.02.002
Li, X., Song, W., Lian, L., & Wei, X. (2015). Forest fire smoke detection using back-propagation neural network based on MODIS data. *Remote Sensing*, *7*(4), 4473–4498. https://doi.org/10.3390/rs70404473
Li, X., Wang, J., Song, W., Ma, J., Telesca, L., & Zhang, Y. (2014). Automatic smoke detection in MODIS satellite data based on K-means clustering and fisher linear discrimination. *Photogrammetric Engineering & Remote Sensing*, *80*(10), 971–982. https://doi.org/10.14358/PERS.80.10.971
Li, X., Zhang, G., Tan, S., Yang, Z., & Wu, X. (2023). Forest fire smoke detection research based on the random forest algorithm and sub-pixel mapping method. *Forests*, *14*(3), 485. https://doi.org/10.3390/f14030485
Li, Y., Zhang, X., Wu, H., Gao, P., & Xia, D. (2007). An enhanced contextual fire detection algorithm based on remote sensing images. *Journal of Image and Graphics*, *12*(9), 1627–1632. https://doi.org/10.11834/jig.20070922
Li, Z., Kaufman, Y. J., Ichoku, C., Fraser, R., & Yu, X. (2001). A review of AVHRR-based active fire detection algorithms: Principles limitations and recommendations. In: Ahern FJ, Goldammer JG, Justice CO (eds), *Global and regional vegetation fire monitoring from space: planning and coordinated international effort* (pp. 199–225).
Li, Z., Nadon, S., & Cihlar, J. (2000). Satellite-based detection of Canadian boreal forest fires: Development and application of the algorithm. *International Journal of Remote Sensing*, *21*(16), 3057–3069. https://doi.org/10.1080/01431160050144956
Lin, Z., Chen, F., Li, B., Yu, B., Shirazi, Z., Wu, Q., & Wu, W. (2017). FengYun-3C VIRR active fire monitoring: Algorithm description and initial assessment using MODIS and landsat data. *IEEE Transactions on Geoscience and Remote Sensing*, *55*(11), 6420–6430. https://doi.org/10.1109/TGRS.2017.2728103
Ling, F., Du, Y., Xiao, F., Xue, H., & Wu, S. (2010). Super-resolution land-cover mapping using multiple sub-pixel shifted remotely sensed images. *International Journal of Remote Sensing*, *31*(19), 5023–5040. https://doi.org/10.1080/01431160903252350
Liu, S., Li, X., Qin, X., Sun, G., & Liu, Q. (2020). Adaptive threshold method for active fire identification based on GF-4 PMI data. *Journal of*

Remote Sensing, *24*(3), 215–225. https://doi.org/10.11834/jrs.20208297
Lu, N., & Gu, S. (2016). Review and prospect on the development of meteorological satellites. *Journal of Remote Sensing*, *20*(5), 832–841. https://doi.org/10.11834/jrs.20166194
Lv, D., Wang, P., Qiu, J., & Tao, S. (2003). An overview on the research progress of atmospheric remote sensing and satellite meteorology in China. *Chinese Journal of Atmospheric Sciences*, *27*(4), 552–566. https://doi.org/10.3878/j.issn.1006-9895.2003.04.09
Maeda, E. E., Formaggio, A. R., Shimabukuro, Y. E., Arcoverde, G., & Hansen, M. C. (2009). Predicting forest fire in the Brazilian Amazon using MODIS imagery and artificial neural networks. *International Journal of Applied Earth Observation Geoinformation*, *11*(4), 265–272. https://doi.org/10.1016/j.jag.2009.03.003
Nakayama, M., Maki, M., Elvidge, C. D., & Liew, S. C. (1999). Contextual algorithm adapted for NOAA-AVHRR fire detection in Indonesia. *International Journal of Remote Sensing*, *20*(17), 3415–3421. https://doi.org/10.1080/014311699211444
Peng, G., Shen, W., Hu, D., Li, J., & Chen, Y. (2008). Method to identify forest fire based on smoke plumes mask by using modis data. *Journal of Infrared and Millimeter Waves*, *27*(3), 185–189. https://doi.org/10.3321/j.issn:1001-9014.2008.03.007
Peterson, D., Wang, J., Ichoku, C., Hyer, E., & Ambrosia, V. (2013). A sub-pixel-based calculation of fire radiative power from MODIS observations: 1: Algorithm development and initial assessment. *Remote Sensing of Environment*, *129*, 262–279. https://doi.org/10.1016/j.rse.2012.10.036
Pozo, D., Olrno, F. J., & Alados-Arboledas, L. (1997). Fire detection and growth monitoring using a multitemporal technique on AVHRR mid-infrared and thermal channels. *Remote Sensing of Environment*, *60*(2), 111–120. https://doi.org/10.1016/S0034-4257(96)00117-4
Pu, R., Gong, P., Li, Z., & Scarborough, J. (2004). A dynamic algorithm for wildfire mapping with NOAA/AVHRR data. International Journal of Wildland Fire. *Journal of the International Association of Wildland Fire*, *13*(3), 275–285. https://doi.org/10.1071/WF03054
Qin, X., Chen, X., Zhong, X., Zu, X., Sun, G., & Yin, L. (2015). Development of forest fire early warning and monitoring technique system in China. *FOREST Resources MANAGEMENT*(6), 45–48. https://doi.org/10.13466/j.cnki.lyzygl.2015.06.009
Qin, X., Li, X., Liu, S., Liu, Q., & Li, Z. (2020). Forest fire early warning and monitoring techniques using satellite remote sensing in China. *Journal of Remote Sensing*, *24*(5), 511–520. https://doi.org/10.11834/jrs.20209135
Qin, X., & Yi, H. (2004). A method to identify forest fire based on MODIS data. *Fire Safety Science*, *13*(2), 83–89. https://doi.org/10.3969/j.issn.1004-5309.2004.02.005
Rafik, G., Jmal, M., Mseddi, W. S., & Attia, R. (2020). Recent advances in fire detection and monitoring systems: A review. *Proceedings of the 8th International Conference on Sciences of Electronics, Technologies of Information and Telecommunications*
Santos, S. M. B. d., Bento-Gonçalves, A., & Vieira, A. (2021). Research on wildfires and remote sensing in the last three decades: A bibliometric analysis. *Forests*, *12*(5), 604. https://doi.org/10.3390/f12050604
Sathishkumar, V. E., Cho, J., Subramanian, M., & Naren, O. S. (2023). Forest fire and smoke detection using deep learning—based learning without forgetting. *Fire Ecology*, *19*(1), 9. https://doi.org/10.1186/s42408-022-00165-0
Schroeder, W., Oliva, P., Giglio, L., & Csiszar, I. A. (2014). The new VIIRS 375m active fire detection data product: Algorithm description and initial assessment. *Remote Sensing of Environment*, *143*, 85–96. https://doi.org/10.1016/j.rse.2013.12.008
Schroeder, W., Prins, E., Giglio, L., Csiszar, I., Schmidt, C., Morisette, J., & Morton, D. (2008). Validation of GOES and MODIS active fire detection products using ASTER and ETM+ data. *Remote Sensing of Environment*, *112*(5), 2711–2726. https://doi.org/10.1016/j.rse.2008.01.005
Segal-Rozenhaimer, M., Li, A., Das, K., & Chirayath, V. (2020). Cloud detection algorithm for multi-modal satellite imagery using convolutional neural-networks (CNN). *Remote Sensing of Environment*, *237*, 111446. https://doi.org/10.1016/j.rse.2019.111446
Setzer, A. W., & Pereira, M. C. (1991). Amazonia biomass burnings in 1987 and an estimate of their tropospheric emissions. *Ambio*, *20*(1), 19–22. https://doi.org/10.2307/4313765
Shu, L., Wang, M., Zhao, F., Li, H., & Tian, X. (2005). Comparison and application of satellites in forest fire monitoring. *World Forestry Research*, (6), 49–53. https://doi.org/10.13348/j.cnki.sjlyyj.2005.06.008
Sun, F., Li, X., Li, Z., & Qin, X. (2020). Near-real-time forest fire monitoring system with medium and high spatial resolutions. *Journal of Remote Sensing*, *24*(5), 543–549. https://doi.org/10.11834/jrs.20209137
Sun, W., Yang, G., Chen, C., Chang, M., Huang, K., Meng, X., & Liu, L. (2020). Development status and literature analysis of China's earth observation remote sensing satellites. *Journal of Remote Sensing*, *24*(5), 479–510. https://doi.org/10.11834/jrs.20209464
Sun, Z., Shen, W., Wei, B., Liu, X., Su, W., Zhang, C., & Yang, J. (2010). Object-oriented land cover classification using HJ-1 remote sensing imagery. *Science China Earth Sciences*, *53*(1), 34–44. https://doi.org/10.1007/s11430-010-4133-6
Tang, S., Qiu, H., & Ma, G. (2016). Review on progress of the Fengyun meteorological satellite. *Journal of Remote Sensing*, *20*(5), 842–849. https://doi.org/10.11834/jrs.20166232
Tian, Y. P., Wu, Z. C., Li, M. Z., Wang, B., & Zhang, X. D. (2022). Forest fire spread monitoring and vegetation dynamics detection based on multi-source remote sensing images. *Remote Sensing*, *14*(18), 4431. https://doi.org/10.3390/rs14184431
Tsagkatakis, G., Aidini, A., Fotiadou, K., Giannopoulos, M., Pentari, A., & Tsakalides, P. (2019). Survey of deep-learning approaches for remote sensing observation enhancement. *Sensors*, *19*(18), 3929. https://doi.org/10.3390/s19183929
Wang, W., Qu, J. J., Hao, X., & Liu, Y. (2009). Analysis of the moderate resolution imaging spectroradiometer contextual algorithm for small fire detection. *Journal of Applied Remote Sensing*, *3*(1), 031502. https://doi.org/10.1117/1.3078426
Wang, W., Qu, J. J., Hao, X., Liu, Y., & Sommers, W. T. (2007). An improved algorithm for small and cool fire detection using MODIS data: A preliminary study in the southeastern United States. *Remote Sensing of Environment*, *108*(2), 163–170. https://doi.org/10.1016/j.rse.2006.11.009
Wooster, M. J., Xu, W., & Nightingale, T. (2012). Sentinel-3 SLSTR active fire detection and FRP product: Pre-launch algorithm development and performance evaluation using MODIS and ASTER datasets. *Remote Sensing of Environment*, *120*, 236–254. https://doi.org/10.1016/j.rse.2011.09.033
Wu, X., Lu, X., & Leung, H. (2020). A motion and lightness saliency approach for forest smoke segmentation and detection. *Multimedia Tools Applications*, *79*, 69–88. https://doi.org/10.1007/s11042-019-08047-5
Xie, Y., Qu, J. J., Xiong, X., Hao, X., Che, N., & Sommers, W. (2007). Smoke plume detection in the eastern United States using MODIS. *International Journal of Remote Sensing*, *28*(10), 2367–2374. https://doi.org/10.1080/01431160701236795
Xie, Z., Song, W., Ba, R., Li, X., & Xia, L. (2018). A spatiotemporal contextual model for forest fire detection using Himawari-8 satellite data. *Remote Sensing*, *10*(12), 1992. https://doi.org/10.3390/rs10121992
Xu, G., & Zhong, X. (2017). Real-time wildfire detection and tracking in Australia using geostationary satellite: Himawari-8. *Remote Sensing Letters*, *8*(11), 1052–1061. https://doi.org/10.1080/2150704X.2017.1350303

Xu, H., Zhang, G., Zhou, Z., Zhou, X., & Zhou, C. (2022). Forest fire monitoring and positioning improvement at subpixel level: Application to Himawari-8 fire products. *Remote Sensing*, *14*(10), 2460. https://doi.org/10.3390/rs14102460

Xu, W., Wooster, M. J., He, J., & Zhang, T. (2020). First study of Sentinel-3 SLSTR active fire detection and FRP retrieval: Night-time algorithm enhancements and global intercomparison to MODIS and VIIRS AF products. *Remote Sensing of Environment*, *248*, 111947. https://doi.org/10.1016/j.rse.2020.111947

Xu, W., Wooster, M. J., Polehampton, E., Yemelyanova, R., & Zhang, T. (2021). Sentinel-3 active fire detection and FRP product performance—Impact of scan angle and SLSTR middle infrared channel selection. *Remote Sensing of Environment*, *261*, 112460. https://doi.org/10.1016/j.rse.2021.112460

Yi, H., Ji, P., He, X., & Zhang, Y. (1996). Study on monitoring and early alarm technique of forest fire using satellite data. *Remote Sensing Technology and Application*, *11*(1), 40–46. https://doi.org/10.11873/j.issn.1004-0323.1996.1.40

Yin, J., He, R., Zhao, F., & Ye, J. (2023). Research on forest fire monitoring based on multi-source satellite remote sensing images. *Spectroscopy and Spectral Analysis*, *43*(3), 917–926. https://doi.org/10.3964/j.issn.1000-0593(2023)03-0917-10

Yin, Z., Chen, F., Lin, Z., Yang, A., & Li, B. (2020). Active fire monitoring based on FY-3D MERSI satellite data. *Remote Sensing Technology and Application*, *35*(5), 1099–1108.

Yu, J., Li, Y., Zheng, X., Zhong, Y., & He, P. (2020). An effective cloud detection method for Gaofen-5 images via deep learning. *Remote Sensing*, *12*(13), 2106. https://doi.org/10.3390/rs12132106

Zhang, D., Huang, C., Gu, J., Hou, J., Zhang, Y., Han, W., Zhang, Y., Han, W., Dou, P., & Feng, Y. (2023). Real-Time wildfire detection algorithm based on VIIRS fire product and Himawari-8 data. *Remote Sensing*, *15*(6), 1541. https://doi.org/10.3390/rs15061541

Zhang, N., Sun, L., & Sun, Z. (2022). GF-4 satellite fire detection with an improved contextual algorithm. *IEEE Journal of Selected Topics in Applied Earth Observations and Remote Sensing*, *15*, 163–172. https://doi.org/10.1109/JSTARS.2021.3132360

Zhang, Q. X., Lin, G. H., Zhang, Y. M., Xu, G., & Wang, J. J. (2018). Wildland forest fire smoke detection based on faster R-CNN using synthetic smoke images. *Procedia Engineering*, *211*, 441–446. https://doi.org/10.1016/j.proeng.2017.12.034

Zhang, T., Wooster, M. J., & Xu, W. (2017). Approaches for synergistically exploiting VIIRS I- and M-Band data in regional active fire detection and FRP assessment: A demonstration with respect to agricultural residue burning in Eastern China. *Remote Sensing of Environment*, *198*, 407–424. https://doi.org/10.1016/j.rse.2017.06.028

Zheng, W., Shao, J., Wang, M., & Liu, C. (2013). Dynamic monitoring and analysis of grassland fire based on multi-source satellite remote sensing data. *Journal of Natural Disasters*, *22*(3), 54–61. https://doi.org/10.13577/j.jnd.2013.0308

Zheng, Y., Zhang, G., Tan, S., Yang, Z., Wen, D., & Xiao, H. (2023). A forest fire smoke detection model combining convolutional neural network and vision transformer. *Frontiers in Forests and Global Change*, *6*. https://doi.org/10.3389/ffgc.2023.1136969

Zhou, X., Feng, D., Xie, Y., Tao, Z., Lv, T., & Wang, J. (2021). Radiometric Cross-Calibration of GF-4/IRS Based on MODIS measurements. *IEEE Journal of Selected Topics in Applied Earth Observations and Remote Sensing*, *14*, 6807–6814. https://doi.org/10.1109/JSTARS.2021.3091977

Zhou, X., & Wang, X. (2006). Validate and improvement on arithmetic of identifying forest fire based on EOS-MODIS data. *Remote Sensing Technology and Application*, *21*(3), 206–211. https://doi.org/10.3969/j.issn.1004-0323.2006.03.007

Zhukov, B., Lorenz, E., Oertel, D., Wooster, M., & Roberts, G. (2006). Spaceborne detection and characterization of fires during the bi-spectral infrared detection (BIRD) experimental small satellite mission (2001–2004). *Remote Sensing of Environment*, *100*(1), 29–51. https://doi.org/10.1016/j.rse.2005.09.019

Agricultural & Rural Studies

Article

The Relationship Between Agri-Food Production and Macro-Economic Dynamics: A Study on Soybeans in Brazilian South and Chinese Mainland

Ângelo Belletti [1,*] and Sérgio Schneider [2]

[1] Department of Rural Development, Federal University of Rio Grande do Sul, Porto Alegre 90050-160, Brazil
[2] Department of Sociology and Rural Development and Food Studies, Federal University of Rio Grande do Sul, Porto Alegre 90050-160, Brazil; schneide@ufrgs.br
* Correspondence: angelo.belletti@hotmail.com

Abstract: This research article aims to establish a relationship between regional conditions of agri-food production and their correlations with macroeconomic structures. To this end, soybeans production in Rio Grande do Sul, Brazil, and its trade with Chinese Mainland are observed. The analysis draws on the Food Regimes approach in dialogue with institutionalist theory, especially considering the construction of agricultural production habits and models. The argument takes secondary quantitative data on soybeans production and trade, triangulating them with information gathered from international platforms—primarily FAOSTAT and Trase Platform—and with qualitative data collected during field research—using landscape analysis and interviews conducted with soybean cooperatives (in the Brazilian case). Findings on the formation of the soybean market between Rio Grande do Sul and Chinese Mainland reveal historically constituted elements that shaped trade flows as they are configured contemporarily. A correlation between the Third Food Regime and effects on agricultural practice in the Brazilian region was also observed.

Keywords: markets; soybean; Chinese Mainland; commodities; agrifood system; food chains

Citation: Belletti, A.; Schneider, S. The Relationship Between Agri-Food Production and Macro-Economic Dynamics: A Study on Soybeans in Brazilian South and Chinese Mainland. *Agricultural & Rural Studies*, 2023, *1*, 0009. *https://doi.org/10.59978/ar01020009*

Received: 10 August 2023
Revised: 25 August 2023
Accepted: 5 September 2023
Published: 12 September 2023

Publisher's Note: SCC Press stays neutral with regard to jurisdictional claims in published maps and institutional affiliations.

1. Introduction

Approximately 238 million tons of soybeans were produced in Rio Grande do Sul, Brazil, between 2000 and 2020, most of which were destined for export. The grains traveled along highways, railways and waterways towards the main port in the region. A significant part of its shipment was destined for the Asian continent, specifically for Chinese ports. Such logistics involved individuals, corporations and States throughout its stages—processes made possible by a historical framework of practices that underpin contemporary operations.

The pointed historical framework is characterized by a global economy in which public and private actors possess different capacities of socioeconomic power, depending on the path of relations established over the decades. Since the founding of the People's Republic of China, especially since the launch of reform and opening up, this relation was developed through bridges connecting an internal development project to the international capitalist economy. In the rural area, these bridges are highly illustrated by the soy-meat chain (Escher, 2022). Through the import of oilseed, China established contact with international private actors, becoming the country with the largest quantity of imports since 2004. Meanwhile, it provided raw materials to stimulate its internal production of animal protein, mostly pork (Lander et al., 2020). On the other hand, the relation established between Rio Grande do Sul and the international market economy was marked by a dependence of the region (and the Brazilian country as a whole) on the capital stock obtained through the export of commodities (Oliveira, 2016; Wesz Junior, 2014). In the field, however, distinct types of agriculture were developed by producers according to their land and capital availability, generating institutions in dialogue with the pre-existing social bases. Given the intricate nature of this subject, our research delves into the formation of the soybean market between Rio Grande do Sul and China spanning from 1970 to 2020. The crux of our investigation lies in examining the role of influential actors in shaping this market dynamic. Specifically, we place a spotlight on the institutions that were either established anew or underwent transformation, instrumental in enabling the facilitation of these substantial commodity flows.

To this end, our objective here divides into three questions: How does soybean export supply originate and is organized by the state of Rio Grande do Sul? How does China's soybean demand in the international market originate and is organized? What elements permeate trade flows between both regions?

To settle down the scope, three choices require justifications: the markets, the geographical area and the time frame. The first one regards interpretation of "the market" as an outcome of human sociability. General reflections on varieties of capitalism and economic forms add to the debate in Political Economy and to development perspectives, by regarding the various elements that comprise socioeconomic relations. In this research market analysis aims to contribute to the aforementioned debate by observing a transnational commodity chain (Azevedo, 2016; Wesz Junior, 2014). The second delimitation regards the geographical focus on China and Rio Grande do Sul. China was chosen because of its significance in oilseeds worldwide imports in the 21st century, its geopolitical potential and its adopted path of development (Escher, 2016; Jabbour, 2010; Schneider, 2011; Zhang & Zeng, 2021). Rio Grande do Sul, on the other hand, presents an economic path linked to soybean, as well as significant social connections in its structure currently (Benetti, 2004; Escher & Wilkinson, 2019). It should be noted that the focus on a Brazilian state rather than the country stems from the possibility of greater depth by avoiding generalizations that would be required in the analysis of the whole national scenario. The selection of these two regions is also due to the possibility of making a comparative analysis between institutional frameworks and their effects on the socioeconomic development of localities. Finally, the adopted time frame (1970 to 2020) is justified by the dynamism of sociopolitical movements in the period in both territories, which led to local agricultural transformations (Chen, 2019; Delgado, 2013).

Two theoretical pillars underpin the elaboration of this article. The first one, aligned with a global and regulative approach, namely the Food Regimes, suggests that the formation of macroeconomic structures defines the position of countries in international trade (Bernstein, 2016; Friedmann, 2005; McMichael, 2009). A second pillar is related to the cultural and cognitive dimensions. We draw on scholars of Historical and Sociological Institutionalism stream because, despite regulative global compositions, everyday practices are performed by actors in contexts that are demarcated by formal and informal factors (Beckert, 2017; Hodgson, 2006). The institutionalist approach also underpins our interpretation of markets, taking them as social elements (Azevedo, 2016). To connect these spheres, we draw especially on the perspective of embeddedness regarding *structural* and *local* dimensions (Cassol & Schneider, 2022; Dimaggio & Louch, 1998).

The analysis resorted to quantitative and qualitative data and combined theoretical and statistical processes to build macro and meso analytical perspectives of the researched theme. Quantitative data were retrieved from the National Waterway Transport Agency (ANTAQ); the National Bureau of Statistics of China (NBSC); the Municipal Agricultural Production database—Brazilian Institute of Geography and Statistics (PAM/IBGE); the Foreign Trade Statistics/Brazilian Ministry of Economy; the Brazilian National Supply Company (CONAB); the Brazilian Association of Vegetable Oils (ABIOVE); and the platform Trase.earth. As to qualitative data, the research drew on two practices: reading the landscape of the northeastern region of Rio Grande do Sul (RS) and conducting semi-structured interviews with representatives of cooperatives located in RS and engaged in the soybean market.

In response to the three aforementioned guiding questions, the research inferred a social, artificial and politically induced nature of the soybean market formed between Rio Grande do Sul and China. A feat accomplished by means of five factors: the dilution of production costs, in RS' agricultural export model, throughout the social body; correlations between the Third Food Regime's dynamics and the practice located in Rio Grande do Sul; the Chinese development model and its balance between domestic and foreign markets; China's global expansion and the consequent changes in the international economy; and the distinct social relationships—such as trust and personal ties—that define the soy market. This research article makes a contribution by delving deeper into the analysis of market development and structuring. It engages in a critical discourse with paradigms that endorse conventional mainstream economic approaches that often ascribe a natural and self-regulating character to capitalist markets. Instead, this research aligns with perspectives advocating for social-based interpretation of economic relations.

In addition to this introduction, the article follows with three sections that address the research questions. The next section presents the production context in Rio Grande do Sul, the third one discusses the Chinese demand for grains and the fourth examines the commercial relationship between Rio Grande do Sul and China, while identifying observable elements related to the Food Regimes' approach as well as institutional elements. Then, it presents final considerations.

2. Supply of Soybeans by Rio Grande do Sul

The first signs of soybean commercial cultivation in Rio Grande do Sul date back to the 1940s. From then on, the grain's trajectory in the region can be outlined according to three periods: from

1950 to 1970; from 1970 to 1990; and from 1990 to 2020 (Wesz Junior, 2014; Delgado, 2013; Da Ros, 2006; Conçalves, 1984).

Between 1950 and 1970, soy gained ground in food consumption and in animal feeding (Conçalves, 1984). Complementarily with wheat crops, the oleaginous plant expanded territorially—especially fostered by local agricultural cooperatives. Its rapid expansion introduced new processes in the rural environment, such as greater mechanization and chemicalization of production (Da Ros, 2006).

Between the 1970s and the 1990s, soybean cultivation became predominant in the region as a result of four socioeconomic movements: changes in international supply due to reduction in the United States' domestic production (Bertrand et al., 1987); increasing consumption of the grain by European countries for production of animal protein and vegetable oils (Singh & Shivakumar, 2010); government subsidies for technological improvements related to the Green Revolution, which enabled soybean cultivation in new regions (Da Ros, 2006); and the rise in commodity prices that expanded the use of agricultural products as a capital inflow channel (Bertrand et al., 1987).

If the period 1970 to 1990 saw a significant expansion of soybean cultivation in Rio Grande do Sul, it was between 1990 and 2020 that its commercial importance became preponderant. At the beginning of the 21st century, economic destabilization in Asian countries caused international retraction of private credit. To maintain capital inflow, the Brazilian government fostered agricultural exports, with the addition of a new identify: agribusiness. In the Brazilian context, the term referred to the political project promoted and organized by agricultural conglomerates based on private capital and government support, especially fiscal incentives, export credits, infrastructure and the like (Oliveira 2016; Pereira & Alentejano, 2015). The sociopolitical construction was in tune with the enactment, in 1996, of the Kandir Law, which exempted primary products from the tax on products transacted, thus benefiting and encouraging the export of unprocessed raw materials. The law aimed to promote foreign trade to guarantee foreign currency inflow to the country's economy (Lemos et al., 2017). This new tax policy replaced the previous one, which levied a 13% tax on non-processed grains transacted, 11% on bran and 8.5% on processed oils. Such elements, together with the liberalization of the national market, reinforced Brazil's connection with the world economy (Benetti, 2004).

As a consequence, indices registered by CONAB on soybean cultivated area in the state show a substantial change over the last five decades: from 3.49 million hectares in 1976/1977, to 2.97 million in 2000/2001 and reaching 6.05 million hectares in 2020/2021. Regarding production, from 5.6 million tons in 1976/1977, production reached 7.1 million in 2000/2001 (indicating increase in productivity) and 20.78 million in 2020/2021—a 271% growth.

As regards the mode of production, the use of fertilizers is an emerging element throughout the 1990s. According to ANTAQ records, trade flows in the two main port complexes of Rio Grande do Sul—Porto Alegre and Rio Grande—recorded for the years 1979/1980/1981 totaled, altogether, three million tons of imported fertilizers, which corresponds to 35.8% of total imports unloaded in the state. In the period 1999/2000/2001, 4.4 million tons were recorded—7.8% of the total. In the recent period (2018/2019/2020), 15.28 million tons of imported fertilizers were recorded, reaching 40.7% of total imports.

This greater inflow of fertilizers points to the consolidation of a farming system based on external inputs, which becomes dependent on markets to make its production cycle viable (Van der Ploeg, 2018). Such trend occurs concomitantly with the opening of Brazilian national market and privatization of state-owned companies in the sector—especially phosphorus- and potassium-based fertilizers (Benetti, 2004)—corroborating the assertion by McMichael (2009, 2016) that the neoliberal discourse on removal of protections to domestic industries in favor of foreign competition has deepened in the Third Food Regime. In the long term, this process led to the concentration, in 2014, of 86% of Brazilian nitrogen-, phosphorus- and potassium-based fertilizers market in five companies (Bunge, Fertipar, Mosaic, Yara, Heringer) and, for pesticides and seeds, in eight companies that dominate 75% of the market (Syngenta, Bayer, Basf, Monsanto, Dupont, Dow, Makhteshim & FMC) (Wesz Junior, 2014).

The case of authorized cultivars for seed production in RS is also illustrative. According to the National Registry of Cultivars (RNC/MAPA), thirteen authorized companies account for 127 registered cultivars. However, all of them have a genetic load associated to three patent registrations—A5547-127, MON87701 x MON89788, GTS-40-3-2—which are linked to the Bayer CropScience / Monsanto Company complex. Therefore, the 127 transgenic cultivars available for cultivation in the state must pay royalties to a company that centralizes ownership of the registered biological material. Such patents began to be regulated in Brazil in 1996, in the wake of international negotiations involving registration of private intellectual property conducted by the World Trade Organization (WTO) (Pereira & Alentejano, 2015). This points to a correlation between macroeconomy and the daily practice of actors, since access to seeds in Rio Grande do Sul is limited by commercial conditions defined by international organizations.

In the stages that follow cultivation, the reconfiguration of soybean processing and refining units in Rio Grande do Sul stands out. ABIOVE data point to an 80% reduction in the number of active soybean oil refining manufacturers between 2002 and 2020, resulting in a 41% decrease in refining capacity in RS in two decades. Such fact relates to the promotion of exports of unprocessed grains, which leads to less value-adding activities in the region (Lemos et al., 2017).

As regards the spatiality of cultivation, in 1975 soybean crops were preponderant in the Northwest region of the state, with relative expansion towards Southwest—regions where wheat predominated earlier (Conçalves, 1984). A spatiality that changes massively in contemporary times—as shown in Figure 1, with significant expansion of the area destined to soybean.

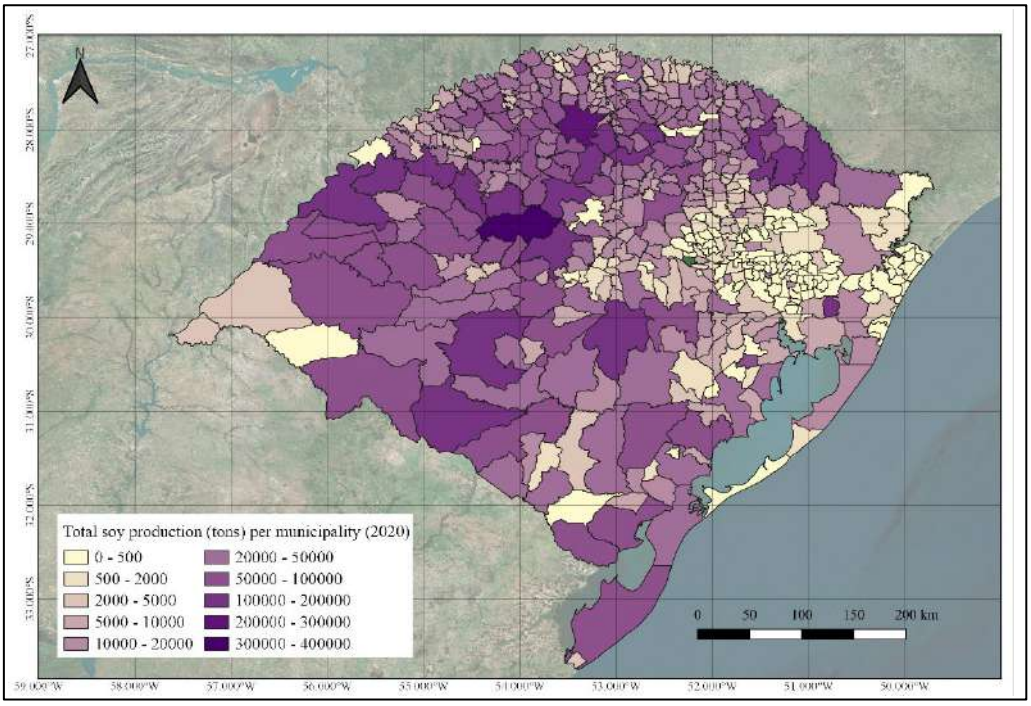

Figure 1. Distribution of soybean crops by municipality in Rio Grande do Sul, 2020. Source: Elaborated by the authors on QGIS using data from Produção Agrícola Municipal (PMA/IBGE).

All regions now have potential sites for soybeans cultivation, with emphasis on its expansion in the pampas region. This expansion took different features according to the local context within the state and to the background of involved actors. On this point, Vennet, Schneider and Dessein (2016) analyzed agricultural units that produced soybeans in southern Brazil and identified three categories of practice: niche farming, colonial farming and farming enterprise.

Niche farming is characterized by diversified production aimed at the sustainability of the farm against pressures exerted by the market economy. These farmers seek specific trade channels, such as organic production, rural tourism and the like. Soybean appears as a single element in a multiple composition, having no primacy in farmers' income. In this category, social integration focused on locality is observed, which establishes community and regional connections as forms of market entry and permanence.

The colonial farming involves agri-food production aimed at the market, while keeping diversified farming for local subsistence. The commercial activities prioritize soybean, corn and wheat crops and pig and poultry farming. This category is characterized by family labor and smallholding properties. Technology is implemented to the extent of availability of capital. Technical assistance, especially from cooperatives, is quite usual in this group, although it varies between properties. Rural succession and the low profitability of small-scale production are elements that put the existence of this group under strain.

Farming enterprise, in turn, focuses on specialized production aimed at the market. It is characterized by extensive use of machinery and chemicals in the farming process. Over the last few decades, it has been marked by continuous technical improvement mainly enabled by academic training of family members, in areas related to agronomy, who implement the acquired knowledge on their properties. Despite the smaller number of farms in this category, the group predominates in soybean production in Rio Grande do Sul.

For a quantitative approximation of the presented categories, data from the Agricultural Census relating access to land and rural category to soybean cultivation are illustrative, as shown in Table 1.

Table 1. Number of soybean growers by farming type and land tenure condition, RS, 2017.

	Total	**Family farming**		**Non-family farming**		**Others**	
		Category total	Category %	Category total	Category %	Category total	Category %
Total	67.268	51.582	100,00%	14.337	100,00%	1.349	100,00%
Owner	59.061	45.518	88,24%	12.422	86,64%	1.121	83,09%
Settler	2.048	1.966	3,81%	82	0,57%	-	-
Tenant	4.556	2.854	5,53%	1.511	10,53%	191	14,19%
Partner	733	543	1,05%	165	1,15%	25	1,85%
Lending Contract	663	522	1,01%	128	0,89%	13	0,96%
Occupant	183	164	0,31%	17	0,11%	2	0,17%
Producer Without Land	24	15	0,02%	12	0,08%	-	-

Source: Agricultural Census (IBGE, 2017).

Agricultural units under the category of Family Farming predominate among soybean growers (76,68%), who also are predominantly landowners. In the data utilized, these category points to agricultural units with extension smaller than four fiscal modules, predominance of family labor and profitability mostly linked to farming. They also have annual incomes of up to R$ 415,000. It is worth highlighting that under the category of family farming, 6.278 properties have an annual income below R$ 23,000. Regarding producers which are not categorized under family farming, the high number of tenant status stands out (10,53%). In the data utilized, they are composed by properties with a maximum annual income of R$ 2,4 million. An element that confirms McMichael's (2016) claim that greater integration into the market economy is related to a more distant relationship with the land as a living space.

Elements that dialogue with information obtained in interviews carried out at grain growers' cooperatives in the region, different interviewees pointed out that around 90% of the associated producers were smallholders who grew modest crops and accounted for only 10% of the total production traded by the cooperative, while the other part originated from bigger properties.

The different modes of production and agricultural integration are also related to the ways soybean farmers choose to trade their produce. According to Schneider (2016), agricultural markets can be thought of as proximity markets, local markets, institutional markets or conventional markets. Farmers, especially family farmers, generally access multiple distribution channels. However, colonial farmers and soybean farming enterprises generally adopt conventional markets, understood as those based on trading of commodities. Therefore, we assume here that these categories of farmers will be at the center of operations when considering the relationship between RS' soybean market and the Chinese economy, the focus of the next section.

3. Chinese Demand for Soybeans

Average per capita income per Chinese household grew by 187% between 1978 and 2020, from 171.2 yuan to 32,188.8 yuan, according to data from China Statistical Yearbook (2021). The radical change was the result of institutional reforms initiated in the 1949 revolution and sustained throughout the ruling of the Communist Party of China (CPC) (Jabbour, 2010).

China's policies aimed at development of the country have been complementary, enabling both domestic economic growth and expansion in the international capitalist market. This process was concomitant with fragmentation of production chains in the 1980s and expansion of international private conglomerates (McMichael, 2016). In such international context, China emerged as a market with wide labor availability and high consumption potential based on rising average income. Thus, reforms implemented by the Communist Party of China administration recognized the international situation and leveraged elements in dispute to catalyze the national economy, interconnecting the domestic and foreign spheres (Jabbour, 2010).

Regarding the agricultural sector, Chinese internationalization was motivated by limited availability of arable land in the country. In a nation with such a huge population, this required establishing relationships with other countries for assuring food supply (Escher, 2016). Such need and the interconnection with preponderant actors in the global trade supply chain—food conglomerates—attributed special economic prominence to the grain-meat complex, for two reasons. On the one hand, international agro-industrial conglomerates saw meat as a channel for maintaining and expanding capital, given the possibility of geographic distribution and expansion of the sector (Weis, 2013). On the other hand, the Chinese administration envisaged the possibility of expanding domestic consumption by fostering animal protein consumption, thus promoting domestic channels for generating and accumulating capital. In this context, the grain became central for both direct feeding and processing (Escher & Wilkinson, 2019). This dynamic coincided with the expansion of purchasing power, creating a framework for social modernization. Such elements are again related with CPC's goal of establishing a balance between the benefits of a market economy and the aspired national development (Chen, 2019).

Pork is the predominant category of meat in Chinese food culture, a practice rooted in the country's history, as evidence points to the domestication of suiformes since 10,000 BC and maintained as a habit today (Schneider, 2011). According to NBSC data, pig production is the predominant livestock in the country historically. In 2020, for example, 406 million pigs were produced.

Regarding production characteristics, until 1985, 95% of pig production in China came from producers that did up to five slaughters per year. During the collectivization period, pigs were part of the farmers' supply obligations to the State (Schneider & Sharma, 2014). However, following socioeconomic reforms implemented in the late 1970s, a new paradigm was established seeking integration, specialization and internationalization of rural production processes (Zhang & Donaldson, 2008). As a result, swine production underwent industrialization (Schneider & Sharma, 2014). The exclusivity of small agricultural units ceased with the promotion of two production systems: specialized production units and large conglomerates (Zhang & Zeng, 2022).

Specialized production units are aimed at capital accumulation in rural areas by means of State investment and rural dynamics of differentiation (Zhang & Donaldson, 2008). It involves properties with larger land areas, which obtain high productivity rates that enable their maintenance as independent pig farmers who produce between 50 and 500 pigs per year (Escher & Wilkinson, 2019). This system can be managed by family members, small enterprises or cooperatives, according to local specificities (Zhang & Zeng, 2021).

Large swine conglomerates, in turn, are characterized by large-scale production— between 500 and 50 thousand pigs per year—and high technological investment in the production process, typically through confinement with high density of animals (Schneider, 2011). Stemming from accumulation processes that are exogenous to the rural environment, they mostly comprise properties linked to foreign private entities— consequence of the opening of Chinese markets in the 20th century—or state-owned enterprises (Zhang & Zeng, 2022). From the operational perspective, they are not homogeneous, distinguishing by two different operational modes: large-scale own productions or vertical integration (Schneider & Sharma, 2014).

The first case refers to companies that directly control production on their farms. A private example of these is the WH Group, an international conglomerate based in China and the United States self-proclaimed "the largest pork company in the world". It conducts research into breed development, feed, animal production, slaughter, meat processing and marketing. In 2021, the company announced revenues of US $27.293 billion. A state-owned example of these conglomerates is China National Cereals, Oils and Foodstuffs Corporation (COFCO). In 2019, it produced approximately five million hogs. Besides this figure, the high investment in different segments of the production process stands out, turning the conglomerate into owner of most of the technologies that induce changes in the supply chain (Schneider, 2011).

Vertical integration is the production strategy adopted by a considerable part of the "Dragon Head Enterprises" in Chinese territory. In this modality, private enterprises outsource the process to other producers. While the first provide the animals, feed and credit for production improvements, the second group provides the property and labor to manage the animals (Huang, 2011). The producer's loss of autonomy, for becoming dependent on the contracting company, would be compensated by the reduction of economic risks (Zhang & Zeng, 2022).

It is under the control of conglomerates (in both forms of operation) that most Chinese pork production takes place. In 2020, 57.1% of slaughters were carried out in properties with more than 500 animals per year. Nine companies (Muyuan, Zhegbang, Wen's, New Hope Liuhe, Tiangbang, COFCO, Aonong, Trs, Haid) accounted for 10.1% of all slaughters, an increase compared to the 6.9% concentration observed in 2018 (Han et al., 2022). Simultaneously with the increase in concentration in large companies, a reduction is observed in small properties: in 1995, about 95%

of Chinese agricultural properties farmed at least one pig, a number that dropped to 27% in 2009 (Escher et al., 2017).

Within the framework of those production models, three moments characterize the relationship between pigs farming, China and the international market (Schneider & Sharma, 2014). The first one follows the beginning of reforms in 1979, when new technologies introduced in China's countryside allowed for commercial farming to supersede the predominant subsistence farming (Schneider, 2011). In the following period, during the turn of the century, China's accession to WTO was allowed under its commitment to apply non-discriminatory economic treatment to imports (Escher, 2016). The last period of changes started in the wake of porcine reproductive and respiratory syndrome (PRRS) outbreak in 2006, which demanded sacrifice of animals in Asia. To reduce the chance of new biological outbreaks, a series of investments addressed to large-scale pigs farming was made, seeking to standardize the production chain (Schneider & Sharma, 2014). As a result, the number of both animals and production regions expanded again (Zhang & Donaldson, 2008). Table 2 shows the distribution of the main production areas in 2020. Sichuan is historically the center for pigs farming and has witnessed, besides the growth in its territory, the expansion of this production to neighboring locations in the Southeast (Schneider, 2011).

The expansion of pigs farming within the Chinese territory gave rise to a situation of nutrition transition in the country. The traditional Chinese diet, composed of eight parts of grains, one part of vegetables and one part of proteins, has progressively been replaced by a western pattern of four parts of grains, three parts of vegetables and three parts of proteins (Huang, 2011). Considering annual proportions, meat consumption in China quadrupled between 1980 and 2010, when it reached an average of 61 kilograms per person in comparison to a world average of 42 kilograms (Escher et al., 2017).

As already mentioned, pigs farming in the country underwent a special change when China joined the WTO. Negotiations linked to its accession led China to give up on increasing taxes on soybeans imports as a food security strategy and to revise the import duty on the oilseed (Yan et al., 2016). Previously to revision, a 13% duty on the value of soybean imports was applied, which was reduced to 3% post-agreements (Jamet & Chaumet, 2016). Furthermore, legislative restrictions on the entry of transgenic grains were loosened, and transgenic soybeans import was authorized, although a ban on domestic cultivation was kept (Yan et al., 2016).

Table 2. Distribution of pork production covering 31 provinces, autonomous regions and municipalities on the Chinese mainland, 2020.

Province	Total Pork Production (million tons.)
Anhui	40,54
Beijing	0,29
Chongqing	10,75
Fujian	4,94
Gansu	11,63
Guangdong	12,41
Guangxi Zhuang	13,32
Guizhou	10,51
Hainan	1,45
Hebei	37,39
Heilongjiang	75,03
Henan	66,95

Table 2. *Cont.*

Province	Total Pork Production (million tons.)
Hubei	27,25
Hunan	29,75
Inner Mongolia	36,53
Jiangsu	37,06
Jiangxi	21,57
Jilin	38,78
Liaoning	24,3
Ningxia Hui	3,73
Qinghai	1,06
Shaanxi	12,31
Shandong	53,57
Shanghai	0,96
Shanxi	13,62
Sichuan	34,99
Tianjin	2,23
Tibet	1,04
Xinjiang	15,27
Yunnan	18,7
Zhejiang	5,92

Source: Data adapted from the National Bureau of Statistics of China (NBSC).

Nonetheless, duty reduction affected only whole grain imports, evidencing a preference for the entry of unprocessed raw materials to which domestic processing could add value (Escher, 2016). The amount of processed grain bran increased from eight million tons in 1997/1998 to 54 million tons in 2014/2015. The industrial production of feed, which still had no records in the 1980s, reached 200 million tons in 2012—the largest production in the world (Jamet & Chaumet, 2016). This point highlights the importance of animal protein production as a value-adding channel (Weis, 2013).

Regarding characterization of the processing sector, until 2004 most companies were Chinese. In that year, international instabilities in the grain price—due to increased phytosanitary control by China, the country's accession to WTO and the crisis in global supply—affected the sector's profitability (Schneider, 2011). Consequently, several local companies lost market position for failing to pay back foreign loans. In this context, international actors such as ADM, Bunge, Cargill and Louis Dreyfus, as well as Asian groups like Noble, Olam and Wilmar, occupied major positions in processing operations in the country. In 2009, these groups controlled 60% of total soybean crush in China (Escher & Wilkinson, 2019). Afterward, especially because of workers' mobilizations, the State reintroduced incentives for national companies. So, in 2016, local companies such as

COFCO, Heilongjiang Oil and Fat, Hopefull Grain and Oil, Chongqing Gran and Shandong Bohai regained economic and social influence, accounting, in that year, for 60% of crush operations (Escher, 2016). Between 2000 and 2018, the total amount of soybeans imported into China grew by 745.24%, being the fourth product in absolute total amount in annual imports—behind other raw materials such as coal and cotton, according to NBSC data.

These described trade processes took place under different formal and informal institutional layers. Changes in import tariffs required by WTO, diplomacy between different nations and construction of logistical channels are some of the most apparent elements of this construction. Throughout the 20th century, for example, policies were implemented by China's government aimed at establishing diplomatic ties with countries in the global South so that to guarantee supply for its import needs (Furtado & Alves, 2020). It was in this context that trade between Rio Grande do Sul and China developed—a topic addressed in the next section.

4. The Grain-meat Complex, Rio Grande do Sul and China

Since the 1980s, commercial relations between China and Brazil have been progressively closer (Furtado & Alves, 2020). Considering the soybean case, although direct investments have been made in both greenfield and brownfield projects (Escher & Wilkinson, 2019), the main results are found in exports. Taking data of FAOSTAT for the 21st century as reference, soybean exports increased from US $390 million in 2000 to US $27 billion in 2018. For comparison, corn crop exports reached a peak of US $59 million in 2015, a quite small figure as compared to soybeans. It is in this context that trade relations between China and Rio Grande do Sul intensified.

Throughout the 1970s to 1990s the main importers of goods from Rio Grande do Sul were in Europe—Germany standing out. According to ANTAQ data, total exports through the Port of Rio Grande added up less than six million tons per year and were scattered among several countries. As for the characterization of these exports, soybeans already comprised most of them, though in the form of bran. In 1980, considering exports volume, soy bran was the leading exported good, totaling 2.24 million tons, followed by soybeans, with 719 thousand tons. In the Port of Porto Alegre, although total trade flows did not exceed two million tons, soy bran was predominant with 119,000 tons exported.

The characterization of trade flows from Rio Grande do Sul reveals that, in the Second Food Regime, crops initially linked to the central economies spread to the periphery of the economic system (McMichael, 2016). After the second half of the 20th century, especially, such process spread to Latin American countries (Bertrand et al., 1987).

Soybean international market changed in the turn of the century, enabling the entry of Rio Grande do Sul. As Furtado and Alves (2020) point out, in 2004 China's acting president, Hu Jintao, visited Latin America and established diplomatic and commercial agreements that were expanded in the following years. As shown in Figure 2, in 2004 other countries were still the predominant destination of RS' exports—Thailand and Turkey stood out. In the following year, South Korea was the largest importer. After 2006, however, China became the destination of most soybean exports from RS—in 2014, for example, 77% of cargo were destined to China.

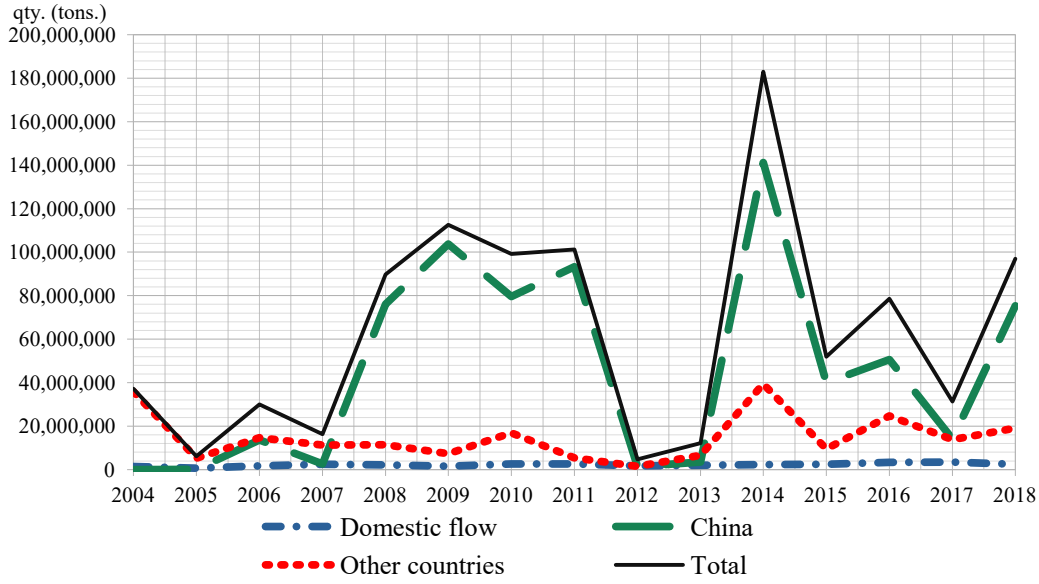

Figure 2. Volume of soybean exported from Rio Grande do Sul by destination, 2004–2018. Source: Elaborated by the authors based on Trase and ComexStat, several years.

Figure 2 also reveals the low participation of soybean domestic consumption, highlighting the agri-export character adopted for the crop. In addition to soybeans quantitative growth, its share in the state's Gross Domestic Product (GDP) is also rising. According to ComexStat data, between 2000 and 2015, while total trade flow for Rio Grande do Sul increased by 29.4%, soybeans trade flow alone grew by 344.88% demonstrating that a significant part of the region's total exports growth was due to soybean expansion. It is worth noting that until 2005 the main soybean products were flour and bran. In the following years, due to both the Kandir Law and the Chinese preference for unprocessed grains, unprocessed soybeans became predominant, with negligible values for soybean oil, sauces and proteins.

It also important to note that, during the 2000s, China strategically shifted its primary source of soybeans from the US to Brazil as part of a deliberate effort to diversify its suppliers and reduce reliance on any single country for this crucial commodity. This transition was driven by China's aim to safeguard its food sovereignty and construct an economic framework less dependent on US dominance in the commodity market. The increasing significance of soybeans for food security and economic stability compelled China to establish a more resilient supply chain. Brazil's emergence as a major soybean producer with ample production capabilities provided a fitting solution to China's strategy. By diversifying its soybean sources and diminishing dependence on the US, China pursued a more balanced and secure trade structure, aligning with its broader economic and geopolitical goals (Furtado & Alves, 2020; McMichael, 2009).

In this context, the correlation between institutional aspects (diplomatic agreements and revision of tariffs on imports) and trade practices (China as main destination and kind of exported products) stands out. These factors reveal the social context of inclusion in this particular market (Azevedo, 2016). Such correlation can also be established by observing the actors in the supply chain. From a global perspective, the grain flow was historically controlled by four transnational corporations: the US ADM and Cargill, the Dutch Bunge and the French Louis Dreyfus (Bertrand et al., 1987; Lemos et al., 2017);. Nowadays, Singaporeans Wilmar and Olam and the Chinese Noble and COFCO show significant international growth (Escher, 2016). The emphasis on these conglomerates' points to international actors with huge social, political and economic influence on the grains market, therefore enjoying primacy over other links in the supply chain, both horizontally and vertically. Understanding existing power disparities is essential for finding out the conditions under which different actors can operate.

Considering the companies involved in soybean trade flow between Rio Grande do Sul and China, Bunge is leading in soybean exports in the South region, according to Trase.earth. Between 2004 and 2018 (period available in the database), the corporation accounted for 36.24% of the total 704 million tons exported. Regarding the other companies that follow Bunge as the main exporters, there are two from the United States, CHS Inc., accounting for 10.60% of soybean exports, and Cargill, with 1.06%. All other companies are originally Brazilian, among which C. Vale (22.10%), Camera (6.89%), Três Tentos (6.33%), Giovelli (0.98%) and José Dinon (2.56%) have their origins

in Rio Grande do Sul. Also worth mentioning is Amaggi (1.64%), a Brazilian group with growing presence in the global soybean supply chain.

Similar picture is observed in the composition of China's importers of soybeans from Rio Grande do Sul. Bunge appears again as a central player in the supply chain, with 38.72% of the 704 million tons imported. Among the other companies, the Brazilian Amaggi stands out (5.07%), reaffirming its participation in the international market. The other importers have varied origins: the Japanese Marubeni (18.52%), US CHS (10.58%), Cargill (8.41%) and Engelhart (5.05%), Bulgarian Agrograin (2.89%), Swiss Glencore (1.95%), Chinese COFCO (1.40%) and Portuguese Concordia (0.62%). Therefore, the grain that enters China is processed by actors of different nationalities.

It is worth noting that the Chinese company COFCO has recently started operations in Rio Grande do Sul. The company, that is controlled by the Chinese State, acts as a guide of national policies to guarantee internal soybean prices and pigs' production. Its operations occur in tandem with State interests by acting internationally as a preponderant actor and strategically for the maintenance of the Chinese national economy (Escher & Wilkinson, 2019).

Besides those mentioned companies, throughout the studied period 94 companies exported soybeans from Rio Grande do Sul to China. In China, in turn, there were 63 importing companies. Despite the considerable number of actors, most of the traded grains was traded by the most powerful actors, what brings back the argument on disparate powers between actors, which can be perceived in two operational strands: the control of international logistics and the influence on the established price of the grain.

Regarding destination of goods, when asked about the group's commercial operation in the soybean market, Interviewee 1 replied: "Today we only work with the domestic market. We do not work with foreign markets. It is because of the size of the cooperative... We are unable to complete a ship load [...]. We already worked, a few years ago, within a pool of companies, cooperatives, non-cooperatives... And then there was a quality problem! We are all together in this process and then, one does everything right, another one doesn't and then, it delays... you can't ship because the quality is not adequate. The ship delays. At that time, it was $25,000 a day. It delays, and then what? So, what did we do? We gave up group working, because you get into trouble if the other doesn't play its part, right? So, what do we work on today? Most of it goes to the foreign market, but it's through trading, right? One of those international players. That's how we work … It goes to there." (Interviewee 1)

The interviewee points out that the cost of hiring a vessel makes it unfeasible for the cooperative—with around 5,300 members—to operate privately in exports. Despite the possibility of cooperation among smaller actors, the narrative emphasizes that factors such as trust and commitment affect practices in this direction. Hence, the most powerful actors in the supply chain take control of trade flows.

Such trade flows are also permeated by relationships of trust and security between actors and their practices (Cassol, 2018). Elements that are apparent in the response of Interviewee 2, when asked about the grain acquisition regime: "We work with 92%, 8% would come from third parties. But we work with third parties [...]. When we are able to store, whether we have a space or not... It is how we work. So, the primacy is for associate producers. Of course, we have the problem that cooperatives have a surname—the associate producer, when you go to a cereals wholesaler, nobody says that the wholesaler 'A' went bankrupt there... you know, in the cooperative system many cooperatives ended up going bankrupt, right? Closing here in our region [...] 'I've already lost money with a cooperative, I don't want to!', so there's all that when we go to a new region to gain associates, right? So, it's not that simple, is it? That's why I always talk to the farmer and say, 'Look how many wholesalers have gone bankrupt, have also let them down'. Then he said he no longer would deliver to a cooperative; so, I said, I said in a meeting: 'Sir, and how many cereal wholesalers have already gone bankrupt in the region? But these don't have a surname, right? If you act so, will you have to stop planting because you will have no one to sell your produce.' You must trust someone, you will see that there are cooperatives and cooperatives, there are manufacturers and manufacturers, there are exporters and exporters [...]" (Interviewee 2)

The interviewee's account brings three elements connected with trust. The first is the relationship between associate members and their cooperatives. Beyond a cooperative's interest in associating farmers aiming at its economic viability (Da Ros, 2006), the certainty about adopted farming procedures by members guarantees that the goods will be as required by the export market. The second element relates to the "cooperative surname", which means that the company has a history and responds in the present for historical processes. This symbolic relationship refers, beyond a specific cooperative, to the construction of discourses about the idealized category, which generically permeate actors' perception of risks in negotiation. And third, stemming from the latter, the interviewee highlights how the duality between trust and distrust affects the relationships between the links in the supply chain—whether manufacturers, exporters or producers— indicating

a context in which organizations operate within a framework conditioned by the relationships between actors and sometimes waiving profit maximization in the face of uncertainties.

As regards grain prices establishment, financialization plays a central role by means of two mechanisms. The first is the relation between grain pricing and the dollar standard as a fiduciary currency, reaffirming US primacy over the international structure initiated during the Second Food Regime (McMichael, 2016). The second regards the establishment of prices by financial platforms that project pricing based on the Chicago Board of Trade (CBOT), a board of trade located in the United States that intermediates the different indices of values and transactions—therefore, again related to financialization (Ávila, 2015). In this context, Brazilian producers face price variations directly affected by international fluctuations in currency and grain prices.

Exchange rates and price fluctuations through financialization are anchored in the temporal logic promoted by capitalism. According to Beckert (2017), the current economic system produces a relation between actors and the environment that is based on monetary gains on available items and on the constant projection of the future as linked to the expansion of material availability. This opens up the possibility that different actors relate to agricultural commodities aiming exclusively at speculative gain. According to Clapp (2014), the financial element gets disconnected from the material element on which it is based. As a result, price volatility, unequal distribution and environmental damage become secondary factors in the rationality shaped by the expectation of future gain.

In soybean supply chain, this practice is noticeable when companies concentrating a large part of transactions (ABCD) are in the ascendant in the financial market. All of them have branches dedicated exclusively to shares acquisition and transaction. Besides direct speculation on the grain's value and possibilities for future contracts, they also operate in different food segments, benefiting from informational advantages on production, processing and distribution sectors (Clapp, 2014).

According to an interviewee, costs related to logistics, storage and taxes add to international pricing. Therefore, price received by growers in Rio Grande do Sul is affected by both international dynamics of grain price fluctuation and regional dynamics of logistics costs (Ávila, 2015). Domestic market flow is affected by the international pricing, since the export price will determine the better profitability in directing the goods either inside or outside the country. This factor also affects the market of processed products—such as soy oil—since it implies the opportunity cost linked to the raw material.

Regarding actors' possibilities of influencing international price, when referring to China's economic power in the market, the same interviewee stated: "When it wants something, it eases off, slows down, right?" (Interviewee 3). Thus, changes in prices are not only determined by dynamics related to balance between supply and demand, but also by the agency of central actors in promoting or withdrawing trade at certain times.

The quoted statement underlines that the economic maintenance of soybean farmers in Rio Grande do Sul becomes dependent on international elements based on financialized fluctuation. That is, the production structure depends on means under control of preponderant actors in the international sphere. Therefore, the formation of the institutional environment is an outcome of macroeconomic dynamics operated by transnational conditions combined with processes linked to the locality—such as relationships of trust. These elements show the correlation between institutions and the trajectory of constitution of the places under analysis (Hodgson, 2008). It is observed that components linked to both structural and local dimensions limit operational possibilities related to the trade flow while immersed in different dimensions of social practices (Cassol, 2018). Consequently, actors in Rio Grande do Sul (producers, traders and public administration) operate within margins imposed by economic dynamics to which they acquiesce.

Building on this, the developed argument regarding the soybean trade between Rio Grande do Sul and China illustrates the food regimes approach (McMichaeL 2016; Friedmann, 2005). Soybean production in southern Brazil emerged in a period when agriculture became fundamental for accumulating capital and guaranteeing exchange rate stability—the so-called second food regime (McMichael, 2016). In this context, animal protein was fostered as a food source for western populations, with soybeans playing a crucial role in this production. Intensive animal production boosted feed manufacturing, creating a continuous market for soybeans and corn. As a result, meat, eggs and milk processing, packaging and transporting companies grew rapidly (Friedma & McMichael, 1989).

In the 1970s, the oil crisis increased the costs of international logistics and boosted the search for alternative use of grains, such as biodiesel, causing a rise in commodity prices. Countries indebtedness related to US technological packages significantly increased and other players emerged in the international grain market, such as Brazil, Argentina and the Soviet Union (Bernstein, 2016).

During this period, the system was restructured following two interconnected changes. The first was the end of exchange rates based on the gold convertibility of the dollar, replaced by flexible exchange rates. The second was the furthering of the General Agreement on Tariffs and Trade (GATT), which, together with the promotion of neoliberalism by other entities, allowed large conglomerates to act internationally without depending on state power. This occurred because tariffs, legislation and incentives began to be considered by multilateral organizations (McMichael, 2016). Thus, throughout the 1980s, a new phase of agri-food circulation emerged, marked by decrease in the power of States and expansion of corporate dominance—the Third Food Regime (Bernstein, 2016).

In the context here analyzed, Brazilian revision of duties on unprocessed raw materials—through Kandir Law—and adoption by China of internationally standardized prices for soybeans are examples of those changes. As is the predominance of international conglomerates in agricultural trade flow between Rio Grande do Sul and China. Although this finding does not deny the relevance of the role of States, it highlights that most disputes occur under coordination of private capital actors. The case of the Chinese company COFCO exemplifies this situation: the company, with state support, compete with other international conglomerates for export markets and, simultaneously, support policies designed by the Chinese State.

The various international influences—transnational conglomerates, States and multilateral bodies—have created environments within which particular formal and informal norms circumscribe the possibilities of economic practices (Hodgson, 2006), thus corroborating the postulation of markets as a result of historically rooted institutional processes, with contemporary correlations of operationalization, surrounded by values, laws and culture (Azevedo, 2016) and conditioned by their historical and geographic dimensions (Hodgson, 2008). Hence, we can infer that the studied market only occurs in the form observed because it is the result of processes characteristic of RS (and, indirectly, of Brazil) and of specific and characteristic Chinese processes—dynamics that, in turn, characterize and condition the actors' way of acting and positioning themselves. However, these practices also interact with relationships of trust and synergy between the elements. Therefore, two layers, sometimes complementary and sometimes contrasting, characterize the economic positions of different actors: one structural and the other local (Cassol & Schneider, 2022; DiMaggio & Louch, 1998). Both dimensions exist in a dialectical regime of influence and coordination of collective actions.

In summary, the soybean trade between Rio Grande do Sul and China is marked by institutions comprising formal layers (laws, policies, international agreements) and informal layers (culture, habit, trust) that define the environment where individuals operate, circumscribing their actions. Such institutions, in turn, originate from the historical dialectics of power relations in both geographic contexts and between them. Processes that were illustrated making use of the food regimes approach, by characterizing global agrifood flows over the last century. In this environment, the analyzed market emerges as an amalgam of formal and informal institutions, immersed in both local and structural dynamics in their different dimensions.

5. Final Remarks

Based on the presented data, we bring the three guiding questions back, seeking possible inferences: How does soybean export supply originate and is organized by the state of Rio Grande do Sul? How does China's soybean demand in the international market originate and is organized? What elements permeate trade flows between both regions?

Regarding the first question, Rio Grande do Sul appears as being historically characterized as an economy aligned with an agri-export model and having a strong relationship—albeit not exclusive—with the soybean market. A factor reinforced throughout the state's history and maintained in contemporary times by action of local actors (for instance, cooperatives inciting farmers to grow wheat and replace it with soybeans), through international reverberations (fluctuation in grain prices and the corresponding economic advantage) and through State support (lines of agricultural credits, technological financing packages and integration into market). Rio Grande do Sul supplies the foreign market with unprocessed grains (boosted by Kandir Law) and its trade flow is centered in the Port of Rio Grande. Such dynamics are related to an identity associated with agribusiness, similarly to the country, and to public costs incurred, especially in infrastructure, resulting from the expansion of cargo transports and the reduced fiscal contribution of the sector to the state.

As to the second question, we noted that the Chinese demand for soybeans stem from two related dynamics. On the one hand, China's development plan exploited the international economy as a factor aligned with domestic strategies, especially by using foreign trade to guarantee food security. On the other hand, international trade flows are guided by cooperation between the Chinese State and conglomerates linked to the grain-meat complex, seeking mutual gains. As a result, China facilitated soybean imports to fulfil terms of accession to the WTO. Such imports

were used as a source for domestic capital accumulation through promoting consumption of animal protein—especially pigs —a market in which large transactional corporations found a lucrative operating space.

The third question relates to mass production of commodities throughout the 21st century, based on the possibility of externalizing phenomena linked to the production cycle—which brings social and, mainly, environmental consequences. Soybean production and distribution rely on public investment—maintenance of local infrastructure and credit channels, for example. Something also promoted by international conglomerates linked to the grain-meat complex. It is through the agency of international private capital that certain consumption practices were developed throughout the 20th century, resulting in contemporary trade channels linked to soybeans. For example, in trade flow between Rio Grande do Sul and China, particularly, one of the identified conglomerates was responsible for a third of the total volume traded. Circumstances that also lead to financialization, turning soybeans into a prospect of both real and fictitious profit. Such elements give rise to the social character of the soybean market, since its existence is subject to structural arrangements—such as the guarantee of financialized operations based on floating exchange rates and international pricing—and local ones—as trust between actors in the supply chain and in construction of identities.

This article warns of the urgency of considering production sectors as immersed in their contexts and linked to local dynamics. Therefore, it points to the need for economic flows to be considered as social processes and, so, for public policies and civil society actions to devise economic integration alternatives based on the premise that all practices are exclusively based on human sociability.

CRediT Author Statement: Ângelo Belletti: Conceptualization, Methodology, Data curation, Writing – original draft, Visualization and Writing – review & editing; **Sérgio Schneider:** Conceptualization, Methodology, Supervision and Writing – review & editing.

Data Availability Statement: Not applicable.

Funding: This research was funded by FAPERGS – Foundation for Research Support of the State of Rio Grande do Sul, Brazil (Call FAPERGS/CAPES 06/2018, 19/2551-0000724-8), and CNPQ – National Council for Scientific and Technological Development, Brazil (Master's Scholarship).

Conflicts of Interest: The funders had no role in the design of the study; in the collection, analyses, or interpretation of data; in the writing of the manuscript, or in the decision to publish the results.

Acknowledgments: Not applicable.

References

Ávila, D. F. (2015). *A influência da Bolsa de Chicago e do câmbio na formação do preço médio da soja praticada no Estado do Rio Grande do Sul* (Brasil), 1999 –2013. [Master Thesis,Universidade Regional do Noroeste do Estado do Rio Grande do Sul].

Azevedo, P. F. (2016). Emergência de Instituições de Mercado: A criação de mercados como política para a agricultura. In F. C. Marques, M. A. Conterato & S. Schneider (Eds.), *Construção de Mercados e Agricultura Familiar: Desafios para o Desenvolvimento Rural* (pp. 209–229). UFRGS.

Beckert, J. (2017). Reimaginando a dinâmica capitalista: Expectativas ficcionais e o caráter aberto dos futuros econômicos. *Tempo Social*, 29, (1), 165–185. https://doi.org/10.11606/0103-2070.ts.2017.119003

Benetti, M. D. (2004). A internacionalização real do agronegócio brasileiro—1990-03. *Indicadores Econômicos FEE*, *32*(2), 26.

Bernstein, H. (2016). Agrarian political economy and modern world capitalism: The contributions of food regime analysis. *Journal of Peasant Studies*, *43*(3), 611–647. https://doi.org/10.1080/03066150.2015.1101456

Bertrand, J. P., Laurent, C., & Leclerq, V. (1987). *O mundo da soja*. Editora USP.

Cassol, A. P. (2018). Instituições sociais e mercados alimentares tradicionais: Barganha, preços, variedade, qualidade e consumo em feiras. [Doctoral dissertation,Universidade Federal do Rio Grande do Sul].

Cassol, A., & Schneider, S. (2022). A imersão social da economia em mercados alimentares brasileiros: Uma abordagem institucionalista. *Revista de Economia e Sociologia Rural*, *60*(2). https://doi.org/10.1590/1806-9479.2021.233766

Chen, G. (2019). Introduction: Zhejiang's social development and the Chinese dream. In G. Chen & J. Yang (Eds.), *Chinese dream and practice in Zhejiang-Society*. (pp. 1–32). Springer.

Clapp, J. (2014). Financialization, Distance and Global Food Politics. *Journal of Peasant Studies*, *41*(5), 794 –814. https://doi.org/10.1080/03066150.2013.875536

Da Ros, C. A. (2006). *As políticas agrárias durante o Governo Olívio Dutra e os embates sociais em torno da questão agrária gaúcha (1999–2002)*. [Doctoral dissertation, Universidade Federal Rural do Rio de Janeiro].

Delgado, G. (2013). *Do "capital financeiro na agricultura" à economia do agronegócio: Mudanças cíclicas em meio século (1965–2012)*. UFRGS.

Dimaggio, P., & Louch, H. (1998). Socially embedded consumer transactions: For what kinds of purchases do people most often use networks? *American Sociological Review*, *63*(5), 619–637.https://doi.org/10.2307/2657331

Escher, F. (2022). A economia política do desenvolvimento rural na China: Da questão agrária à questão agroalimentar. *Revista de Economia Contemporânea*, *26*, 1–29. https://doi.org/10.1590/198055272610

Escher, F. (2016). *Agricultura, Alimentação e Desenvolvimento Rural: Uma análise institucional comparativa entre Brasil e China*. Doctoral dissertation, Universidade Federal do Rio Grande do Sul].

Escher, F., Schneider, S. & Ye, J. (2017). The agrifood question and rural development dynamics in Brazil and China: Towards a protective countermovement. *Globalizations*, *15*(1), 92–113. https://doi.org/10.1080/14747731.2017.1373980
Escher, F., & Wilkinson, J. (2019). A economia política do complexo Soja-Carne Brasil-China. *Revista de Economia e Sociologia Rural*, *57*(4), 656–678. https://doi.org/10.1590/1806-9479.2019.191017
Friedmann, H. (2005). From colonialism to green capitalism: Social movements and food regimes. In F. H. Buttel & P. McMichael (Eds.), *New directions in the sociology of global development* (pp. 227–624). Emerald Group Publishing Limited. https://doi.org/10.1016/S1057-1922(05)11009-9
Friedmann, H., & McMichael, P. (1989). Agriculture and the state system: The rise and decline of national agricultures, 1870 to the present. *Sociologia Ruralis*, *29*(2), 93–117. https://doi.org/10.1111/j.1467-9523.1989.tb00360.x
Furtado, P. C., & Alves, V. E. (2020). "Investimentos chineses, reestruturação produtiva e transformações no espaço agrário do bioma de Cerrados do Centro Norte do Brasil." *Revista OKARA*: Geografia em debate, *14*(2), 473–492.
Conçalves, O. A. (1984). *A expansão da soja no Rio Grande do Sul* (1950–1975). Porto Alegre.
Yan, H., Chen, Y., & Bun, K. (2016). China's soybean crisis: The logic of modernization and its discontents. *Journal of Peasant Studies*, *43*(2), 373–395. https://doi.org/10.1080/03066150.2015.1132205
Han, M., Yu, W., & Clora, F. (2022). Boom and bust in China's pig sector during 2018–2021. *Sustainability*, *14*(11), 6748. https://doi.org/10.3390/su14116784
Hodgson, G. M. (2006). What are institutions? *Journal of Economic Issues*, *40*(1), 1–25.
Hodgson, G. M. (2008). Darwinismo e ciências sociais: um diálogo possível. *Estudos Avançados*, *22*(63), 271–280. https://doi.org/10.1590/S0103-40142008000200020
Huang, P. C. C. (2011). China's new age small farming and their vertical integration: Agrobusiness or co-ops? *Modern China*, *37* (2), 107–135. https://doi.org/10.1177/0097700410396476
Jabbour, E. M. (2010). Projeto Nacional, Desenvolvimento e Socialismo de Mercado na China de hoje. [Doctoral dissertation, Universidade de São Paulo].
Jamet, J. P., & Chamet, J. (2016). Soybean in China: adapting to the liberalization. *OCL*, *23*(6), D604. https://doi.org/10.1051/ocl/2016044
Lander, B., Schneider, M., & Brunson, K. (2020). A history of pigs in China: From curious omnivores to industrial pork. *Journal of Asian Studies*, *79*(4), 865–889. https://doi.org/10.1017/S0021911820000054
Lemos, M. L., Guimarães, D. D., Maia, G. B. D. S., & Maia, G. B. (2017). *Agregação de valor na cadeia da soja*. Relatório BNDES Setorial. https://web.bndes.gov.br/bib/jspui/bitstream/1408/14138/2/BNDES-Setorial-46_Soja_P_BD.pdf
McMichael, P. (2009). A food regime genealogy. *The Journal of Peasants Studies*, *36*(1), 139–169. https://doi.org/10.1080/03066150902820354
McMichael, P. (2016). *Regimes Alimentares e Questões Agrárias*. Editora UFRGS.
Oliveira, G. d. L. T. (2016). The geopolitics of Brazilian soybeans. *The Journal of Peasant Studies*, *43*(2), 348–372. https://doi.org/10.1080/03066150.2014.992337
Pereira, J. M., & Alentejano, P. (2015). El agro brasileño: de la modernización conservadora a la hegemonia del agronegocio. In G. Almeyra, L. Bórquez, & J. M. Pereira (Eds.). *Capitalismo, tierra y poder en America Latina*. Ediciones Continente.
Van der Ploeg, J. D. (2018). *The new peasantries*: *rural development in times of globalization*. Routledge.
Schneider, M. (2011). *Feeding China's Pigs: Implications for the environment, China's smallholder farmers and food security*. Institute for Agriculture and Trade Policy.
Schneider, M., & Sharma, S. (2014). *China's pork miracle? Agribusiness and development in China's pork industry*. Institute for Agriculture and Trade Policy.
Schneider, S. (2016). Mercados e Agricultura Familiar. In F. Marques, M. Conterato, & S. Schneider (Eds.), *Construção de mercadose agricultura familiar: desafios para o desenvolvimento rural* (pp. 93–142). Porto Alegre.
Schneider, S., Schubert, M. N., & Escher, F.(2016). "Regimes Agroalimentares e o lugar da agricultura familiar–umaapresentação ao debate." *Revista Mundi Meio Ambiente e Agrárias*, *1*(1), 1–20.
Guriqbal Singh, G. S. & Shivakumar, B. G. (2010). The role of soybean in agriculture. In G. S. Guriqbal Singh. *The Soybean: Botany, production and uses*. Punjab Agricultural University.
Vander Vennet, B., Schneider, S., & Dessein, J. (2016). Different farming styles behind the homogenous soy production in southern Brazil. *Journal of Peasant Studies*, *43*(2), 396–418. https://dx.doi.org/10.1080/03066150.2014.993319
Weis, T. (2013). The meat of the global food crisis. *Journal of Peasant Studies*, *40*(1), 65–85. https://doi.org/10.1080/03066150.2012.752357
Wesz Junior, V. (2014). O mercado da soja e as relações de troca entre produtores rurais e empresas no Sudeste de Mato Grosso (Brasil). [Doctoral dissertation., Universidade Federal Rural do Rio de Janeiro].
Zhang, Q. F., & Donaldson J. (2008). The rise of agrarian capitalism with Chinese characteristics: agricultural modernization, agribusiness and collective land rights. *China Journal*, 60, 25–47.
Zhang, Q. F., & Zeng, H. (2021). Politically directed accumulation in rural China: the making of the agrarian capitalist class and the new agrarian question of capital. *Journal of Agrarian Change*, *21*(4), 677–701. https://doi.org/10.1111/joac.12435
Zhang, Q. F., & Zeng, H. (2022). Producing industrial pigs in southwestern China: The rise of contract farming as a coevolutionary process. *Journal of Agrarian Change*, *22*(1),97–117. https://doi.org/10.1111/joac.12457

Agricultural & Rural Studies

Article

Analysis of Spatial Unbalance and Convergence of Agricultural Total Factor Productivity Growth in China—Based on Provincial Spatial Panel Data From 1978 to 2020

Chaozhu Li [1] and Xiaoliang Li [2,*]

[1] China Institute for Rural Studies, Tsinghua University, Beijing 100084, China; lizhaozhu326@tsinghua.edu.cn
[2] Jiyang College, Zhejiang A&F University, Zhuji 311800, China
* Correspondence: lixiaoliang@zafu.edu.cn

Abstract: Using the provincial panel data from 1978 to 2020 as the research object, this study employs the fixed effect SFA-Malmquist model to measure the agricultural total factor productivity of each province and city, and the spatial correlation of China's agricultural total factor productivity is determined by Moran's I. On this basis, three weights (adjacency, economy, geography) are included as spatial factors in three spatial β-convergence models (SAR, SEM and SDM), and the spatial convergence characteristics of China's agricultural total factor productivity are analyzed in different time periods and different regions. The study found that: First, China's agricultural total factor productivity shows a growing trend, but as time goes on, its growth rate gradually slows down, and the growth rate in the eastern region is higher than that in the central and western regions. Second, China's agricultural total factor productivity has significant spatial correlation and spatial convergence characteristics. The differences in agricultural total factor productivity in various regions are shrinking over time, and the spatial spillover effect significantly shortens the convergence process. Due to spatial convergence, while carrying out agricultural production, all regions should thoroughly consider the advantages of agricultural resources in neighboring regions and strengthen cooperation and exchanges between regions.

Keywords: agriculture; total factor productivity; spatial convergence; unbalance

Citation: Li, C.; Li, X. Analysis of Spatial Unbalance and Convergence of Agricultural Total Factor Productivity Growth in China—Based on Provincial Spatial Panel Data From 1978 to 2020. *Agricultural & Rural Studies*, 2023, *1*, 0010. *https://doi.org/10.59978/ar01020010*

Received: 8 May 2023
Revised: 18 July 2023
Accepted: 9 June 2023
Published: 5 September 2023

1. Introduction

Agricultural production is an important foundation for national stability and security (Hou & Yao, 2018). Since 1978, relying on the increase of factor input and the improvement of total factor productivity, China's agriculture has made great achievements. The output and productivity of all major agricultural sectors have increased rapidly (Gong, 2018b; Lin, 1992). It has created a miracle that less than 10 % of the world's arable land has fed 20 % of its population (Li, 2014). The total agricultural output increased from 111.8 billion yuan in 1978 to 7174.8 billion yuan in 2020. However, with the increasing scarcity of land resources, the shortage of rural labor force caused by the acceleration of urbanization, and the diminishing marginal returns caused by the continuous improvement of fertilizer and machinery inputs, the contribution of the increase in agricultural factor inputs to agricultural growth is constantly decreasing. The way to promote agricultural development by relying on factor inputs is unsustainable. Continuously improving agricultural total factor productivity has almost become the only choice (Gao, 2015; Yang & Yang, 2013).

Due to the critical role of total factor productivity (TFP) in agricultural production, TFP has become an essential focus of scholars at home and abroad. Scholars use different methods (parametric methods and nonparametric methods), different data (macro statistical data, micro survey data), and different production function settings (Translog production function or C-D function) to measure China's agricultural TFP to make an accurate judgment on the trend of China's agricultural TFP and its key influencing factors (Pan & Ying, 2012). Still, the existing research has not reached a more consistent conclusion. This difference is not only reflected in the measurement value of China's agricultural TFP (Wu et al., 2001; Xu, 1999). More importantly, they have severe differences in China's agricultural TFP trend after the 1990s (Gong, 2018a). Some scholars believe that the growth rate of China's agricultural TFP continued to increase in the late 1990s and began to slow down until 2000 (Nin Pratt et al., 2008; Wang et al., 2013). Other scholars believe that the

growth rate of China's agricultural TFP has slowed down since the 1990s (Chen et al., 2008; Zhou & Zhang, 2013).

In addition, since 1978, with the improvement of China's agricultural market and the continuous improvement of regional openness and exchange, the flow of agricultural production factors between regions has become increasingly frequent (Wu, 2010). Spatial factors have become a negligible factor affecting China's agricultural TFP, but few scholars have included spatial factors in the analysis of agricultural TFP (Wang et al., 2010). Productivity caused by differences in resource endowments and agricultural development levels in different regions spatially distributed? How will this spatial difference evolve? Does the difference in total factor productivity among regions show a convergence trend over time? If so, what form of convergence? What are the characteristics of convergence in different regions and stages of development? Therefore, the scientific measurement of China's agricultural TFP since 1978 and the analysis of its differences in spatial distribution and the convergence law over time will help to understand the growing trend of China's agricultural TFP since the reform and opening up. An objective understanding of the spatial differences and temporal evolution of agricultural TFP is of great significance for strengthening the scientific flow of agricultural production factors between regions, the sustainable development of China's agriculture, and the realization of modern agriculture.

2. Literature Review

Based on the critical role of TFP in China's agricultural development, scholars have conducted detailed and in-depth research on it, which has laid a good foundation for the writing of this paper. Throughout the existing literature, the research on China's agricultural TFP can be elaborated from three aspects: research methods, research contents, and research conclusions.

Research methods. Currently, the mainstream methods for measuring the TFP of China's agriculture are Data Envelopment Analysis (DEA) and Stochastic Frontier Analysis (SFA). Huo et al. (2011), Yang and Yang (2013), Wang and Zhang (2018) all used the DEA method to measure the TFP of Chinese agriculture. Considering that agricultural production is a complex process and will be affected by many factors in the production process, DEA can only consider the primary input and cannot attribute other factors to the residual term, which may affect measurement accuracy to a certain extent (Shi et al., 2016). For this reason, some scholars suggest using the SFA method to measure the TFP of China's agriculture. Quan (2009), Kuang (2012), Zhang and Cao (2013) began to use the SFA method to measure China's agricultural TFP. Although the total factor productivity measured by the SFA method is more in line with the characteristics of agricultural production, and the measurement results are better than DEA to a certain extent (Fan & Li, 2012), the existing literature on the measurement of agricultural TFP by SFA ignores the personal effect in the non-efficiency term, which may overestimate the technical efficiency, thus affecting the measurement results of TFP (Kumbhakar, 1990).

In the research content aspect, the scholars' research on agricultural TFP has been measured in detail from different levels, such as micro (Gao et al., 2016; Jia & Xia, 2017) and macro (Wang & Zhang, 2018), and the critical factors affecting TFP have been studied (Li & Yin, 2017; Zeng et al., 2018). However, the above studies regard different regions as independent individuals and do not include the inter-regional flow of production factors and the resulting spatial relationship. With the development of spatial econometrics and economic geography, some scholars began to consider the role of spatial factors in agricultural production. For example, Wang et al. (2010) used the spatial econometric model to study the growth of China's agricultural TFP and its influencing factors from 1992 to 2017. Yang and Yang (2013) studied the spatial correlation of China's agricultural TFP and concluded that the agricultural TFP in the adjacent areas has obvious spatial effects.

In terms of research conclusions, there are some differences in the existing research on the measurement value of China's agricultural TFP. For example, for the study of the average annual growth rate of China's agricultural TFP from 1981 to 1995, Xu (1999) showed that the average annual growth rate of the above interval was −1.48 %, while Wu et al. (2001) obtained an average annual growth rate of 2.41 %. In addition, scholars have significant differences in the trend of China's agricultural TFP after the 1990s (Gong, 2018a). Nin et al. (2008), Wang et al. (2013) believe that the growth rate of China's agricultural TFP continued to increase in the late 1990s, while Chen et al. (2008), Zhou and Zhang (2013) believe that the growth rate of China's agricultural TFP has slowed since the 1990s.

In summary, the existing literature can still be expanded from the following aspects. Considering that the SFA method has more advantages than DEA in the measurement of agricultural TFP, the existing research on the measurement of agricultural TFP using SFA ignores the individual effects in the non-efficiency term, so the SFA-Malmquist method with fixed effects can be used to solve this problem. In addition, with the strengthening of inter-regional exchanges, spatial factors play an increasingly important role in agricultural production. The convergence model considering spatial effects can deeply analyze the evolution of agricultural TFP in time and space. Based on

this, this paper will take China's provincial agricultural production data from 1978 to 2020 as the research unit and use the fixed effect SFA-Malmquist model, which can separate the individual effect and the non-efficiency term to re-measure China's agricultural TFP. On this basis, Moran's I and spatial convergence model are used to study the evolution of agricultural TFP in time and space and the influence of spatial factors on agricultural TFP.

3. Research Methods

3.1. Fixed Effect SFA-Malmquist Model

DEA and SFA are the mainstream methods to measure Total factor productivity (TFP), the Malmquist index is a specific index established by Caves et al. (1982) to measure the change in total factor productivity based on the Malmquist consumption index and Shepherd distance function. In practical research, the distance function in the Malmquist index is generally calculated by parametric methods (such as SFA) or non-parametric methods (such as DEA) and then decomposed (Shi et al., 2016). As mentioned before, the agricultural production process is affected by many factors. SFA can incorporate these random factors into the classical white noise term and has more advantages than the DEA method in measuring agricultural production efficiency. Considering that previous studies ignore the individual effects of regions, this may cause bias in the measurement results (Kumbhakar, 1990). Therefore, this paper will use the fixed effect SFA model proposed by Greene (2005) to measure technical efficiency (TE) and then use the Malmquist index decomposition method to obtain total factor productivity (TFP), technical change (TPCH), technical efficiency change (TECH). The basic model of SFA-Malmquist with fixed effect is as follows:

$$\ln Y_{it} = lnf\left(X_{it};\beta\right) + \alpha_i + v_{it} - \mu_{it} \tag{1}$$

Here, Y_{it} is the output of province i in t years, X_{it} is the input of i in t years, β is the parameter to be estimated, $f(\cdot)$ is the efficient production function, α_i is the fixed effect of the province, v_{it} is the random error term, and assume that $v_{it} \sim iid\mathcal{N}\left(0,\sigma_v^2\right)$, μ_{it} is the technical inefficiency term. The setting of $f(\cdot)$ has many forms in practical research. The C-D and Translog functions are the most commonly used function forms. To study the accuracy of this paper, the authors employed the LR test. LR test shows that the model in the form of the Translog function is more in line with the data of this paper. Therefore, Formula (1) can be rewritten as follows:

$$\ln Y_{it} = \beta_0 + \sum_j \beta_j lnx_{ijt} + t\times\beta_t + \sum_i\sum_l \beta_{jl} lnx_{ijt}\times lnx_{ilt} + t^2\times\beta_{tt} + \sum\beta_{jt} t\times lnx_{ijt} + \alpha_i + v_{it} - \mu_{it} \tag{2}$$

Technical efficiency (TE) can be expressed as:

$$TE_{it} = \exp\left(-\mu_{it}\right), 0 \le \exp\left(-\mu_{it}\right) \le 1 \tag{3}$$

According to the formula (3), the change of technical efficiency from t to t + 1 can be calculated and denoted as $TECH_i^{t,t+1}$,

$$TECH_i^{t,t+1} = TE_{i,\ t+1} / TE_{it} \tag{4}$$

The technical change ($TPCH_i^{t,t+1}$) can be derived from the derivation of formula (2). Because under the assumption of non-neutral technical change, technical change will change with the change of input, the technical change value of adjacent periods should be taken as the geometric average value, that is

$$TPCH_i^{t,t+1} = \exp\left(\frac{1}{2}\left(\frac{\partial ln Y_{it}}{\partial t} + \frac{\partial ln Y_{i,t+1}}{\partial\left(t+1\right)}\right)\right) \tag{5}$$

Considering that most scholars believe that agricultural production conforms to the characteristics of constant returns to scale (Xu et al., 2011), in addition, it is assumed that the TFP obtained under variable returns to scale will be affected by the scale of production (Liu & Meng, 2002). Therefore, under the condition of constant returns to scale, Malmquist index decomposition see formula (6),

$$TFP_i^{t,t+1} = TECH_i^{t,t+1} \times TPCH_i^{t,t+1} \tag{6}$$

3.2. Moran's I Index

Different regions have differences in agricultural TFP due to different resource endowments. However, according to Tobler (1970), "the first law of geography", there is a specific relationship between everything, and with the shortening of distance, this relationship will become closer and closer. (Tobler, 1970) A specific spatial correlation in agricultural TFP may exist. Therefore, testing the spatial correlation of agricultural TFP is crucial. This paper will use the most popular Moran's I to measure the spatial correlation of agricultural TFP in different regions. Moran's I can be expressed as:

$$\mathrm{I} = \frac{\sum_{i=1}^{n}\sum_{j=1}^{n} w_{ij}\left(x_i - \overline{x}\right)\left(x_j - \overline{x}\right)}{S^2 \sum_{i=1}^{n}\sum_{j=1}^{n} w_{ij}} \tag{7}$$

Where, $S^2 = \frac{\sum_{i=1}^{n}\left(x_i - \overline{x}\right)^2}{n}$ is the variance of the sample, w_{ij} is the spatial weight matrix, and x_i and x_j are the observed values of spatial positions i and j. The value of I is between −1 and 1, greater than 0 indicates positive spatial correlation, less than 0 indicates negative spatial correlation, and equal to 0 indicates no spatial correlation.

In this paper, three spatial weight matrices will be selected, which are geographical adjacency spatial weight matrix (W_1), economic distance spatial weight matrix (W_2) and spatial distance weight matrix (W_3).

Geographical adjacency space weight matrix: $w_1 = w_{ij} = \begin{cases} 1, & i \text{?} s\ adjacent\ to\ j \\ 0, & i \text{?} s\ not\ adjacent\ to\ j \end{cases}$

Economic distance spatial weight matrix: $w_2 = w_{ij} = \begin{cases} \dfrac{1}{\left|\overline{Y_i} - \overline{Y_j}\right|}, & i\ is\ adjacent\ to\ j \\ 0, ? & i = j \end{cases}$

Spatial distance weight matrix: $w_3 = w_{ij} = \begin{cases} 1/d, & i \neq j \\ 0, & i = j \end{cases}$

Among them, i and j represent region i and region j respectively, $\overline{Y_j}$ represents the average per capita real GDP of region j in the sample interval, and d represents the geographical distance between the provincial capitals of region i and region j.

3.3. Spatial Convergence Model

There are three classical convergence models, σ convergence, β convergence, and club convergence, among which β convergence is the most widely used. β-convergence can be divided into absolute β-convergence and conditional β-convergence. It mainly tests whether the growth rate of inter-provincial agricultural TFP converges. The main difference between absolute β-convergence and conditional β-convergence is that absolute β-convergence assumes that the resource endowments of each region are the same. In contrast, conditional β-convergence considers the differences in resource endowments in different regions, which is more in line with actual production activities (Zhang et al., 2015). Therefore, this paper will use β convergence to test the convergence of agricultural TFP, and compare the difference between absolute β-convergence and

conditional β-convergence. The classical conditional β-convergence model is shown in formula (8). If $\sum_{k=1}^{n}\theta_k lnX_{k,i,t}$ is removed, it is absolute β-convergence.

$$\ln TFP_{i,t+1} - \ln TFP_{i,t} = \alpha + \beta \ln TFP_{i,t} + \sum_{k=1}^{n}\theta_k lnX_{k,i,t} + \varepsilon_{i,t} \tag{8}$$

Since the traditional β-convergence model does not consider the spatial influence, the convergence conclusion is biased (Yu, 2015). Therefore, this paper constructs a β-convergence model considering spatial factors and compares the differences between the traditional β-convergence model and the spatial β-convergence model. Since spatial models can be divided into the spatial autoregressive model (SAR), spatial error model (SEM), and spatial Dubin model (SDM), the corresponding β-convergence models considering spatial factors can be divided into the following three types:

The β-convergence model of SAR:

$$ln\frac{TFP_{i,t+1}}{TFP_{i,t}} = \alpha + \rho\sum_{j=1}^{n} w_{ij} ln\frac{TFP_{j,t+1}}{TFP_{j,t}} + \beta \ln TFP_{i,t} + \sum_{k=1}^{n}\theta_k lnX_{k,i,t} + \varepsilon_{i,t} \tag{9}$$

The β-convergence model of SEM:

$$ln\frac{TFP_{i,t+1}}{TFP_{i,t}} = \alpha + \beta \ln TFP_{i,t} + \sum_{k=1}^{n}\theta_k lnX_{k,i,t} + \varphi_{i,t}; \varphi_{i,t} = \rho\sum_{j=1}^{n} w_{ij}\varphi_{i,t} + \varepsilon_{i,t} \tag{10}$$

The β-convergence model of SDM:

$$ln\frac{TFP_{i,t+1}}{TFP_{i,t}} = \alpha + \rho\sum_{j=1}^{n} w_{ij} ln\frac{TFP_{j,t+1}}{TFP_{j,t}} + \beta \ln TFP_{i,t} + \sum_{k=1}^{n}\theta_k lnX_{k,i,t} + \varnothing_k \sum_{j=1,k=1}^{n} w_{ij} lnX_{k,i,t} + \varepsilon_{i,t} \tag{11}$$

Among them, $TFP_{i,t}$ and $TFP_{i,t+1}$ are the agricultural TFP of province i in period t and period $t+1$, respectively, and β is the convergence judgment coefficient. If β is significantly negative, it indicates convergence, and the convergence speed ω can be calculated according to $\beta = -(1-e^{-\omega T})/T$. θ_k is the estimated coefficient of the control variable $X_{i,t}$. When $\theta_k = 0$, it is absolute β-convergence. Otherwise, it is conditional β-convergence. $\varepsilon_{i,t}$ is a random error term and is assumed to satisfy $\varepsilon_{i,t} \sim iid\left(0, \sigma^2\right)$. ϱ is the spatial auto-regressive coefficient, $\varphi_{i,t}$ is the error term of spatial autocorrelation, and $\varnothing_k$ is the regression coefficient of the interaction effect between the control variable and the spatial weight matrix. w_{ij} is the spatial weight matrix.

4. Index Selection and Data Sources

To conduct in-depth research on China's agricultural total factor productivity, the starting year of this study was selected as 1978, and all data were from the "China Statistical Yearbook", "China Rural Statistical Yearbook", "New China 50 Years Statistical Data Compilation". Considering the problem of merging Sichuan and Chongqing before, Chongqing is classified into Sichuan. Hainan, and Tibet, not within the scope of this study due to the lack of data. This paper finally obtains the panel data of 28 provinces and cities from 1978 to 2020 for 43 years.

In constructing the input-output index system for measuring agricultural TFP, this paper refers to the general treatment method of the existing literature (Gong, 2018a; Shi et al., 2016). It selects the number of employees in agriculture, forestry, animal husbandry, and fishery (ten thousand people), the sown area of crops (thousand hectares), the total power of agricultural machinery (ten thousand kilowatts), and the application amount of agricultural fertilizer (ten thousand tons) to represent the labor input, land input, capital input and intermediate input in the process of agricultural

production, respectively. Taking the total output value of agriculture, forestry, animal husbandry, and fishery (billion yuan) as output and conducted price index deflations based on the 1978.

By studying the existing literature on the selection of influencing factors of agricultural TFP and considering data availability. This paper selects the proportion of the affected area of crops to the affected area (Gong, 2018a), based on the per capita GDP after the deflator in 1978 (Zhang & Chen, 2015), the proportion of the urban resident population to the total population (Yang et al., 2017), the proportion of the total highway mileage to the land area of the province (Zhuo & Zeng, 2018), the proportion of the added value of the secondary industry to the GDP (Wang & Zhang, 2018), and the proportion of the effective irrigation area to the sown area of crops (Gong, 2018a), representing the disaster situation (Disas), economic development (Gdppc), urbanization level (Citil), transportation convenience (Trans), the development of the secondary industry (Indus) and irrigation level (Irrig). A total of 6 variables are used as the driving factors affecting the spatial and temporal changes of agricultural TFP.

5. Empirical Results and Analysis

5.1. The Measurement and Timing Analysis of China's Agricultural TFP

Before measuring the TFP of agriculture, this paper first analyzes the input-output data of provincial agricultural production from 1978 to 2020. The first two lines of Table 1 show the annual agricultural input-output level in 1978 and 2020. The last six lines show the agricultural input-output's average annual growth rate in different agricultural development stages. The total agricultural output value continued to increase throughout the study period, with an average annual growth rate of more than 4 %. Regarding input factors, the input of land, fertilizer, and machinery has shown an increasing trend. Only the labor input has shown a decreasing trend in individual stages. This is mainly due to the advancement of urbanization and industrialization. The large-scale transfer of rural surplus labor to the city has reduced the labor engaged in agricultural production.

Table 1. Input and output of agricultural production.

		Total Agricultural Output Value	Labour	Land	Fertilizer	Mechanics
		Billion Yuan	Ten Thousand People	Hectares	10000 Tons	10000 Kilowatts
Annual Value	1978	1397	28318	146379	884	11749.9
	2020	137782.2	17715	167487	5250.7	105622.1
Average Annual Growth Rate	1978–1984	6.9%	2.1%	9.4%	11.8%	9.4%
	1985–1989	6.2%	−0.4%	7.4%	7.4%	7.4%
	1990–1993	5.5%	0.6%	3.2%	7.5%	3.2%
	1994–1998	7.6%	0.3%	5.6%	5.9%	5.6%
	1999–2003	4.7%	−0.7%	5.1%	1.3%	5.1%
	2004–2020	4.5%	−1.0%	3.6%	1.9%	3.6%

Note: According to Gong (2018a)' s division of agricultural production stages, China's agricultural development since 1978 can be divided into six stages, namely, the transition period from a collective economy to a family-based agricultural system from 1978 to 1984, the dual-track system period from 1985 to 1989, the in-depth reform stage of the joint procurement and marketing system from 1990 to 1993, the tax and fee system reform stage from 1994 to 1998, the comprehensive economic reform period of rural development from 1999 to 2003, and the focus on the development period of agriculture, rural areas, and farmers from 2004 to the present.

The agricultural TFP of 28 provinces for 42 years from 1979 to 2020 was calculated using the fixed effects SFA Malmquist model in Stata software. It analyzes the development trend of China's agricultural TFP since 1979. Figure 1 shows the average annual growth rate of China's agricultural TFP. By observing the figure, it can be found that the Malmquist productivity index calculated each year is greater than 1, indicating that the TFP of China's agriculture has shown a growing trend in the past four decades. However, over time, the growth rate of agricultural TFP gradually slowed down, especially since 1993, the average annual growth rate of TFP began to decline, which also verified the previous research conclusions, that is, from the 1990s, the growth rate of China's agricultural TFP slowed down (Chen et al., 2008; Zhou & Zhang, 2013).

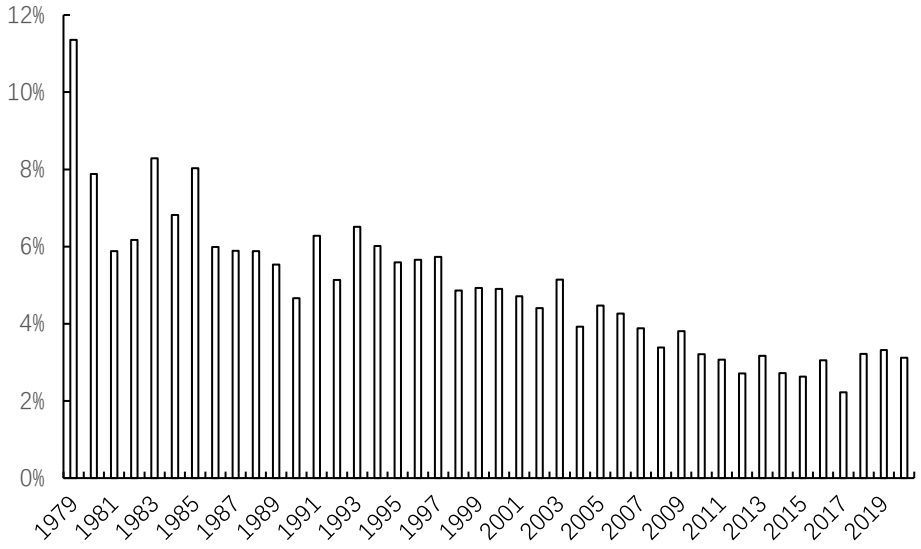

Figure 1. Annual growth rate of agricultural total factor productivity in China.

To further analyze the changing trend of China's agricultural TFP growth before and after the 1990s and the difference of agricultural TFP in different regions, figure 2 lists the changing trend of agricultural TFP growth in three stages (1979–2020,1979–1990 and 1991–2020) and three regions (eastern, central and western). First, agricultural TFP growth in 1979–1990 was significantly higher than in 1991–2020 and 1979–2020, further verifying the previous conclusions. Although the growth rate of China's agricultural TFP slowed down after the 1990s, it is still growing, which shows that a series of agricultural reforms and agricultural support policies implemented since 1979 have effectively promoted the improvement of agricultural TFP. Secondly, by comparing the growth of agricultural TFP in the three regions of the Middle, East, and West, it can be found that the Eastern region is the highest, which shows that the agricultural technology level in the Eastern region has made significant progress, and attaches great importance to scientific and technological innovation in the process of agricultural production. The low growth of TFP in the central and western regions shows that the above two regions rely too much on the initial factor input in agricultural production. The role of agricultural science and technology innovation in agricultural production is relatively small, and agricultural production is still in a relatively extensive state.

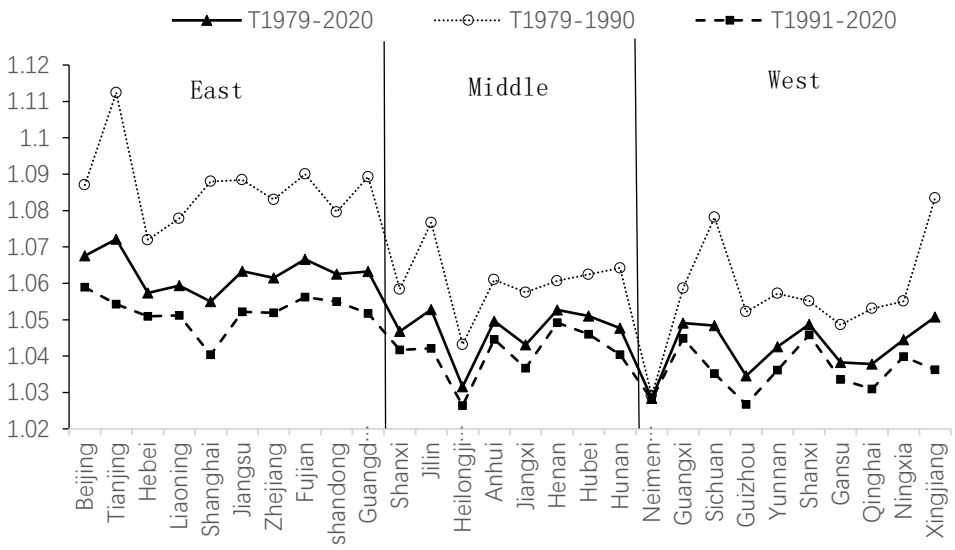

Figure 2. Growth and changing trend of agricultural total factor productivity in China.

The above analysis shows that China's agricultural TFP has been growing since 1979. What is the reason for the growth of TFP? According to Equations (4), (5), and (6), the growth of TFP can be decomposed into technological progress (TPCH) and changes in technical efficiency (TECH), and the factor decomposition diagram of TFP growth since 1978 is obtained. It can be seen from Figure 3 that the value of technical progress (TPCH) is all greater than 1, and some values of Technical Efficiency Change (TECH) are less than 1. This shows that the growth of China's agricultural total factor productivity mainly depends on the progress of agricultural technology. In contrast, technical efficiency sometimes plays the opposite role, which to some extent offsets the effect of the improvement of agricultural technology level. Further analysis of the trend of technological progress and technical efficiency changes before and after 1990 shows that after the 1990s, the growth rate of technological progress began to slow down, and the growth rate of technical efficiency showed a slow upward trend, indicating that the impact of technical efficiency on agricultural total factor productivity began to strengthen gradually.

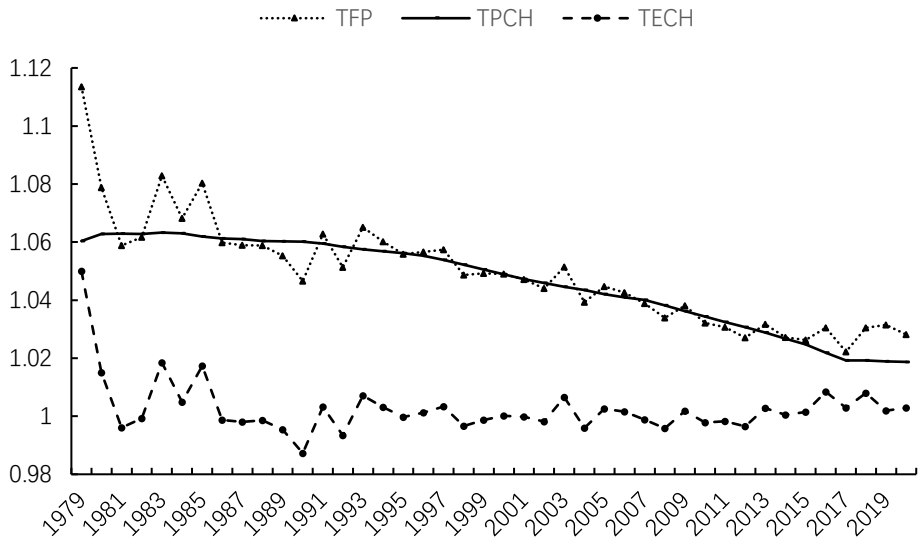

Figure 3. Decomposition of China's agricultural total factor productivity growth from 1979 to 2020.

5.2. Spatial Correlation Analysis of Agricultural TFP in China

To test whether there is a spatial correlation in the TFP of agricultural production, Table 2 lists the global Moran's I calculated based on the geographical adjacency spatial weight matrix. The results show that Moran's I index from 1985 to 2020 is between 0.21 and 0.47. Both are significant at the 5 % significance level, indicating a spatial correlation in the TFP of agriculture in various provinces and cities in China. In addition, this spatial correlation is becoming increasingly obvious over time. This phenomenon may be due to the flow of agricultural production factors between regions, the promotion of agricultural technology extension projects, and mechanical cross-regional operations (Gao & Song, 2014). Notably, the TFP of 1978–1984 did not pass the global correlation test. Further, it is necessary to examine the local spatial correlation of the above years through local Moran's I. Table 3 lists the LISA clustering results for insignificant years. Table 3 shows that although there was no global correlation between 1979 and 1984, there is a specific regional accumulation in the local area, reflecting the imbalance of agricultural development in China to a certain extent. This paper also uses the economic distance spatial weight matrix and the geospatial distance weight matrix to measure the spatial correlation of agricultural TFP in each province and city. The results are very similar to Table 2 and Table 3. Due to the length of the article, it is not shown here.

Table 2. Moran's I index of agricultural total factor productivity from 1979 to 2020.

Year	Moran's I	P-value	Year	Moran's I	P-value
1979	0.087	0.314	2000	0.400	0.000
1980	0.105	0.238	2001	0.427	0.000
1981	0.073	0.336	2002	0.441	0.000
1982	0.051	0.465	2003	0.447	0.000
1983	0.112	0.205	2004	0.449	0.000
1984	0.150	0.126	2005	0.454	0.000
1985	0.210	0.039	2006	0.454	0.000
1986	0.233	0.025	2007	0.460	0.000
1987	0.239	0.022	2008	0.464	0.000
1988	0.271	0.012	2009	0.466	0.000
1989	0.289	0.008	2010	0.470	0.000
1990	0.329	0.003	2011	0.473	0.000
1991	0.305	0.005	2012	0.472	0.000
1992	0.311	0.005	2013	0.478	0.000
1993	0.343	0.002	2014	0.483	0.000
1994	0.351	0.002	2015	0.486	0.000
1995	0.375	0.001	2016	0.482	0.000
1996	0.384	0.001	2017	0.470	0.000
1997	0.376	0.001	2018	0.479	0.000
1998	0.382	0.001	2019	0.483	0.000
1999	0.366	0.001	2020	0.476	0.000

Table 3. LISA clustering results in insignificant years.

	H-H	L-L	H-L	L-H
1979		Shanxi, Shaanxi	Sichuan	
1980		Shaanxi, Gansu, Ningxia	Sichuan, Xinjiang	
1981		Shanxi, Shaanxi, Ningxia	Jilin	NeiMongol
1982		Shanxi., Shaanxi, Gansu, Ningxia	Jilin, Sichuan, Xinjiang	NeiMongol
1983		NeiMongol, Shaanxi, Gansu, Ningxia	Xinjiang	
1984	Tianjin	Shanxi, NeiMongol, Shaanxi, Gansu, Ningxia	Sichuan, Xinjiang	

Note: H-H represents high value surrounded by high value, L-L represents low value surrounded by low value, H-L represents high value surrounded by low value, and L-H represents low value surrounded by high value.

5.3. Convergence Analysis of Agricultural Total Factor Productivity in China

For the traditional β-convergence model, the Hausman test is first carried out to determine that the fixed effect should be selected to analyze the convergence of China's agricultural TFP. As mentioned, China's agricultural TFP has a spatial correlation. Based on three spatial econometric models, three spatial β-convergence models (SAR spatial β-convergence model, SEM spatial β-convergence model, and SDM spatial β-convergence model) are constructed. According to the Wald test, the SDM spatial β-convergence model is optimal, and the spatial Hausman test results still support the fixed effect.

It can be seen from Table 4 that the coefficients of $lnTFP_{i,t}$ in all models are significantly negative, which indicates that there is an apparent convergence trend in China's agricultural total factor productivity and the gap between regional agricultural total factor productivity is shrinking. Through comparing the traditional absolute convergence and conditional convergence, the study found that the convergence speed of conditional convergence (0.065) is greater than that of absolute convergence (0.049). The same conclusion can be drawn by comparing spatial absolute and spatial conditional convergence. That is, the convergence speed of spatial conditional convergence (0.088) is greater than that of spatial absolute convergence (0.074). This is because conditional convergence considers the differences in production factors between regions, shortens the period of convergence, and makes the convergence test closer to reality; Spatial factors have the effect of accelerating

convergence. By comparing the convergence speed of the three models of spatial absolute β-convergence and spatial conditional β-convergence, it can be found that the convergence speed of SAR, SEM, and SDM with spatial conditional β-convergence is significantly faster than that of spatial absolute β-convergence. This phenomenon may be because the spatial spillover effect or diffusion effect narrows the inter-regional agricultural production gap, thus accelerating the convergence speed. For the control variables, the direction and significance level of the influence of the coefficients of the traditional convergence model and the spatial convergence model on the TFP of agriculture is the same. There are some differences in the size of the coefficients. Because the control variables are not the focus of this study, they are not explicitly analyzed.

Table 4. The β convergence of agricultural total factor productivity in China.

Variable	Traditional Absolute β-convergence	Spatial Absolute β-convergence			Traditional Conditional β-convergence	Spatial Conditional β-convergence		
		SAR	SEM	SDM		SAR	SEM	SDM
$lnTFP_{i,t}$	−0.048***	-0.047***	-0.052***	-0.071***	−0.063***	-0.061***	-0.065***	-0.077***
	(0.011)	(0.005)	(0.005)	(0.007)	(0.015)	(0.006)	(0.006)	(0.007)
Trans					0.010	0.010***	0.010**	−0.006
					(0.006)	(0.004)	(0.004)	(0.006)
Citil					0.003	0.003	0.003	0.004
					(0.003)	(0.004)	(0.004)	(0.004)
Irrig					0.018	0.019	0.019	0.012
					(0.020)	(0.013)	(0.013)	(0.014)
Disas					0.001	0.001	0.001	0.001
					(0.006)	(0.005)	(0.005)	(0.005)
Indus					−0.016	−0.016	−0.019	−0.030*
					(0.026)	(0.015)	(0.015)	(0.016)
$\ln(\mathrm{Gdppc})$					0.023***	0.022***	0.023***	0.022***
					(0.006)	(0.005)	(0.005)	(0.005)
Constant	0.114***				−0.048			
	(0.022)				(0.036)			
Rho		0.104**	0.145***	0.145***		0.098**	0.129***	0.140***
		(0.040)	(0.041)	(0.041)		(0.040)	(0.041)	(0.041)
R-squared	0.468	0.154	0.146	0.031	0.484	0.095	0.095	0.188
Convergence Rate	0.049	0.048	0.053	0.074	0.065	0.063	0.067	0.080
Fixed Effect	Yes	Yes	Yes	Yes	Yes	Yes	Yes	Yes

Based on analyzing the influence of spatial effect on the convergence of China's agricultural total factor productivity, the following will further study the spatial convergence characteristics of China's agricultural total factor productivity by period (before and after the 1990s), by region (eastern, central and western) and by using different spatial weight matrices (geographical adjacency spatial weight matrix W_1, economic distance spatial weight matrix W_2 and spatial distance weight matrix W_3).

Table 5 reports the regression results of the SDM conditional β-convergence model with fixed effects in different periods. On the whole, the results of each convergence model with different spatial weight matrices in different periods show that China's agricultural TFP has the characteristics of convergence, which also shows that the convergence trend of China's agricultural TFP is robust; The convergence rate of China's agricultural TFP shows a decreasing trend. The convergence rate between 1979–1990 is significantly higher than between 1991–2020. This may be due to the lack of production resources in the early stage of reform and opening up. The agricultural

production conditions in various regions vary considerably. With the reform and opening up, the flow rate of agricultural production factors between regions continues to increase. Agricultural production in various regions has released great potential, and inefficient regions are growing faster. However, with the deepening of the reform, the gap in resource endowments between regions has gradually narrowed, the conditions for agricultural production have been continuously improved, and agriculture has been continuously transformed from 'quantity growth' to 'quality growth', which has slowed down the convergence rate to a certain extent.

Table 5. Conditional β convergence of agricultural total factor productivity in different periods based on SDM.

Variable	1979–1990			1991–2020			1979–2020		
	W_1	W_2	W_3	W_1	W_2	W_3	W_1	W_2	W_3
$lnTFP_{i,t}$	−0.377***	−0.415***	−0.338***	−0.032***	−0.030***	−0.025***	−0.077***	−0.067***	−0.063***
	(0.025)	(0.029)	(0.026)	(0.008)	(0.007)	(0.007)	(0.007)	(0.007)	(0.006)
Rho	0.161**	−0.159**	0.120	0.283***	−0.128**	0.252**	0.140***	−0.132***	0.182*
	(0.071)	(0.077)	(0.183)	(0.048)	(0.054)	(0.107)	(0.041)	(0.045)	(0.094)
R-squared	0.260	0.214	0.161	0.059	0.188	0.217	0.188	0.159	0.025
Convergence Rate	0.473	0.536	0.412	0.033	0.030	0.025	0.080	0.069	0.065
Control	Yes	Yes	Yes	Yes	Yes	Yes	Yes	Yes	Yes
Fixed Effect	Yes	Yes	Yes	Yes	Yes	Yes	Yes	Yes	Yes

Note: The control variables are the disaster situation (Disas), economic development (Gdppc), urbanization level (Citil), transportation convenience (Trans), secondary industry development (Indus), and irrigation level (Irrig) mentioned above.

Table 6 reports the regression results of the conditional β-convergence model of SDM with fixed effects in different regions. Overall, the convergence model results of different regions and spatial weight matrices show that China's agricultural TFP has convergence characteristics. The convergence speed of China's agricultural TFP shows a spatial distribution pattern decreasing in the western, eastern, and central regions. The western region has the fastest convergence rate. The possible reason is that the western region is rich in agricultural resources. Still, the social and economic development level is low, and the level of agricultural production technology is relatively low. However, with the advancement of the Western development strategy, the Western region has developed rapidly. The acceleration of inter-regional resource and technology flow has shortened the convergence cycle of agricultural TFP. The central region is primarily the prominent grain-producing area, the agricultural production conditions are relatively perfect, and the overall level of agricultural production technology is relatively high. Although the eastern region is economically developed, agricultural production is not its primary goal. The marginal effect of technology and capital investment in the central and eastern regions is decreasing, and the convergence rate of agricultural TFP is slow.

Table 6. Conditional β convergence of agricultural total factor productivity in different areas based on SDM.

Variable	Eastern			Central			Western		
	W_1	W_2	W_3	W_1	W_2	W_3	W_1	W_2	W_3
$lnTFP_{i,t}$	−0.125***	−0.174***	−0.093***	−0.098***	−0.172***	−0.145***	−0.192***	−0.096***	−0.282***
	(0.022)	(0.027)	(0.025)	(0.022)	(0.029)	(0.029)	(0.017)	(0.013)	(0.025)
Rho	−0.094	−0.761***	−0.569***	−0.288***	−0.230***	−0.191**	−0.487***	−0.221***	−0.932***
	(0.061)	(0.083)	(0.118)	(0.048)	(0.079)	(0.088)	(0.076)	(0.069)	(0.148)
R-squared	0.350	0.433	0.367	0.217	0.161	0.267	0.207	0.099	0.232
Conver-gence Rate	0.134	0.191	0.098	0.103	0.189	0.157	0.213	0.101	0.331
Control	Yes	Yes	Yes	Yes	Yes	Yes	Yes	Yes	Yes
Fixed Ef-fect	Yes	Yes	Yes	Yes	Yes	Yes	Yes	Yes	Yes

Note: The control variables are the disaster situation (Disas), economic development (Gdppc), urbanization level (Citil), transportation convenience (Trans), secondary industry development (Indus), and irrigation level (Irrig) mentioned above.

6. Conclusions and Policy Recommendations

With the improvement of China's agricultural market and the continuous improvement of regional openness and communication, the flow of agricultural production factors among regions is becoming increasingly frequent. Spatial factors have become a non-negligible factor affecting the change in China's agricultural TFP. This paper takes the provincial panel data from 1978 to 2020 as the research object, uses the fixed effect SFA-Malmquist model to measure each province and city's agricultural TFP, and determines the spatial correlation of China's agricultural TFP through Moran's I. On this basis, the spatial factors are included in the β-convergence model. The spatial convergence characteristics of China's agricultural TFP are analyzed in different periods and regions. Through analysis, the following main conclusions are obtained:

First, since 1978, the TFP of China's agriculture has shown a growing trend, but its growth rate has gradually slowed over time. This conclusion is consistent with the research results of Chen et al., (2008) and Zhou and Zhang (2013). Comparing the growth of agricultural TFP in the central, eastern, and western regions, it can be found that the eastern region has the highest TFP growth. In contrast, the central and western regions have lower TFP growth. The growth of agricultural TFP in China mainly depends on the progress of agricultural technology. Still, the impact of technical efficiency on agricultural TFP has gradually strengthened.

Second, China's agricultural TFP has significant spatial correlation and spatial convergence characteristics. The differences in agricultural TFP in various regions are shrinking over time, and the spatial spillover effect significantly shortens the convergence process. By studying the convergence process in different periods, it is found that the convergence speed between 1979 and 1990 is significantly higher than that between 1991 and 2020. By studying the convergence process in different regions, it is found that the convergence speed of China's agricultural TFP shows a spatial distribution pattern of decreasing in the west, east, and middle.

Practical implications of this research include:

First, China's agricultural TFP still has a lot of room for improvement. In the future, the use of digital technology, advanced equipment, and other means will continue to improve technical efficiency to achieve the growth of China's agricultural TFP. In recent years, digital technology and digital equipment have been gradually applied to the agricultural field, and smart agriculture and digital agriculture have also been continuously promoted everywhere, which will effectively improve China's agricultural TFP. In the future, efforts should be made to continuously promote digital technology, advanced equipment, and other technologies in the agricultural field.

Second, while strengthening its own agricultural production, the regional government should also take complete account of the advantages of agricultural resources in neighboring regions, strengthen cooperation and exchanges between regions, and constantly play the spillover effect of regions with high agricultural TFP. This paper has proved that China's agricultural TFP has significant spatial agglomeration specificity and spatial effect, which benefits from the flow of production factors, technology, personnel, etc., among regions. In the future, based on constantly strengthening cooperation and exchange between regions, we should give full play to the role of digital

technology, break down barriers between regions, and promote the entire flow of technology, personnel, and factors to achieve the goal of jointly improving agricultural TFP.

CRediT Author Statement: Chaozhu Li: Conceptualization, Methodology, Data curation, Writing original draft, Software and Validation; **Xiaoliang Li:** Methodology, Visualization, Investigation, Supervision and Writing–review & editing.

Data Availability Statement: Not applicable.

Funding: Soft Science Project of Zhejiang Provincial Department of Science and Technology (2022C35066), General Project of Zhejiang Provincial Department of Education (Y202145961), and Doctor Training Program of Jiyang College, Zhejiang Agriculture and Forestry University (RC2022D03).

Conflicts of Interest: The authors declare no conflict of interest.

Acknowledgments: We would like to acknowledge all the people who have contributed to this paper.

References

Caves, D., Christensen, L., & Diewert, W. (1982). The economic theory of index numbers and the measurement of input, output, and productivity. *Econometrica: Journal of the Econometric Society*, 1393–1414.

Chen, P., Yu, M., Chang, C., & Hsu, S. (2008). Total factor productivity growth in China's agricultural sector. *China Economic Review*, *19*(4), 580–593. https://doi.org/10.1016/j.chieco.2008.07.001

Fan, L., & Li, G. (2012). Total factor productivity and its research progress in the field of agriculture. *Modern Economic Science*, *34*(1), 109–119+128.

Gao, F. (2015). Evolution trend and internal mechanism of regional total factor productivity in Chinese agriculture. *The Journal of Quantitative & Technical Economics*, *32*(5), 3–19+53. https://doi.org/10.13653/j.cnki.jqte.2015.05.001

Gao, M., & Song, H. (2014). The spatial convergence of grain production technical efficiency and the difference of functional areas also on the spatial ripple effect of technology diffusion. *Management World*, (7), 83–92. https://doi.org/10.19744/j.cnki.11-1235/f.2014.07.010

Gao, M., Song, H., & Carter, M. (2016). The impact of grain direct subsidies on wheat productivity of farmers with different scales of operation based on data of rural households in fixed observation points nationwide. *Chinese Rural Economy*, (8), 56–69.

Gong, B. (2018a). Agricultural reforms and production in China: Changes in provincial production function and productivity in 1978–2015. *Journal of Development Economics*, *132*, 18–31. https://doi.org/10.1016/j.jdeveco.2017.12.005

Gong, B. (2018b). The contribution of inputs and productivity to agricultural growth in China. *Journal of Agrotechnical Economics*, (6), 4–18. https://doi.org/10.13246/j.cnki.jae.2018.06.001

Greene, W. (2005). Reconsidering heterogeneity in panel data estimators of the stochastic frontier model. *Journal of Econometrics*, *126*(2), 269–303. https://doi.org/10.1016/j.jeconom.2004.05.003

Hou, M., & Yao, S. (2018). Spatial-temporal evolution and trend prediction of agricultural eco-efficiency in China: 1978–2016. *Acta Geographica Sinica*, *73*(11), 2168–2183. https://doi.org/10.11821/dlxb201811009

Huo, Z., Wu, Y., & Zhou, Z. (2011). Evaluation of agricultural productivity China based on input-output. *Economic Geography*, *31*(6), 999–1002.

Jia, L., & Xia, Y. (2017). Scale efficiency of grain production and influencing factors based on survey data from Heilongjiang, Henan and Sichuan. *Resources Science*, *39*(5), 924–933. https://doi.org/10.18402/resci.2017.05.12

Kuang, Y. (2012). Technology efficiency, technology progress, factor accumulation and China's agricultural economic growth. *The Journal of Quantitative & Technical Economics*, *29*(1), 3–18. https://doi.org/10.13653/j.cnki.jqte.2012.01.009

Kumbhakar, S. (1990). Production frontiers, panel data, and time-varying technical inefficiency. *Journal of Econometrics*, *46*(1–2), 201–211. https://doi.org/10.1016/0304-4076(90)90055-X

Li, G. (2014). The green productivity revolution of agriculture in China from 1978 to 2008. *China Economic Quarterly*, *13*(2), 537–558. https://doi.org/10.13821/j.cnki.ceq.2014.02.011

Li, S., & Yin, X. (2017). Analysis of the impact of rural labor transfer on agricultural total factor productivity in China. *Journal of Agrotechnical Economics*, (9), 4–13. https://doi.org/10.13246/j.cnki.jae.2017.09.001

Lin, J. (1992). Rural reforms and agricultural growth in China. *The American Economic Review*, 34–51.

Liu, Y., & Meng, L. (2002). SFA method for measuring Malmquist productivity index. *Journal of Beijing Institute of Technology (Social Sciences Edition)*, (S1), 42–44.

Nin Pratt, A., Yu, B., & Fan, S. (2008). The total factor productivity in China and India: New measures and approaches. *China Agricultural Economic Review*, *1*(1), 9–22. https://doi.org/10.1108/17561370910915339

Pan, D., & Ying, R. (2012). Spatial-temporal differences of agricultural total factor productivity: Restudy of previous literatures. *Economic Geography*, *32*(7), 113–117+128. https://doi.org/10.15957/j.cnki.jjdl.2012.07.018

Quan, J. (2009). Empirical analysis of China's agricultural total factor productivity growth: 1978 ~ 2007-Based on Stochastic Frontier Analysis (SFA) method. *Chinese Rural Economy*, (9), 36–47.

Shi, C., Zhu, J., & Jie, C. (2016). Regional differences and convergence analysis of agricultural total factor productivity growth in China-based on fixed effect SFA model and panel unit root method. *Inquiry Into Economic Issues*, (4), 134–141.

Tobler, W. (1970). A computer movie simulating urban growth in the Detroit region. *Economic Geography*, *46*, 234–240.

Wang, B., & Zhang, W. (2018). Cross-provincial differences in determinants of agricultural eco-efficiency in China: An analysis based on panel data from 31 provinces in 1996-2015. *Chinese Rural Economy*, (1), 46–62.

Wang, S., Tuan, F., Gale, F., Somwaru, A., & Hansen, J. (2013). China's regional agricultural productivity growth in 1985–2007: A multilateral comparison. *Agricultural Economics*, *44*(2), 241–251. https://doi.org/10.1111/agec.12008

Wang, Y., Song, W., & Han, X. (2010). Spatial econometric analysis of agricultural total factor productivity and its influencing factors in China-Based on provincial spatial panel data from 1992 to 2007. *Chinese Rural Economy*, (8), 24–35.

Wu, S., Walker, D., Devadoss, S., & Lu, Y. (2001). Productivity growth and its components in Chinese agriculture after reforms. *Review of Development Economics*, *5*(3), 375–391. https://doi.org/10.1111/1467-9361.00130

Wu, Y. (2010). An estimation of output elasticity of regional agricultural production factors in China—An empirical study with spatial econometric models. *Chinese Rural Economy*, (6), 25-37+48.
Xu, Q., Yin, R., & Zhang, H. (2011). Economies of scale, returns to scale and the problem of optimum-scale farm management: An empirical study based on grain production in China. *Economic Research Journal*, *46*(3), 59–71+94.
Xu, Y. (1999). Agricultural productivity in China. *China Economic Review*, *10*(2), 108–121.
Yang, G., & Yang, M. (2013). The spatial correlation effect of agricultural total factor productivity in China—An empirical study based on static and dynamic spatial panel models. *Economic Geography*, *33*(11), 122–129.
Yang, Y., Lin, W., & Zhang, L. (2017). Agricultural technology progress, technical efficiency and grain production—An empirical analysis based on provincial panel data in China. *Journal of Agrotechnical Economics*, (5), 46–56. https://doi.org/10.13246/j.cnki.jae.2017.05.005
Yu, Y. (2015). Research on the dynamic spatial convergence of provincial total factor productivity in China. *The Journal of World Economy*, *38*(10), 30–55. https://doi.org/10.19985/j.cnki.cassjwe.2015.10.003
Zeng, Y., Lv, Y., & Wang, X. (2018). Multidimensional analysis of the impact of farmland transfer on the technical efficiency of grain production—An empirical study based on stochastic frontier production function. *Journal of Huazhong Agricultural University (Social Sciences Edition)*, (1), 13–21+156–157. https://doi.org/10.13300/j.cnki.hnwkxb.2018.01.002
Zhang, L., & Cao, J. (2013). China's agricultural total factor productivity growth: The introduction of allocative efficiency change—An empirical analysis based on stochastic frontier production function method. *Chinese Rural Economy*, (3), 4–15.
Zhang, L., & Chen, S. (2015). Empirical Analysis on spatial-temporal evolution and driving forces of per capita grain possession in China. *Economic Geography*, *35*(3), 171–177. https://doi.org/10.15957/j.cnki.jjdl.2015.03.025
Zhang, Z., Xue, B., Chen, X., & Li, Y. (2015). Convergence in spatial difference of industrial environmental efficiency in China. *China Population Resources and Environment*, *25*(2), 30–38. https://doi.org/10.3969/j.issn.1002-2104.2015.02.005
Zhou, L., & Zhang, H. (2013). Productivity growth in China's agriculture during 1985–2010. *Journal of Integrative Agriculture*, *12*(10), 1896–1904. https://doi.org/10.1016/S2095-3119(13)60598-5
Zhuo, L., & Zeng, F. (2018). Research on the impact of rural infrastructure on total factor productivity of grain. *Journal of Agrotechnical Economics*, (11), 92–101. https://doi.org/10.13246/j.cnki.jae.2018.11.007

Agricultural & Rural Studies

Article

Evaluation of the Streamflow Response to Agricultural Land Expansion in the Thiba River Watershed in Kenya

Brian Omondi Oduor [1,2,*], Benedict Mwavu Mutua [3], John Ng'ang'a Gathagu [4] and Raphael Muli Wambua [5]

[1] IS-FOOD Institute (Innovation & Sustainable Development in Food Chain), Public University of Navarre, 31006 Pamplona, Spain
[2] Water Engineering, Pan African University Institute of Water and Energy Sciences, Tlemcen 13000, Algeria
[3] Division of Planning, Partnerships, Research and Innovation, Kibabii University, Bungoma P.O Box 1699-50200, Kenya; bmmutua@kibu.ac.ke
[4] Department of Monitoring and Evaluation, Upper Tana-Nairobi Water Fund Trust, Nairobi P.O. Box 76716-00620, Kenya; John.gathagu@nairobiwaterfund.org
[5] Faculty of Engineering, Egerton University, Egerton P.O Box 536-20115, Kenya; raphael.wambua@egerton.ac.ke
* Correspondence: brianomondi.oduor@unavarra.es

Abstract: The increasing global population necessitates increased agricultural production, driving the expansion of agricultural lands and advancement of irrigation farming to supplement the inconsistent and insufficient rainfall patterns prevalent in many regions. This study aimed to evaluate the potential impacts of the expansion of agricultural lands on the streamflow regime of the Thiba River and its impact on the downstream users. The study involved comparing the 2004 and 2014 land uses and using the Hydrologic Engineering Centre's Hydrologic Modelling Systems (HEC-GeoHMS and HEC-HMS) for long-term impact simulations. The results showed a considerable decline in the streamflow in the dry months compared to the wet months, with increasing water abstraction trends from 2007 to 2014. The long-term impact assessment showed an average decline in streamflow in the near (2030) and far (2060) future due to land use and population changes with minimal impact from the increasing precipitation. Based on these findings, there is a need for proper water management and adaptation mechanisms to be put in place to maintain the future water supply from the Thiba River. This study's findings could assist policy and decision-makers in making informed water resource management decisions.

Keywords: agricultural land; irrigation; land use change; streamflow; Thiba River watershed; water abstraction

Citation: Oduor, B. O.; Mutua, B. M.; Gathagu, J. N.; Wambua, R. M. Evaluation of the Streamflow Response to Agricultural Land Expansion in the Thiba River Watershed in Kenya. *Agricultural & Rural Studies*, 2023, *1*, 0011. *https://doi.org/10.59978/ar01020011*

Received: 11 August 2023
Revised: 5 September 2023
Accepted: 9 September 2023
Published: 12 September 2023

1. Introduction

Agricultural production has continuously been increasing all over the world, mainly due to increased food demand due to the growing population (Food and Agriculture Organization of the United Nations [FAO], 2017b; Mateo-Sagasta et al., 2018). This has prompted the expansion of agricultural lands and the development of irrigation farming to supplement most areas' unreliable and low rainfall capacities. Agriculture, by far, consumes the highest amount of global world water resources, with irrigation accounting for the maximum share of global freshwater withdrawals (Siebert et al., 2010). According to Zeng and Cai (2014), approximately 70% of the global freshwater withdrawal is used to meet irrigation water requirements.

In Kenya, just like the rest of the world, agriculture is the leading water consumer accounting for over 80% of the available water (Muema et al., 2018). The Kenyan government has initiated and promoted various agricultural projects, especially irrigation projects, to increase agricultural productivity and enhance food security. Despite the many advantages of irrigation, some adverse effects are experienced in irrigated areas. These negative effects include influences on the hydrological regime such as the decline of the base flow and reduction in discharge of the stream caused by over-exploitation of water resources or disruption of the natural hydrological regime through manmade structures. Additionally, irrigation could result in water erosion caused by inappropriate irrigation methods on sloping fields, as well as affect surface and groundwater quality (Fernández-Cirelli et al., 2009).

The Mwea Irrigation Scheme (MIS) in the Thiba River watershed, one of Kenya's largest irrigation schemes, has tremendously expanded since 2003, after Kenya's Vision 2030 plan

establishment. The Kenyan government has substantially invested in expanding irrigation to bridge the over one million hectares gap required by 2030 to sustain food production (Muema et al., 2018). The MIS was established in 1954, with currently over 30,000 acres of gazetted land, of which 22,000 acres are utilized for paddy rice production and the remainder for settlement, public utilities, and subsistence crop cultivation (National Irrigation Authority, 2023). Paddy rice farming has resulted in the expansion of the area surrounding the scheme by approximately 8,600 acres. This new area was not planned for and has worsened the situation in terms of water availability for the scheme (National Irrigation Authority, 2023). However, there is limited information on actual water abstracted from the river and the potential impacts on streamflow associated with increased commercial agricultural activities.

The continuous expansion of agricultural land in the study area by the government and individual farmers has substantially increased the demand for water from the Thiba River. This demand is further exacerbated by the high population growth in the area, putting extra pressure on the already diminishing water resources. As agricultural productivity rises to meet the growing food demand, the expansion of agricultural lands becomes inevitable, resulting in increased agricultural water demand and more strain on the Thiba River. The escalating agricultural water demand, combined with domestic and industrial needs, has resulted in increased water abstractions from the river, mainly in the upstream areas with higher population densities and agricultural activities, consequently affecting the downstream water availability (Akoko et al., 2020). Furthermore, water pollution by fertilizers, agrochemicals, and sedimentation exported from the cultivated fields affects the river's water quality, compounding the problem.

Despite these challenges, there is a lack of studies examining the impact of continuous agricultural land expansion and increased water abstraction on the Thiba River's flow regime. This knowledge gap hinders the development of effective water and land management strategies for sustainability and appropriate water resource utilization in the watershed. This study aimed to evaluate the streamflow response to agricultural water abstraction and its variability with rainfall for the Thiba River watershed. The relationship between streamflow and water abstraction and the land use change from 2004 to 2014 was examined. The Hydrologic Engineering Centre's Hydrologic Modelling Systems (HEC-HMS) and its Geospatial extension (HEC-GeoHMS) models were used to predict future scenarios based on a practical approach to obtaining long-term land use and climate changes in the near future (2030) and in the far future (2060).

2. Materials and Methods

2.1. Study Area

Thiba River watershed (Figure 1a) is located in Kirinyaga and Embu Counties of Kenya at latitudes 0° 5' S and 0° 47' S, and longitudes 37° 12'E and 37° 32'E and it's approximately 100 km North-East of Kenya's capital city, Nairobi. It covers an estimated area of 1648 km^2. The watershed is located in the upper region of the Tana River basin that is drained by rivers Thiba, Nyamindi, Rupigazi, and several other smaller streams. Thiba River receives its waters from a higher elevation region in Mount Kenya. The watershed has several agricultural activities upstream and downstream, including the MIS, which is well known for paddy rice production in Kenya. The MIS covers over 15% of this watershed and consumes the highest irrigation water in the area. Other agricultural practices in the watershed that depend on irrigation include cultivating maize and other subsistence crops. Thiba River drains its water to the Kaburu hydroelectric dam, one of the seven hydro-power stations in the Upper Tana Basin.

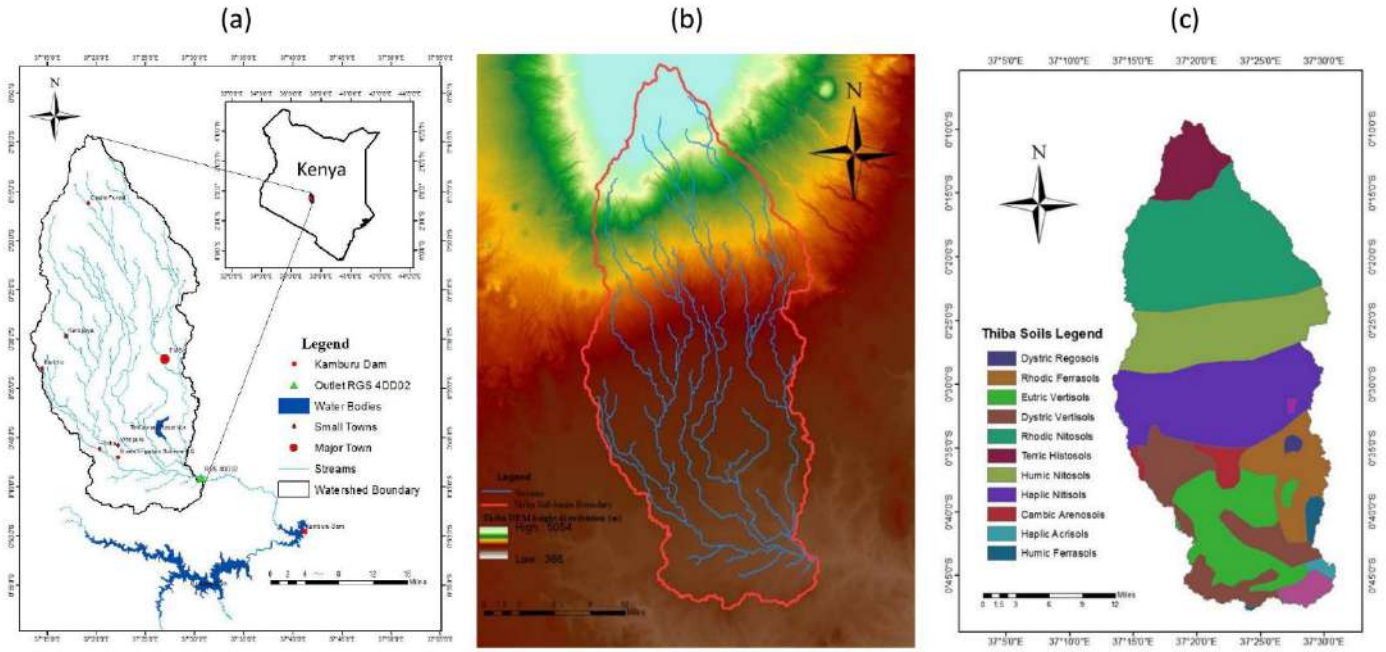

Figure 1. The Thiba River watershed (a) location (b) topography and (c) soil type maps.

The climate in the study area ranges from tropical to semi-arid in the upstream to downstream, having annual precipitation ranging from 400 mm in the lowland areas to about 2000 mm in the highland areas of Mount Kenya. The average annual precipitation in the watershed is 944 mm (Akoko et al., 2020). However, lower rainfall patterns are mostly experienced in January, February, June, July, and August. The temperatures in the watershed range from 13 °C in the highlands to around 30 °C in the lowlands. The hottest months are between January and February, whereas the coolest months are between June and July. The mean temperature for the watershed is about 23 °C. The elevation of the watershed (Figure 1b) varies spatially, ranging from as high as 5000 m in the highland region of Mount Kenya to less than 1000 m in the lowland region. The watershed's soil type (Figure 1c) is mainly black cotton and volcanic soils. The high-elevated regions around Mount Kenya are characterized by histosols and nitisols, which are majorly formed from volcanic ash deposits. These soils are more productive (agriculturally) than most soils in this watershed despite undergoing a series of weathering (FAO et al., 2012).

The watershed's predominant land-use activity is commercial flood irrigation of paddy rice in the MIS. Some farmers in this watershed also practice horticultural farming, whereas others only focus on subsistence farming, such as growing maize and beans (Nyamai et al., 2012). The MIS accounted for 88% of rice produced in Kenya between 2005 and 2010 (National Irrigation Authority, 2023). The scheme receives over 80% of its water supply from Nyamindi and Thiba Rivers, which have a link canal joining them to transfer water from the Nyamidi River to the Thiba River. Irrigation water is abstracted from the rivers by gravity action through fixed intake weirs and then conveyed and distributed in the scheme via unlined open channel systems.

2.2. Data Acquisition

The topography data used a 30 m resolution Digital Elevation Map (DEM) for the Thiba River watershed (Figure 1b) obtained from the Shuttle Radar Topography Mission (SRTM) elevation data was downloaded from the USGS website (United States Geological Survey, 2017). The soil data map for the Thiba River watershed (Figure 1c) was downloaded from the Soil and Terrain (SOTER) database for the Upper Tana catchment, of which the study area is located at the scale of 1:250,000 (Batjes, 2011; Dijkshoorn et al., 2011). The classified land use maps for 2004 and 2014 were downloaded from the FAO's Africover project database (FAO, 2017a). These land use maps are produced from visual interpretation of digitally enhanced Landsat TM images (Bands 4,3,2) (Di Gregorio & Latham, 2003; Jansen & Di Gregorio, 2003). The 2009 Kenyan population grid map obtained from the International Livestock Research Institute (ILRI) website was used to extract the study area's population density grid to project the future population in 2030 and 2060 for future analysis.

The daily observed rainfall data from 2000 to 2009 obtained from the Kenya Meteorological Department (KMD) for three meteorological stations (Embu, Kerugoya, and Castle Forest) within the Thiba River watershed was used for the study. Satellite rainfall data for the study period obtained from the global cleaning weather data was used to fill in the missing gaps. The daily observed streamflow data for Thiba River from 2000 to 2009 was obtained from the Water Resources Management Authority (WRMA) in Embu, Kenya, and National Irrigation Authority (NIA) in MIS, Kirinyaga County, Kenya. The statistical method of data filling was adopted to fill in the missing data. Due to a lack of consistent discharge data from several gauging stations within the watershed, only one gauging station at the watershed outlet, River Gauging Station (RGS) 4DD02 (0° 25' 48' 'S 37° 30' 22''E), was used. Past agricultural water abstraction data from MIS was obtained from the NIB located at the scheme and the WRMA in Embu. The data from the NIB was compared to that from the WRMA to validate it. The available water abstraction data obtained was from 2007 to 2014. This data was used to establish the abstraction trend due to agricultural activities within the watershed. The average monthly potential evapotranspiration data for the Thiba River watershed was obtained using the FAO's Climate and Water balance (CLIMWAT) and Crop Water Requirement (CROPWAT) models for the Embu, Mwea, and Kerugoya stations (FAO, 2015). Then the average value for the three stations was used to represent the whole catchment. This potential evapotranspiration data was calculated using the Penman-Monteith equation in CROPWAT. The potential evapotranspiration ranges from a mean of 1700 mm in the low elevation savannah zone to less than 500 mm annually in the summit region with an overall average of 1000 mm (Notter et al., 2007).

2.3. Model Description

The future impacts of agricultural land expansion on streamflow were analyzed using the HEC-GeoHMS coupled with the HEC-HMS model. The model choice was due to the simplicity and straightforward approach in its application. It analyzes watershed hydrology in both lumped and quasi-distributed forms. HEC-GeoHMS has well-developed data management and visualization functions. It also performs spatial analysis when developing distributed hydrologic parameters, which saves time and costs and helps in accuracy enhancement (United States Army Corps of Engineers [USACE], 2010).

The HEC-GeoHMS is a free public-domain hydrological modeling software that was designed by the United States Army Corps of Engineering (USACE) Hydrologic Engineering Centre (HEC) to help and assist engineers, hydrologists, or those with limited GIS experience to be able to visualize spatial information, perform spatial analysis functions, delineate catchments boundaries and streams, document watershed characteristics, and prepare hydrological model inputs (USACE, 2013). It is a physically based, lumped, semi-distributed, and geospatial hydrological tool that was developed to process geospatial data and create their input files in GIS. HEC-GeoHMS is used to translate GIS spatial data into model files for HEC-HMS. ArcGIS is used for data formatting, processing, and coordinate transformation. HEC-GeoHMS uses DEM for catchment delineation and preparation of various hydrologic inputs. The interconnection between GIS, HEC-GeoHMS, and HEC-HMS is illustrated in Figure 2.

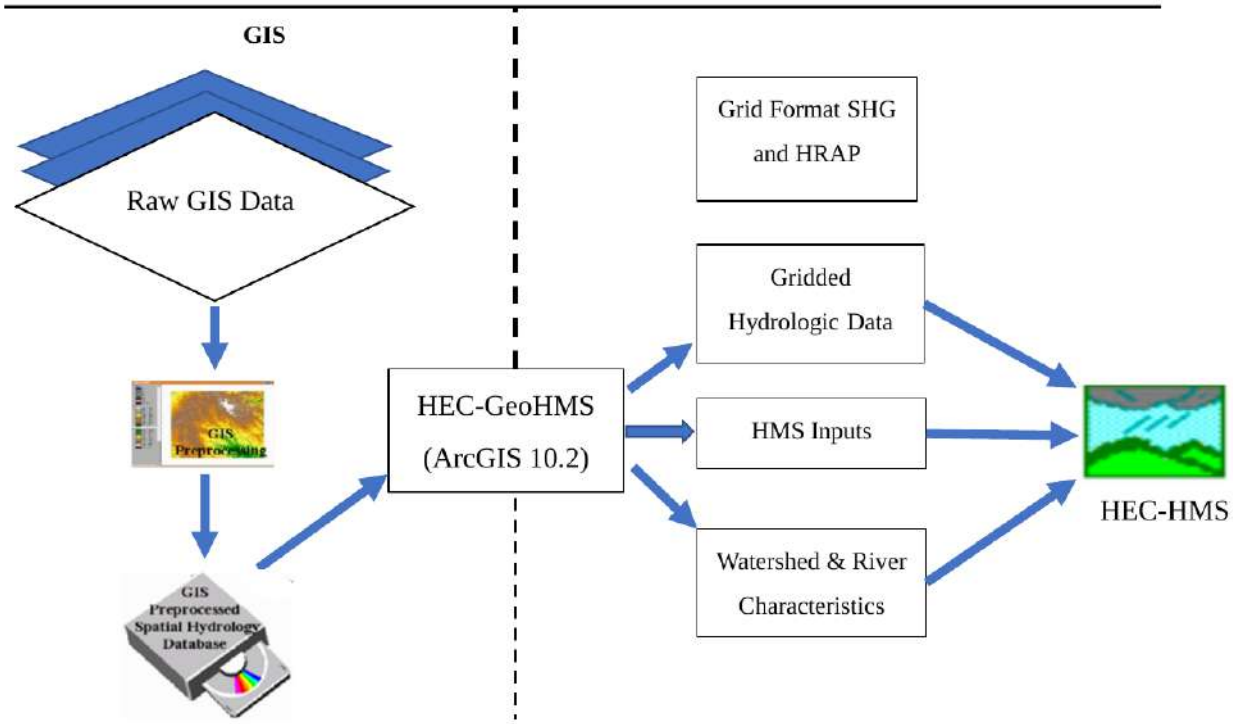

Figure 2. Schematic diagram of the relationship between GIS, HEC-GeoHMS, and HEC-HMS.

The HEC-HMS model divides the watershed into smaller subbasins to simulate the hydrologic cycle's energy and mass flux balances (USACE, 2010). The model runoff simulation components include (i) the precipitation specification option, describing the observed (historical) rainfall at a given location; (ii) the loss models to estimate the runoff volume based on the precipitation and the watershed's characteristics;(iii) the direct runoff models accounting for the overland flow, storage, and energy losses; (iv) the hydrologic routing models accounting for storage and energy flux during water movement through the stream channels; (v) models of naturally occurring confluences and bifurcations; and (vi) models of water control measures such as diversions and storage facilities. The model also contains a distributed runoff model for radar-based precipitation data and a continuous soil moisture accounting model for simulating the watershed's long-term response to wetting and drying

2.4. Model Set-up and Run

HEC-GeoHMS 10.2, which is the ArcGIS 10.2 geo-processing extension, and Arc Hydro tools were used to generate and process geospatial information of the watershed, such as streamflow paths, sub-basins, catchment boundary, elevations, and soil type. The three main data sets that were used in this research to model the agricultural expansion impacts on streamflow included the DEM, which gave the topographic information of the watershed, land use data, and hydrological data (precipitation, streamflow, and evapotranspiration data). These data were then processed and computed using HEC-GeoHMS in ArcGIS 10.2 to generate the parameters required for the HEC-HMS model input to generate runoff simulations.

The HEC-GeoHMS delineated the watershed into 24 subbasins based on their slope characteristics, length of the stream, and number of tributaries joining the main channel. Each of these 24 subbasins had their parameters, but for this study, their averages were used in the simulation process to simplify the processing. The precipitation data from the three rain gauge stations were assigned to each of the 24 subbasin depending on the station's proximity to the centroid of the subbasin. The discharge data at the outlet watershed was used to calibrate and validate the model.

The Soil Conservation Service Curve Number (SCS-CN) method (United States Department of Agriculture, 2016) was used to simulate the watershed hydrology so that when estimating the future land cover changes due to agricultural expansion, the curve number change would be used to represent the changes. The initial abstraction was assumed to be equivalent to 0.2S, where S represented the potential maximum retention capacity for the normal antecedent moisture conditions. This retention was adjusted on a 5-day antecedent rainfall (Chow et al., 1988). Once all the parameters were set, 1000 simulation runs were made from 1998 to 2009, with the first two years set for the model warm-up.

2.5. Model Evaluation

The HEC-HMS model was calibrated (2000–2004) and validated (2005–2009) using the observed daily streamflow data at the watershed outlet. The SCS-CN loss parameters, which included the initial abstraction, the percent imperviousness, and the curve number for each subbasin, were calculated in HEC-GeoHMS as initial values. The time of concentration, T_c, was calculated by obtaining the longest flow path in HEC-GeoHMS (Hoblit & Curtis, 2003). The model calibration was done using the model optimization feature, which automatically adjusts various parameters to obtain a minimum objective function value that matches the observed values (USACE, 2013). The observed actual river flow discharges were input into the time series data manager, after which the simulated flows were compared to these actual flows. Several iterations were made, each with 1000 runs, until the best set of parameter values with the highest efficiency were obtained. The calibrated parameters included the runoff loss functions, such as the initial abstractions and CN, transform functions, such as the lag time, and routing functions, such as the Muskingum routing parameters. The lag time and the Muskingum K value were the most sensitive calibration parameters. The curve number values based on the land use data for 2004 and 2014 were kept as initially estimated in HEC-GeoHMS. The best model parameters obtained after calibration were used to run the model for the land use scenarios in the study area. The model performance was evaluated using the hydrologic goodness of fit based on the Nash-Sutcliff Efficiency (NSE), the coefficient of determination (R^2), and the percent bias (PBIAS). Moriasi et al. (2007) recommended NSE > 0.5, R2 > 0.5, and PBIAS ±25% for a satisfactory streamflow model performance.

2.6. Variation in Agricultural Water Abstraction and Streamflow

The relationship between agricultural water abstraction and streamflow was determined using Spearman's Rank Correlation Test. Correlation methods such as Spearman's Rank, Kendall Rank, and Pearson are commonly used in hydrological studies due to their relative simplicity and high validity (Fowler et al., 2007). The correlation analysis was used to complement regression models in this study by measuring the strength of the relationship between the dependent and the independent variables. It, therefore, provided a test of the statistical significance of the data by showing the degree to which the two variables changed. The Spearman Rank correlation was chosen since it is a non-parametric test that does not make distributional assumptions about the population under investigation. The Spearman's rank coefficient, ρ, was used to measure the linear relationship between two sets of ranked data (Zar, 1972). The coefficient was calculated using Equation (1):

$$\varrho = 1 - \frac{6\sum_{i=1}^{n}\left(x_i - y_i\right)^2}{n\left(n^2 - 1\right)} \tag{1}$$

Where n is the number of values in each dataset, and x_i and y_i represents the two sets of variables under consideration in the i^{th} observation.

2.7. Land Use Change Detection

Land use data for the Thiba River watershed were obtained for 2004 and 2014 to compare the changes in land use within this watershed. The period chosen was ten years apart to show the notable changes in land use in the basin due to increased agricultural area. These land uses were classified into eight classes: irrigated agriculture, rain-fed agriculture, bare land, forests, urban area, shrubs, herbaceous plants, and water. Change detection between the 2004 and 2014 land use maps was determined using comparison statistics whereby each land use area percentage was obtained.

2.8. Long-Term Streamflow Response to Land Use and Climate Changes

The long-term impacts of agricultural land expansion on streamflow were estimated using projected changes in precipitation, land use, and their combinations. The HEC-HMS model has a forecasting manager used to input the projected data. The 2014 land use and population data were used to project the future land use and water demand, while the projected precipitation estimated the future water input.

Future land use scenarios of in 2030 representing the near future and 2060 representing the far future were used to predict future streamflow. A simple but practical approach was adopted to develop the future land use data in ArcGIS by overlaying the 2014 land use shapefile with the projected population density shapefiles for 2030 and 2060. The population density maps for 2030 and 2060 were obtained by applying a constant 1.7% population growth rate per annum to the existing population density map of 2009, obtained from the current census data available for Kenya at that time (Kenya National Bureau of Statistics, 2010). The new population densities were used

to predict the future land uses with the assumption that the future land use will be highly dependent on the population growth. Assumption was also made that as the population increased, the existing forest land would be converted to agriculture land. In that way, the land use maps for 2030 and 2060 were thus created. It's important to note that the relationship between population growth and land use changes is complex and depends on many other factors, including urbanization and the region's transition stage (Acharya & Nangia, 2004). The HEC-HMS model parameters for processing runoff, such as the curve numbers, lag times, and the Muskingum parameters, were then recalculated based on the developed future land use scenarios.

The future precipitation was estimated using the moderate representative concentration pathway (RCP4.5) with an ensemble of three statistically downscaled and bias-corrected Global Climate Models (GFDL-ESM2M, HadGEM2-ES, NorESM1-M) for the region (Bentsen et al., 2013; Dunne et al., 2012; Jones et al., 2011). The climate data used in this study was downloaded from the Water Weather Energy Ecosystem website (www.2w2e.com) at a 0.5º spatial resolution for the coordinates range of latitude −1º to 0º south, and longitude 37º to 38º east. Global climate data are generally more reliable for temperature than precipitation prediction; however, ensemble approaches could reduce these uncertainties (Kawasaki et al., 2010). The ensemble of the climate model projections shows an average annual temperature rise of 0.4 °C in 2030 and 1.4 °C in 2060; and a projected average annual precipitation increase of 2.2% by 2030 and 5.7% by 2060 with higher increases in March (4.1% and 12.5%) and October (9.4% and 18.2%) in the two periods. These estimations align with the Intergovernmental Panel on Climate Change (IPCC) reports projections in East Africa for precipitation that predict no change to 2.5% in the next decade and between 6% to 10% increase by 2100 (Kiem et al., 2008; Meehl et al., 2007).

3. Results and Discussions

3.1. Model Sensitivity Analysis, Calibration, and Validation

The model evaluation was preceded by the sensitivity analysis of the most influential parameters in the watershed. A global sensitivity test was conducted on streamflow parameters obtained from the HEC-GeoHMS and the best parameters used in the HEC-HMS for the model simulation. The HEC-HMS model has an automatic calibration package that can estimate specific model parameters based on their initial conditions. The sensitive parameters were then used to calibrate the model. The SCS-CN and the Muskingum routing parameters were the most sensitive parameters. The curve number is an essential hydrology parameter as it directly affects the rates of surface runoff and infiltration in the watershed. The SCS-CN value is influenced by the watershed's land use, soil characteristics, and the initial soil moisture conditions (Mishra et al., 2012; Rallison & Miller, 1982). A higher SCS-CN value results in higher surface runoff than infiltration, while a lower value results in more infiltration than surface runoff. The Muskingum K value determines the average routing time of runoff from each reach. It is based on a simple finite difference approximation of the continuity equation and considers the storage characteristics of the channel reach (USACE, 2010). The Muskingum parameter also has a dimensionless weight parameter, X, which determines the relative weighting of the inflow and outflow in the storage calculation. The value of X ranged from 0 to 0.5, with 0.2 being the best value used to adjust the behavior of the runoff movement through each reach. If X is set to 0, the model represents a linear reservoir with storage solely determined by the outflow rate and K value. If X is set to 0.5, equal weight is given to inflow and outflow, resulting in a uniformly progressive wave that does not attenuate as it moves through the reach (USACE, 2010).

The model adequately captured the monthly streamflow simulations' magnitude and temporal dynamics, replicating most high and low flows during calibration and validation, as shown in Figure 3. The model produced good performance evaluation results with NSE and R^2 values of 0.66 and 0.68, respectively, during calibration, and 0.61 and 0.65, during validation. The simulations generally underestimated the observations with PBIAS values of 0.18 and 0.14 during calibration and validation, respectively, which is considered acceptable considering the numerous uncertainties associated with modeling. The model's uncertainty could be due to errors in the input data (e.g., meteorological data), measured data errors (e.g., streamflow observations), and model simplifications (Meaurio et al., 2015; Rostamian et al., 2008; Tolson & Shoemaker, 2007). The findings from this study were comparable to those obtained by Yasin et al. (2015), in which they modeled hill torrents in Pakistan using HEC-GeoHMS and HEC-HMS and found an acceptable NSE value of 0.54. From these findings, the model was considered suitable for adoption in the watershed.

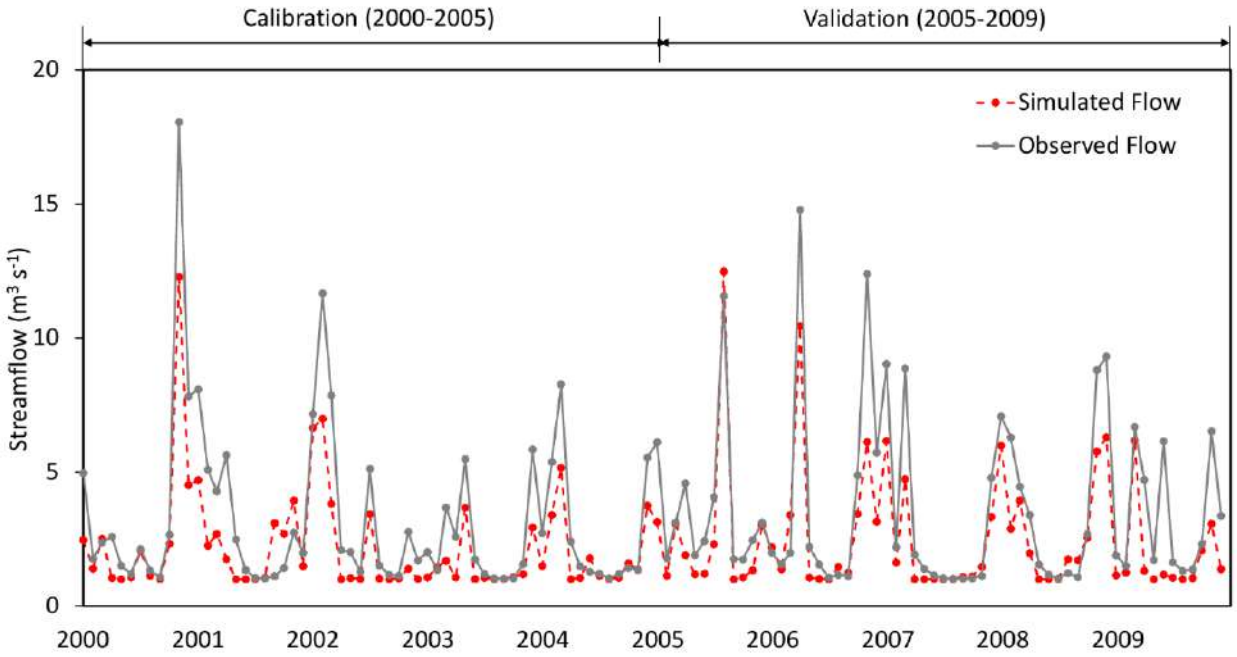

Figure 3. Comparison of monthly observed and simulated streamflow hydrographs during calibration (2000 to 2004) and validation (2005—2009) at the outlet of the Thiba River watershed.

3.2. Agricultural Water Abstraction and Streamflow Analysis

The analysis of the data provided by NIB and WRMA showed an increasing trajectory of water abstraction from the Thiba River between 2007 and 2014, as shown in Figure 4. The highest abstraction of about 9.3 million m^3 happened in 2014, whereas the lowest of about 7.2 million m^3 occurred in 2009. This increase in abstraction in 2014 could be attributed to reduced rainfall due to the drought experienced in Eastern Africa that year. Conversely, water abstraction in 2009 was lower due to high rainfall in that year, thus reducing the dependency on the river water. The seasonal distribution of water abstraction pattern indicated higher abstractions in the dry months of January to February and June to October, coinciding with high irrigation water demand. The changes in the flow regime of Thiba River could be attributed to various factors, with water abstraction considered one of the primary drivers. The largest proportion of water abstraction was due to increased requirements for irrigation, occasioned by the increased land area under irrigation, especially within the MIS. These findings are consistent with previous studies by Ngigi et al. (2007), who observed similar agricultural water abstraction patterns in the Ewaso Ng'iro River.

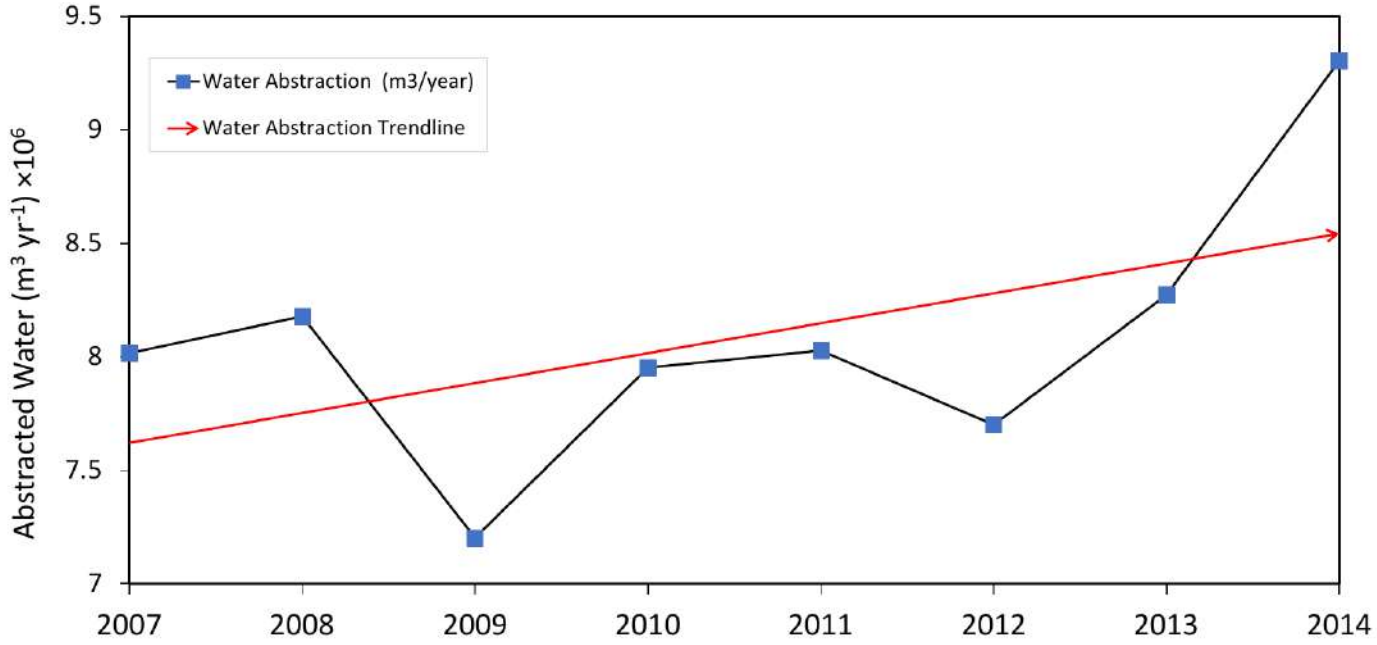

Figure 4. Annual water abstraction trend from the Thiba River between 2007 to 2014.

The correlation between streamflow and agricultural water abstraction from 2007 to 2014 gave a highly significant and strong inverse relationship with a decreasing trend, as shown in Figure 5a. Water abstraction analysis revealed that about 0.23 $m^3 s^{-1}$ (approximately 20000 $m^3 day^{-1}$) was abstracted during the dry seasons, whereas 0.06 $m^3 s^{-1}$ (approximately 5000 $m^3 day^{-1}$) of the river's flow was abstracted during the wet seasons, as demonstrated in Figure 5b. This implies that about 35% of the river's flow during dry season and only 3% of the flow during wet season flow were abstracted from the Thiba River. These findings compare to Ngigi et al. (2007) findings that irrigation water abstraction is a key contributor to streamflow reduction in dry spells, exacerbated by unregulated and illegal water abstraction practices.

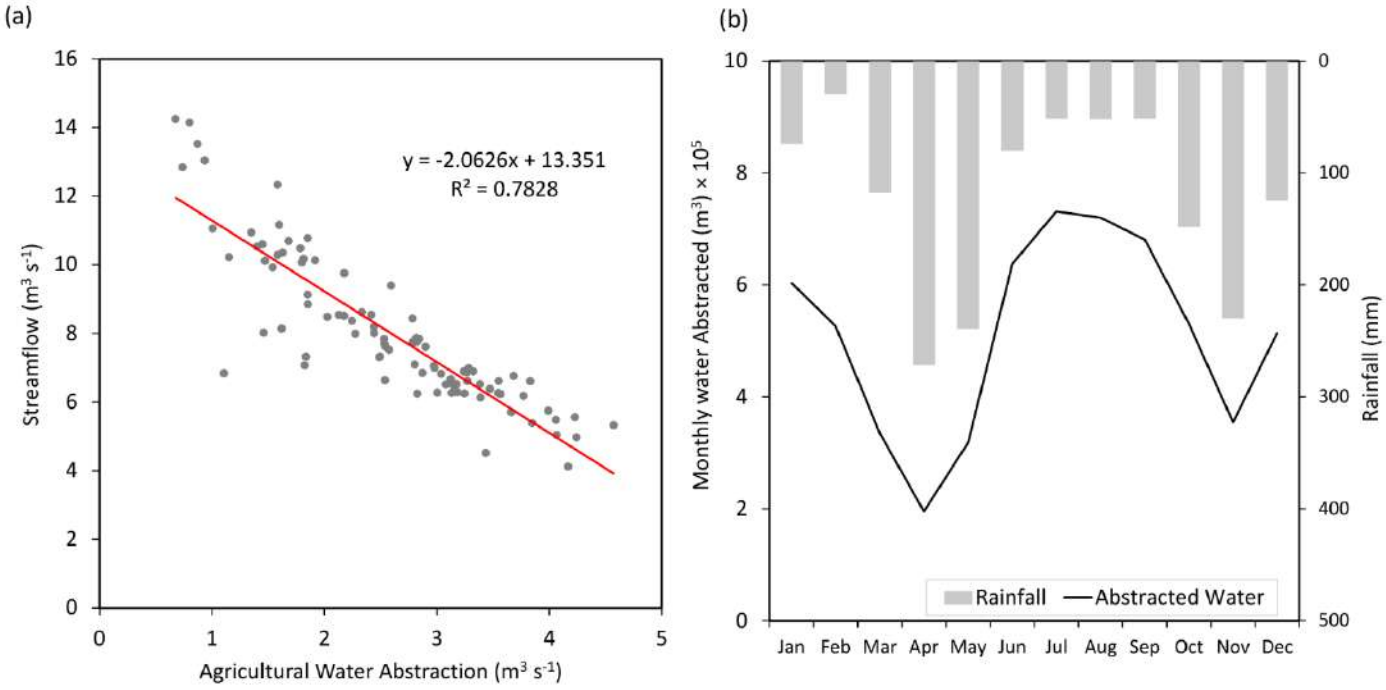

Figure 5. (a) Correlation between agricultural water abstraction and streamflow (b) comparison of monthly average water abstraction and rainfall trends from 2007 to 2014.

The findings from the Thiba River are consistent with previous research across geographical contexts. For instance, in the Ewaso Ng'iro River, Ngigi et al. (2007) observed similar agricultural water abstraction patterns with about 62% of dry season flow and 43% of wet season flow being abstracted from the river. Similarly, in the Naro Moru River, Aeschbacher et al. (2005) reported a 30% streamflow decline between 1960 and 2005 attributed to water abstraction, thus demonstrating the long-term and cumulative nature of water abstraction's influence on river regime. The consistency and reliability of the relationship between irrigation water abstraction and streamflow fluctuations in the Thiba River is further validated by the similarities between our findings and those of other studies. These findings emphasize the need to strike a balance between human activities like agriculture and adopting more sustainable measures to manage our water supplies.

3.3. Land Use Change Analysis

The Thiba River watershed experienced substantial spatial land use changes, within the course of a decade, from 2004 to 2014. The major land use activities include agriculture (> 60%) and forest (>30%) accounting for almost 95% of the watershed area. Land uses in the watershed were classified into eight categories, as illustrated in Figure 6. In the 2014 land use map (Figure 6b), the major land use activity was rainfed agricultural farming (50.5%), which included crops such as maize, coffee, and tea. Approximately 15% of the watershed was used for irrigated agriculture, with paddy rice farming in MIS being predominant. Horticultural crops also form part of the irrigated crops. The forested region around Mount Kenya, which covers almost a third of the watershed, witnessed a decrease in coverage by 6.2% from 2004 to 2014 (Figure 7). This decline in the forested area could be attributed to multiple factors, including deforestation to create room for agricultural activities, residential areas expansion to accommodate more people, and to a lesser extent, population growth driving the demand for timber and fuel. Additionally, the conversion of forest land to agricultural use may have also been influenced by the expansion of rainfed and irrigated agricultural land. Within the same period, the rainfed agricultural land increased by almost 5%, whereas the irrigated agricultural increased by only 1%.

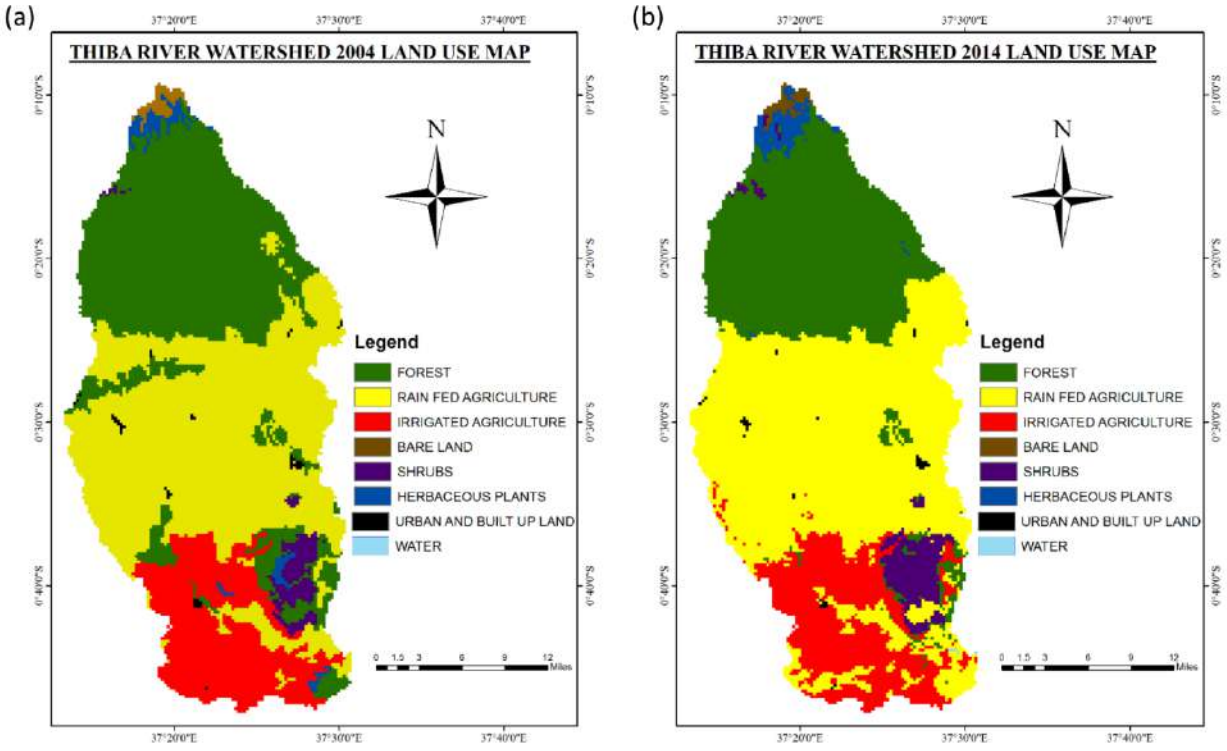

Figure 6. Thiba River watershed spatial distribution of land use maps for (a) 2004 and (b) 2014.

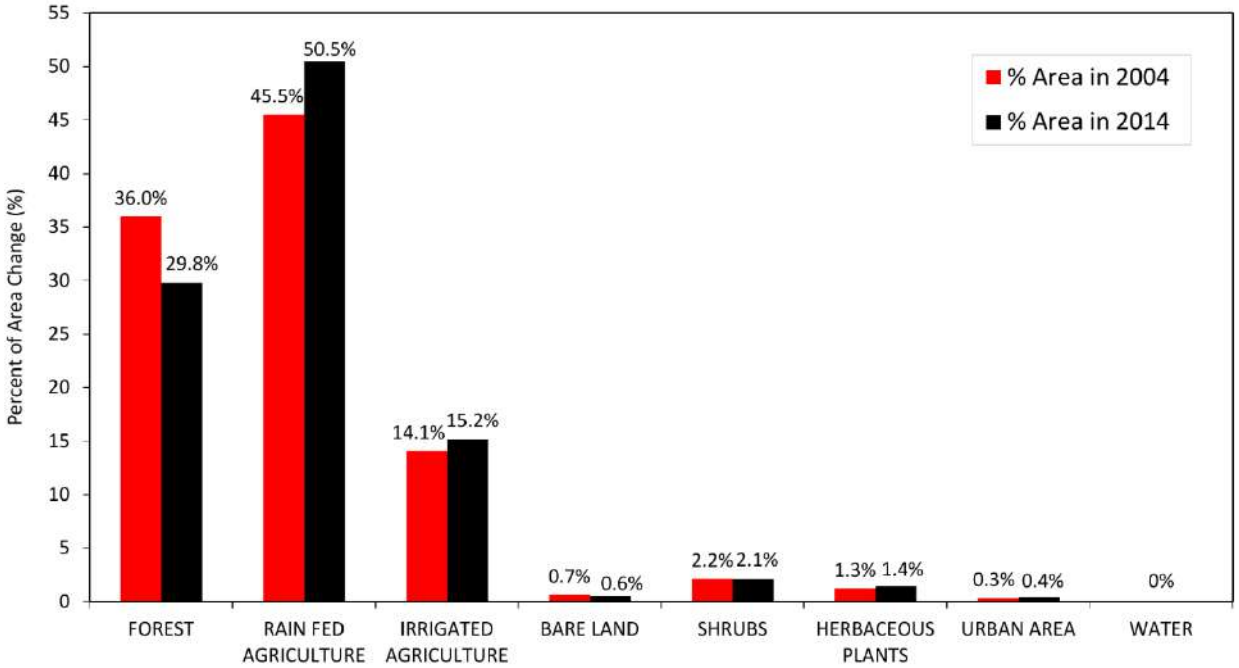

Figure 7. Land use change analysis from 2004 to 2014 in the Thiba River watershed.

The conversion of forests to give way to agricultural land since 2004 could be attributed to the increased population growth within the Upper Tana catchment's rural areas, which encompasses the Thiba River watershed. This population surge has increased the demand for agricultural lands, particularly because most of these communities heavily rely on agriculture for sustenance. Therefore, some of the forested areas could have been converted to small-scale agricultural plots, that predominantly depend on rainfall for food production.

It is worth noting that the adoption of unsustainable agricultural practices in many of these areas has exacerbated environmental challenges such as erosion and sedimentation of the rivers and streams. According to Kitheka and Ongwenyi (2002), some of these unstainable practices, such as continuous tillage, create large bare land, potentially contributing to increased runoff volume. In a related study by Ngigi et al. (2007) in the Ewaso Ng'iro river basin, it was observed that agricultural intensification had increased to unprecedented levels due to high population growth in the basin. The study also pointed out that land use changes resulting from population pressures had adverse effects on river flows, environmental degradation, and decreased agricultural production.

To further emphasize the relevance of these findings, it is noteworthy that similar patterns have been observed in other regions. For instance, a study by Kirui (2008) in the Upper Molo catchment found that the area covered by forested land reduced by 48% between 1986 to 2001 due to encroachment by the local farmers in search of more agricultural land. This study likewise concluded that the high demand for agricultural land in the area resulted from increased population, mirroring the situation in the Thiba River watershed.

Based on these findings and the consistency with previous studies, it is apparent that the land use changes observed in the Thiba River watershed are part of a larger trend influenced by population growth and the subsequent demand for more agricultural land to produce more food. However, the adoption of unsustainable agricultural practices exposes the need for targeted interventions to address environmental concerns and promote sustainable land use practices in these areas.

3.4. Long-Term Impact Scenario Analysis

In generating the land use scenario, the 2014 land use map was reclassified into four categories of agricultural land, forest, residential area, and water and overlaid with the projected population density maps to result in new land use areas, as shown in Figure 8. This categorization provided a foundation for assessing the future impacts of land use changes and population growth on water resources in the Thiba River basin. The population change analysis showed that the agricultural water demand would increase from 9.3 million m^3 in 2014 (baseline scenario) to 11.6 million m^3 in 2030 (near future) and 16 million m^3 in 2060 (far future), representing a 24% and 72% increase in 2030 and 2060 agricultural water demand, respectively. These findings highlight the urgent need for adoption of efficient irrigation practices and alternative water sources to meet this projected increase in agricultural water demand. Furthermore, it would be expected that the water demand

for other uses would also increase as the population increased, and this would exert more pressure on the Thiba River if no new water sources were developed. In this scenario, projected land use was assumed to be only affected by population change, which would affect the future agricultural water demand. However, it is imperative to recognize that other factors beyond population growth, such as future economic growth, climate change trends, and inter-seasonal variability, would greatly influence the amount of agricultural water required, especially during the dry seasons. As the region's economy and living standards continue to improve, higher water consumption would be for various purposes.

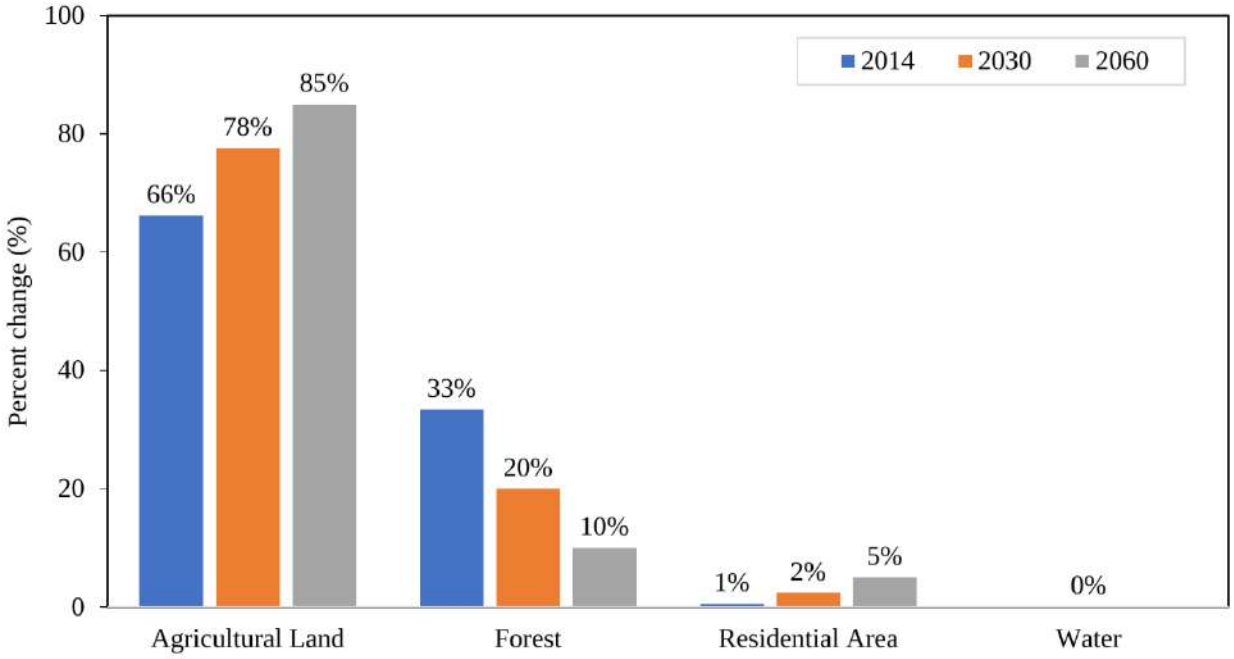

Figure 8. The projected percent land use change in 2030 and 2060 compared to 2014 (baseline).

The land use change scenario findings showed that streamflow was reduced by 18% in 2030 and 52% in 2060 compared to the baseline. This streamflow decrease could be attributed to increased water demand due to land use changes and population increase. The increase in residential area would increase the SCS-CN value, thus increasing the surface runoff, which could have also led to the increased streamflow. However, the increase in residential areas was negligible compared to the increase in agricultural water demand. Reduction of the forest land could have also contributed to an increase in streamflow since there was an increase in the bare land created for agricultural purposes, thus increasing runoff. However, this was also outdone by the high levels of water abstraction from the river.

The precipitation change scenario showed an annual streamflow increase of 3% and 6% in 2030 and 2060, respectively, resulting from climate change. This could be attributed to increased 2.2% and 5.7% precipitation in 2030 and 2060, respectively. According to previous IPCC reports (Meehl et al., 2007), the East African region is projected to experience increased precipitation and temperature; however, the impact on streamflow would be negligible due to the high evapotranspiration rates due to the temperature increase compared to the slight precipitation increase. Similar increasing streamflow patterns caused by climate change have also been observed in other parts of Kenya. For instance, Githui et al. (2009) reported a 2.4% to 23.2% increase in streamflow as a result of a 6% to 11.5% rise in precipitation in the 2020s and 2050s in the Nzoia catchment of the Lake Victoria basin in western Kenya. Similarly, Musau et al. (2015) observed an average annual streamflow increase of up to 4.8% in the 2020s and 17.2% in the 2050s in the Mount Elgon watershed using the B1 scenario, albeit reporting high uncertainties.

The final scenario combined land use and precipitation change had a comparable trend to the land use change scenario. Streamflow declined by 15% and 48% in 2030 and 2060, respectively, under this scenario. This could be attributed to the increased water demand in the land use scenario compared to the slight precipitation increase. Despite increasing precipitation, an increase in water demand, mainly agricultural water demand due to population increase, has a higher effect on the stream flow since there would be increased abstractions from the river. The findings were consistent with those obtained by Kawasaki et al. (2010), who reported that population growth and land development had a greater impact on streamflow change than precipitation in the 50 years studied.

The results of the streamflow response in each of the scenarios discussed above are as shown in Figure 9.

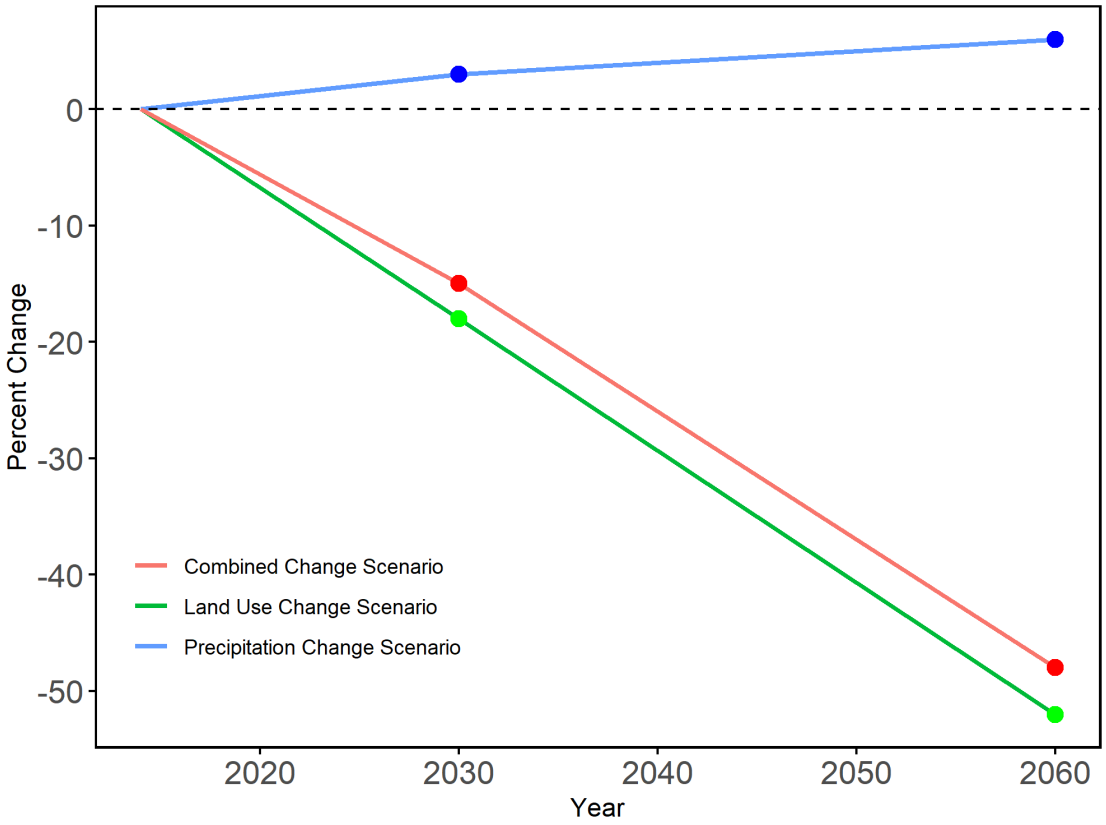

Figure 9. Projected annual streamflow change in the Thiba River watershed for changes in land use, precipitation, and their combination in 2030 and 2060 compared to the baseline (2014).

The projected changes in streamflow and agricultural water demand demonstrate the need for adaptive water resource management. To effectively address these challenges, a multifaceted approach is needed, focusing on optimizing water allocation, investing in efficient irrigation methods, and exploring alternative water sources (Pulighe et al., 2021; Rodrigues et al., 2023). This requires collaborative initiatives involving a diverse group of stakeholders, including practitioners, experts, researchers, policy-, and decision-makers.

The substantial increase in agricultural water demand necessitates prompt action. Implementing sustainable agricultural practices, promoting crop diversification, and embracing water-efficient irrigation methods like drip irrigation and precision farming, are vital to mitigating the potential impacts on crop yields and food security (Oduor et al., 2023). Conducting a comprehensive assessment of vulnerable crops in the study area can help guide targeted interventions, ultimately enhancing resilience and sustainability in the face of evolving environmental conditions.

It is important to recognize that reduced agricultural productivity due to water scarcity may have far-reaching socioeconomic consequences. Therefore, policymakers need to take proactive steps to address the potential economic consequences, such as reduced livelihood opportunities, increased migration, and increased dependence on external food sources. Diversifying income sources and promoting alternative livelihoods can enhance resilience. Furthermore, it is imperative to build climate resilience by ensuring that communities and agriculture adapt to water scarcity and climate variability. To facilitate this adaptation, outreach programs such as education and awareness campaigns could be instrumental in fostering sustainable water use practices among local stakeholders.

4. Conclusions

This study evaluated the long-term streamflow response to changes in agricultural land in the Thiba River watershed. The decrease in streamflow during dry months and the strong correlation with agricultural water abstraction highlight the need for long-term, sustainable water resource management strategies. The results emphasize the urgent need for proactive policies and adaptive measures that balance agricultural needs with ecosystem conservation to ensure consistent and

reliable water supply in the future. The projected decline in future streamflow, exacerbated by population growth and agricultural expansion, requires a paradigm shift in water management practices.

Despite the model simulations providing valuable insights, it is important to acknowledge the inherent uncertainties associated with any modeling approach. The scope of this study was primarily on streamflow dynamics, leaving avenues for future research to explore water quality, ecological impacts, and alternative land management scenarios.

Based on the findings, it would be prudent to implement sustainable water resource management measures such as efficient irrigation techniques, crop selection optimization, and enforcement of water use regulations to mitigate excessive water abstraction. Investing in water-related infrastructure and promoting public awareness regarding responsible water consumption could also contribute to long-term water security.

This research contributes to the state-of-the-art of the complex relationship between land use, hydrology, and water availability. The findings could be useful to water professionals and managers in developing a robust integrated water and land management system, as well as guiding policies and decisions on river water resource management. The methodology and outcomes of this study can be extended to other regions facing similar agricultural and land use management challenges.

CRediT Author Statement: Brian Omondi Oduor: Conceptualization, Methodology, Data curation, Writing – original draft, Visualization, Investigation, Software and Validation; **Benedict Mwavu Mutua:** Conceptualization, Methodology, Supervision and Writing – review & editing; **John Ng'ang'a Gathagu:** Visualization, Investigation and Writing – review & editing; **Raphael Muli Wambua:** Supervision and Writing – review & editing.

Data Availability Statement: Not applicable.

Funding: This research received no external funding.

Conflicts of Interest: The authors declare no conflict of interest.

Acknowledgments: The authors would like to acknowledge the support of the African Union through the Pan African University Institute of Water and Energy Sciences (PAUWES) for the PAU scholarship granted to the authors.

References

Acharya, A. K., & Nangia, P. (2004). Population growth and changing land-use pattern in Mumbai metropolitan region of India. *Caminhos de Geografia*, *5*(11), 168–185. https://doi.org/10.14393/rcg51115332

Aeschbacher, J., Liniger, H., & Weingartner, R. (2005). River water shortage in a highland-lowland system: A case study of the impacts of water abstraction in the Mount Kenya region. *Mountain Research and Development*, *25*(2), 155–162. https://doi.org/10.1659/0276-4741(2005)025[0155:RWSIAH]2.0.CO;2

Akoko, G., Kato, T., & Tu, L. H. (2020). Evaluation of irrigation water resources availability and climate change impacts-a case study of Mwea irrigation scheme, Kenya. *Water (Switzerland)*, *12*(9), 1–22. https://doi.org/10.3390/W12092330

Batjes, N. H. (2011). *Soil property estimates for the Upper Tana, Kenya, derived from SOTER and WISE (Ver. 1.1)*. https://www.isric.org/sites/default/files/isric_report_2010_07b.pdf

Bentsen, M., Bethke, I., Debernard, J. B., Iversen, T., Kirkevåg, A., Seland, Ø., Drange, H., Roelandt, C., Seierstad, I. A., Hoose, C., & Kristjánsson, J. E. (2013). The Norwegian Earth System Model, NorESM1-M – Part 1: Description and basic evaluation of the physical climate. *Geoscientific Model Development*, *6*, 687–720. https://doi.org/10.5194/gmd-6-687-2013

Chow, V. Te, Maidment, D. R., & Mays, L. W. (1988). Applied hydrology. *McGraw-Hill Series in Water Resources and Environmental Engineering*. McGraw-Hill Book Company. https://ponce.sdsu.edu/Applied_Hydrology_Chow_1988.pdf

Di Gregorio, A., & Latham, J. (2003). *Africover Land Cover Classification and Mapping Project*. https://www.eolss.net/sample-chapters/c19/E1-05-01-09.pdf

Dijkshoorn, J. A., Macharia, P. N., Huting, J. R. M., Maingi, P. M., & Njoroge, C. R. K. (2011). *Soil and terrain conditions for the Upper Tana River catchment, Kenya (Version 1.1)*. https://www.isric.org/sites/default/files/isric_gwc_report_k11.pdf

Dunne, J. P., John, J. G., Adcroft, A. J., Griffies, S. M., Hallberg, R. W., Shevliakova, E., Stouffer, R. J., Cooke, W., Dunne, K. A., Harrison, M. J., Krasting, J. P., Malyshev, S. L., Milly, P. C. D., Phillipps, P. J., Sentman, L. T., Samuels, B. L., Spelman, M. J., Winton, M., Wittenberg, A. T., & Zadeh, N. (2012). GFDL's ESM2 global coupled climate-carbon earth system models. Part I: Physical formulation and baseline simulation characteristics. *Journal of Climate*, *25*(19), 6646–6665. https://doi.org/10.1175/JCLI-D-11-00560.1

Food and Agriculture Organization of the United Nations. (2015). CLIMWAT 2.0. for CROPWAT. *Water Development and Management Unit and the climate Change and Bioenergy Unit of FAO* (2.0; Issue September). Land and Water Development Division of FAO. https://www.fao.org/land-water/databases-and-software/climwat-for-cropwat/en/

Food and Agriculture Organization of the United Nations. (2017a). *Spatially Aggregated Multipurpose Landcover Database for Kenya - AFRICOVER*. Africover. https://data.apps.fao.org/map/catalog/srv/api/records/7b07bb4c-bf31-4487-8615-3a6a32643b1f

Food and Agriculture Organization of the United Nations. (2017b). *Water for sustainable food and agriculture: A report produced for the G20 Presidency of Germany*. Food and Agriculture Organization of the United Nations. https://www.fao.org/3/i7959e/i7959e.pdf

Food and Agriculture Organization of the United Nations, International Institute for Applied Systems Analysis, International Soil Reference and Information Centre, Institute of Soil Science, Chinese Academy of Sciences, &Joint Research Centre. (2012). *Harmonized World Soil Database (version 1.2)*. http://webarchive.iiasa.ac.at/Research/LUC/External-World-soil-database/HTML/index.html?sb=1

Fernández-Cirelli, A., Arumí, J. L., Rivera, D., & Boochs, P. W. (2009). Environmental effects of irrigation in arid and semi-arid regions. *Chilean Journal of Agricultural Research* 69(Suppl. 1), 27–40. https://doi.org/10.4067/s0718-58392009000500004

Fowler, H. J., Blenkinsop, S., & Tebaldi, C. (2007). Linking climate change modelling to impacts studies: Recent advances in downscaling techniques for hydrological modelling. *International Journal of Climatology,* 27(12), 1547–1578. https://doi.org/10.1002/joc.1556

Githui, F., Gitau, W., Mutua, F., & Bauwens, W. (2009). Climate change impact on SWAT simulated streamflow in western Kenya. *International Journal of Climatology*, *29*(12), 1823–1834. https://doi.org/10.1002/joc.1828

Hoblit, B. C., & Curtis, D. C. (2003). *Integrating Radar Rainfall Estimates with Digital Elevation Models and Land Use Data to Create an Accurate Hydrologic Model*. (Working Paper). https://onerain.com/wp-content/uploads/2020/10/2001-radar-rainfall-accurate-hydologic-model.pdf

Jansen, L. J. M., & Di Gregorio, A. (2003). Land-use data collection using the "land cover classification system": Results from a case study in Kenya. *Land Use Policy*, *20*(2), 131–148. https://doi.org/10.1016/S0264-8377(02)00081-9

Jones, C. D., Hughes, J. K., Bellouin, N., Hardiman, S. C., Jones, G. S., Knight, J., Liddicoat, S., O'Connor, F. M., Andres, R. J., Bell, C., Boo, K. O., Bozzo, A., Butchart, N., Cadule, P., Corbin, K. D., Doutriaux-Boucher, M., Friedlingstein, P., Gornall, J., Gray, L., … Zerroukat, M. (2011). The HadGEM2-ES implementation of CMIP5 centennial simulations. *Geoscientific Model Development*, *4*, 543–570. https://doi.org/10.5194/gmd-4-543-2011

Kawasaki, A., Takamatsu, M., He, J., Rogers, P., & Herath, S. (2010). An integrated approach to evaluate potential impact of precipitation and land-use change on streamflow in Srepok River Basin. *Theory and Applications of GIS*, *18*(2), 9–20. https://doi.org/10.5638/thagis.18.117

Kenya National Bureau of Statistics (2010). *Kenya Population and Housing Census, Volume 1, Population by Administrative Units*. https://www.knbs.or.ke/2009-kenya-population-and-housing-census-volume-1a-population-distribution-by-administrative-units/

Kiem, A. S., Ishidaira, H., Hapuarachchi, H. P., Zhou, M. C., Hirabayashi, Y., & Takeuchi, K. (2008). Future hydroclimatology of the Mekong River basin simulated using the high-resolution Japan Meteorological Agency (JMA) AGCM. *Hydrological Processes*, *22*(9), 1382–1394. https://doi.org/10.1002/hyp.6947

Kirui, W. K. (2008). *Analysis of Catchment Hydrologic Response Under Changing Land Use: The Case of Upper Molo River Catchment, Kenya* [Egerton University]. http://hdl.handle.net/1834/6858

Kitheka, J. U., & Ongwenyi, G. S. (2002). The Tana River Basin and the opportunity for research on the land-ocean interaction in the Tana Delta. University of Nairobi. http://hdl.handle.net/1834/7842

Mateo-Sagasta, J., Zadeh, S. M., & Turral, H. (2018). More people, more food, worse water? A global review on water pollution from agriculture *Food and Agricultural Organization and International Water Management Institute*. http://www.fao.org/3/ca0146en/ca0146en.pdf

Meaurio, M., Zabaleta, A., Uriarte, J. A., Srinivasan, R., & Antigüedad, I. (2015). Evaluation of SWAT model's performance to simulate streamflow spatial origin. The case of a small forested watershed. *Journal of Hydrology*, *525*, 326–334. https://doi.org/10.1016/j.jhydrol.2015.03.050

Meehl, G. A., Stocker, T. F., Collins, W. D., Friedlingstein, P., Gaye, A. T., Gregory, J. M., Kitoh, A., Knutti, R., Murphy, J. M., Noda, A., Raper, S. C. B., Watterson, I. G., Weaver, A. J., & Zhao, Z.-C. (2007). Global climate projections: Climate Change 2007: The physical science basis. *Working Group I to the Fourth Assessment Report of the Intergovernmental Panel on Climate Change (IPCC)*. Cambridge University Press.

Mishra, S. K., Pandey, A., & Singh, V. P. (2012). Special Issue on Soil Conservation Service Curve Number (SCS-CN) Methodology. *Journal of Hydrologic Engineering*, *17*(11), 1157. https://doi.org/10.1061/(asce)he.1943-5584.0000694

Moriasi, D. N., Arnold, J. G., Van Liew, M. W., Bingner, R. L., Harmel, R. D., & Veith, T. L. (2007). Model evaluation guidelines for systematic quantification of accuracy in watershed simulations. *Transactions of the ASABE*, *50*(3), 885–900. https://doi.org/10.13031/2013.23153

Muema, F. M., Home, P. G., & Raude, J. M. (2018). Application of benchmarking and principal component analysis in measuring performance of public irrigation schemes in Kenya. *Agriculture (Switzerland)*, *8*(10), 162. https://doi.org/10.3390/agriculture8100162

Musau, J., Sang, J., Gathenya, J., & Luedeling, E. (2015). Hydrological responses to climate change in Mt. Elgon watersheds. *Journal of Hydrology: Regional Studies*, *3*, 233–246. https://doi.org/10.1016/j.ejrh.2014.12.001

National Irrigation Authority. (2023). *Mwea Irrigation Scheme*. https://irrigation.go.ke/projects/mwea-irrigation-scheme/

Ngigi, S. N., Savenije, H. H. G., & Gichuki, F. N. (2007). Land use changes and hydrological impacts related to up-scaling of rainwater harvesting and management in upper Ewaso Ng'iro river basin, Kenya. *Land Use Policy*, *24*(1), 129–140. https://doi.org/10.1016/j.landusepol.2005.10.002

Notter, B., MacMillan, L., Viviroli, D., Weingartner, R., & Liniger, H. P. (2007). Impacts of environmental change on water resources in the Mt. Kenya region. *Journal of Hydrology*, *343*, 266–278. https://doi.org/10.1016/j.jhydrol.2007.06.022

Nyamai, M., Mati, B. M., Home, P. G., Odongo, B., Wanjogu, R., & Thuranira, E. G. (2012). Improving land and water productivity in basin rice cultivation in Kenya through system of rice intensification (SRI). *Agricultural Engineering International: CIGR Journal*, *14*(2), 1–9.

Oduor, B. O., Campo-Bescós, M. Á., Lana-Renault, N., & Casalí, J. (2023). Effects of climate change on streamflow and nitrate pollution in an agricultural Mediterranean watershed in Northern Spain. *Agricultural Water Management*, *285*, 1–12. https://doi.org/10.1016/J.AGWAT.2023.108378

Pulighe, G., Lupia, F., Chen, H., & Yin, H. (2021). Modeling climate change impacts on water balance of a Mediterranean watershed using SWAT+. *Hydrology*, *8*(4), 1–14. https://doi.org/10.3390/hydrology8040157

Rallison, R. E., & Miller, N. (1982). Past, present, and future SCS runoff procedure. In V. P. Singh (Ed.), *International Symposium on Rainfall-Runoff Modeling*, 353–364. Mississippi State University.

Rodrigues, D., Fonseca, A., Stolarski, O., Freitas, T. R., Guimarães, N., Santos, J. A., & Fraga, H. (2023). Climate Change impacts on the Côa Basin (Portugal) and potential impacts on agricultural irrigation. *Water (Switzerland)*, *15*(15), 1–17. https://doi.org/10.3390/w15152739

Rostamian, R., Jaleh, A., Afyuni, M., Mousavi, S. F., Heidarpour, M., Jalalian, A., & Abbaspour, K. C. (2008). Application of a SWAT model for estimating runoff and sediment in two mountainous basins in central Iran. *Hydrological Sciences Journal*, *53*(5), 977–988. https://doi.org/10.1623/hysj.53.5.977

Siebert, S., Burke, J., Faures, J. M., Frenken, K., Hoogeveen, J., Döll, P., & Portmann, F. T. (2010). Groundwater use for irrigation – a global inventory. *Hydrology and Earth System Sciences*, *14*(10), 1863–1880. https://doi.org/10.5194/hess-14-1863-2010

Tolson, B. A., & Shoemaker, C. A. (2007). Cannonsville Reservoir watershed SWAT2000 model development, calibration and validation. *Journal of Hydrology*, *337*(1–2), 68–86. https://doi.org/10.1016/j.jhydrol.2007.01.017

United States Army Corps of Engineers. (2010). *Hydrologic Modeling System, HEC-HMS User's Manual, Version 3.5*. https://www.hec.usace.army.mil/software/hec-hms/documentation/HEC-HMS_Users_Manual_3.5.pdf

United States Army Corps of Engineers. (2013). *HEC-GeoHMS: Geospatial Hydrologic Modeling System, Version 10.1, User's Manual*. https://www.hec.usace.army.mil/software/hec-geohms/documentation/HEC-GeoHMS_Users_Manual_10.1.pdf

United States Department of Agriculture. (2016). Natural Resources Conservation Service: Conservation Practice Standard-filter strip code 393. In *United States Department of Agriculture (USDA) - Natural Resources Conservation Service (NRCS)* (Issue September, pp. 1–4). United States Department of Agriculture (USDA) - Natural Resources Conservation Service (NRCS). https://www.nrcs.usda.gov/sites/default/files/2022-09/Filter_Strip_393_CPS.pdf

United States Geological Survey. (2017). *USGS EROS Archive - Digital Elevation - Shuttle Radar Topography Mission (SRTM) 1 Arc-Second Global*. Earth Resources Observation and Science (EROS) Center. https://doi.org/10.5066/F7PR7TFT

Yasin, Z., Nabi, G., & Randhawa, S. M. (2015). Modeling of Hill Torrent Using HEC Geo-HMS and HEC-HMS Models: A Case Study of Mithawan Watershed. *Pakistan Journal of Meteorology*, *11*(22), 1–11. http://www.pmd.gov.pk/rnd/rndweb/rnd_new/journal/vol11_issue22_files/1.pdf

Zar, J. H. (1972). Significance Testing of the Spearman Rank Correlation Coefficient. *Journal of the American Statistical Association*, *67*(339), 578–580. https://doi.org/10.2307/2284441

Zeng, R., & Cai, X. (2014). Analyzing streamflow changes: Irrigation-enhanced interaction between aquifer and streamflow in the Republican River basin. *Hydrology and Earth System Sciences*, *18*(2), 493–502. https://doi.org/10.5194/hess-18-493-2014

Agricultural & Rural Studies

Commentary

An Atlas of Desertification for Spain

Jaime Martínez-Valderrama

Estación Experimental de Zonas Áridas, Consejo Superior de Investigaciones Científicas, 04120 Almería, Spain; jaimonides@eeza.csic.es

1. The Lack of Desertification Maps

As occasions like Desertification and Drought Day draw near or news headlines highlight new temperature records, a renewed interest on desertification is raised. Alongside this, the media often raises customary inquiries. Among the initial queries is the one concerning the scope of the issue. They presume that we experts know all this, and that we have a perfectly quantified variable that measures desertification. They assume that the dense network of satellites allows us to monitor the problem almost instantaneously, and that it is enough to take a look at this map, and issue a brief report: in this province, there is this percentage of desertification, this percentage is severe and this percentage is medium, and this percentage is severe.

We are far from it. We don't really have an answer to something basic, which is the state of desertification. There is a disparate estimation of the global extent of desertified lands provided to date, ranging between 4–74% of drylands (Safriel, 2007). The extent of desertification is an elusive figure, often presented as partial information even in official documents. For example, the Intergovernmental Science-Policy Platform on Biodiversity and Ecosystem Services (2018) equates the problem to population affected (from 2.7 billion in 2010 to 4 billion in 2050) rather than to amount of land. The Intergovernmental Panel on Climate Change (Mirzabaev et al. 2019) gives a precise figure: "9.2% of drylands (±0.5%) experienced declines in biomass productivity" during 1980–2000, which is based on studies that estimate a 24-29% decline in global biomass (Le et al., 2016). Similarly, the United Nations Convention to Combat Desertification (2022) estimates that 20% of global land is degraded to some extent.

This pattern holds true at both the national and regional levels. In the case of Spain, outdated statistics have persisted, such as the assertion that 20% of its land area is undergoing degradation processes. This statistic originates from a study conducted for the period of 2000–2010, which evaluated land condition considering the rain use efficiency paradigm (Sanjuán et al., 2014). However, the assessment of desertification must include more factors, such as the degradation of groundwater bodies (which in the above map are revealed as positive anomalies), a serious problem in the drylands of Spain.

Alongside this map, which reflects the current state, there is another map of desertification risk, constructed using the Mediterranean Desertification and Land Use methodology (European Commission, 1999). Its validity has been questioned due to its lack of statistical and conceptual rigor. Specifically, this map is a simple algebraic operation to add up the effect of four factors (aridity, erosion, use of aquifers and area burnt by forest fires), excluding the possibility of synergy between them. For example, in a territory with higher aridity, and therefore lower productivity rates, soil loss has a greater impact than in less arid areas, since soil formation rates are lower. These types of interactions are not considered in the methodology used in the Spanish National Action Plan against Desertification, which also ignores the causes of the problem. Moreover, the factors are weighed subjectively. For example, if soil erosion estimated by the Revised Universal Soil Loss Equation is between 12 and 25 t ha^{-1} yr^{-1}, the weight of the erosion factor is 2, but nothing justifies these thresholds.

The lack of desertification maps, not only in Spain, but on a global scale, was certified by the latest World Atlas of Desertification (WAD) (Cherlet et al., 2018), which warns on the first page: "Although 'desertification' remains in the title, [...] deterministic maps on global land degradation are not presented." The rationale behind this gap in knowledge is multifaceted and arises from the inherent intricacies of desertification, encompassing a spectrum of degradation processes. These span from erosion and biodiversity loss to the overexploitation of water resources, and include economic degradation. Consequently, the pursuit of an indicator capable of harmonizing this diverse array of variables has encountered obstacles. Another contributing factor is the pronounced level of subjectivity in desertification assessment. Many experts have classified landscapes

Citation: Martínez-Valderrama, J. An Atlas of Desertification for Spain. *Agricultural & Rural Studies*, 2023, *1*, 0012. *https://doi.org/10.59978/ar01020012*

Received: 8 August 2023
Revised: 6 September 2023
Accepted: 9 September 2023
Published: 14 September 2023

characterized by sparse, non-lush vegetation—typical of arid regions and exhibiting ochre hues—as areas undergoing degradation.

2. How to Fill this Critical Gap

Given the impossibility of mapping, the WAD proposes Convergence of Evidence (CE) to detect desertification processes at an early stage. CE emphasizes the importance of the context of each site and considers a series of biophysical and socio-economic variables to portray the potential threat of desertification. Without being an original approach—in 1998 the Surveillance System for Assessing and Monitoring of Desertification project (http://www.eeza.csic.es/surmodes/) already used this idea to identify the "desertification landscapes" of Spain (Martínez-Valderrama et al., 2022)—the idea is a fabulous diagnostic tool, as it makes it possible to anticipate degradation before it leads to irreversible deterioration of the socio-ecosystem.

However, the CE raises doubts. It does not provide a global framework in which to compare desertification states in different places, precisely because it prioritizes the local conceptual component, i.e., by considering that each context provides an idea of what desertification is. Moreover, it leaves empty all those maps that are constantly asked about. The problem with not having a map is that any map will do. Media questions are one thing, but the needs of the administration in decision-making are another, and these often come at a time that is not conducive to reflection. Indeed, when politicians become interested in desertification (or fires, or droughts, or plastic pollution) it is often too late, and there are very short deadlines to respond to very complex problems. In this context, it is not surprising that, for example, aridity maps are used to represent desertification. This is a major error, as aridity maps represent only where desertification can potentially occur.

It is not an option, if the problem is to be tackled with guarantees, to lack desertification maps. An example of this, in the case of Spain, is the express request for a desertification map by the Spanish Government in the latest National Strategy to Combat Desertification. Our project aims to address the challenge through the use of artificial intelligence algorithms. To do so, all available geospatial information on desertification (e.g., aridity index, soil organic carbon, land use changes, state of groundwater bodies, per capita income, etc.) will be gathered, and cases of desertification in Spain will be identified. We then train our prototype with these cases, relating them to the mapped variables under different climate change scenarios. From these relationships we will be able to detect, through the various maps that the project will generate, more cases of desertification that may initially go unnoticed or that have not been identified to date. In order to identify the main predictors and their importance in desertification in Spain, we will carry out a Random Forest permutation analysis (Breiman, 2001). Thus, in addition to having identified the places with desertification, we will have an idea of its causes, which will guide the design of solutions.

Our aim is to provide decision-makers with a useful tool for diagnosing desertification, which is the first step towards tackling the problem with guarantees. Only by knowing where the problems occur and with what intensity, will it be possible to start designing measures to reverse the problem (when it is already too advanced) or to redirect land uses that are beginning to cause land degradation.

CRediT Author Statement: This is a single author paper and the author was solely responsible for the content, including the concept, analysis, writing, and revision of the manuscript.

Data Availability Statement: Not applicable.

Funding: This research is supported by ATLAS project, funded by the Biodiversity Foundation of the Ministry for the Ecological Transition and the Demographic Challenge (MITECO) within the framework of the Recovery, Transformation and Resilience Plan (PRTR), financed by the European Union—NextGenerationEU.

Conflicts of Interest: The author declares no conflict of interest.

Acknowledgments: Not applicable.

References

Breiman, L. (2001). Random forests. *Mach. Learn.*, *45*, 5–32. https://doi.org/10.1023/A:1010933404324

Cherlet, M., Hutchinson, C., Reynolds, J., Hill, J., Sommer, S., & von Maltitz, G. (2018). *World atlas of desertification rethinking land degradation and sustainable land management*. Publication Office of the European Union. https://doi.org/10.2760/9205

European Commission. (1999). *The medalus project: Mediterranean desertification and land use: manual on key indicators of desertification and mapping environmentally sensitive areas to desertification*. Office for Official Publications of the European Communities.

The Intergovernmental Science-Policy Platform on Biodiversity and Ecosystem Services. (2018). *The IPBES assessment report on land degradation and restoration*.

Le, Q. B., Nkonya, E., & Mirzabaev, A. (2016). Biomass productivity-based mapping of global land degradation hotspots. In E. Nkonya, A. Mirzabaev, & J. von Braun (Eds.), *Economics of land degradation and improvement—A global assessment for sustainable development* (pp. 55–84). Springer International Publishing.

Martínez-Valderrama, J., del Barrio, G., Sanjuán, M. E., Guirado, E., & Maestre, F. T. (2022). Desertification in Spain: A sound diagnosis without solutions and new scenarios. *Land*, *11*(2), 272. https://doi.org/10.3390/land11020272

Mirzabaev, A., J. Wu, J. Evans, F. García-Oliva, I.A.G. Hussein, M.H. Iqbal, J. Kimutai, T. Knowles, F. Meza, D. Nedjraoui, F. Tena, M. Türkeş, & R. J. Vázquez, M. W. (2019). Desertification. In J. M. P.R. Shukla, J. Skea, E. Calvo Buendia, V. Masson-Delmotte, H.-O. Pörtner, D.C. Roberts, P. Zhai, R. Slade, S. Connors, R. van Diemen, M. Ferrat, E. Haughey, S. Luz, S. Neogi, M. Pathak, J. Petzold, J. Portugal Pereira, P. Vyas, E. Huntley, K. Kissick, M. (Eds.), *Climate change and land: An IPCC special report on climate change, desertification, land degradation, sustainable land management, food security, and greenhouse gas fluxes in terrestrial ecosystems* (pp. 249–343). UNEP.

Safriel, U. (2007). The assessment of global trends in land degradation. In M. Sivakumar & N. Ndiang'ui (Eds.), *Climate and land degradation* (pp. 1–38). Springer.

Sanjuán, M. E., Barrio, G. del, Ruiz, A., Rojo, L., Puigdefábregas, J., & Martínez, A. (2014). *Evaluación y seguimiento de la desertificación en España: Mapa de la Condición de la Tierra 2000–2010* [*Assessment and monitoring of desertification in Spain: Land condition map 2000-2010*]. Ministerio de Agricultura, Alimentación y Medio Ambiente (Spain). https://digital.csic.es/bitstream/10261/200778/1/2dRUE_ES_EnFinal_v7.pdf

United Nations Convention to Combat Desertification. (2022). *Global land outlook. Land restoration for recovery and resilience*. https://www.unccd.int/sites/default/files/2022-04/UNCCD_GLO2_low-res_2.pdf

To be

a leading academic journal

in the

field of agricultural, rural and farmers' issues and policies.

Agricultural & Rural Studies

Abstracted & Indexed In Google Scholar

Publisher
SCC PRESS
Address: Unit 811, Beverley Commercial Centre, 87-105 Chatham Road South, Tsim Sha Tsui, Kowloon, Hong Kong S.A.R., China.

Zhejiang Editorial Office
Rural Revitalization Academy of Zhejiang Province, Zhejiang A&F University, Hangzhou, Zhejiang, 311300, China.

Academic Open Access Publishing
Since 2023